UNIVERSIDADE DE SÃO PAULO
PROGRAMA INTERUNIDADES EM BIOINFORMÁTICA

ALINE RANGEL POZZO

# 3D NUCLEAR ARCHITECTURE DISTINGUISHES THYROID NEOPLASTIC HISTOTYPES

SÃO PAULO - SP
2024

ALINE RANGEL POZZO

# 3D NUCLEAR ARCHITECTURE DISTINGUISHES THYROID NEOPLASTIC HISTOTYPES

Dissertação apresentado a Universidade de São Paulo, como requisito para o recebimento do Mestrado em Bioinformática.

Orientador: Dr. Pedro A.F. Galante

São Paulo - SP

2024

*“Coincidence is God’s way of remaining anonymous” (Albert Einstein)*

## ACKNOWLEDGMENTS

First, I must thank my supervisor, Dr. Pedro Galante. With his assistance and dedicated involvement in every step throughout the process, this project was accomplished. I want to thank you very much for opening the door to your lab for me.

I would also like to thank the experts who were involved in this research project: Filipe F dos Santos, Dettori Tinuccia, Matteo Giulietti, Daniela Virginia Frau, Dr. Roberta Vanni, Dr. Alok Pathak, Dr. Gabor Fischer, Dr. John Gartner, Dr. Paola Caria and Dr. Sabine Mai. The project could not have been successful participation and input.

My acknowledgement also goes to the Genomic Centre for Cancer Research and Diagnosis, a Canada Foundation for Innovation-funded facility, where the imaging was performed. I thank the Rady Innovation Fund for support of this work and Canada Research Chair (Tier 1) funding. I acknowledge the CeSAR (Centro Servizi Ricerca d'Ateneo) core facility of the University of Cagliari and Marta Costa for assistance with the generation of the sequencing data. I thank Mary Cheang for the statistical analyses.

Finally, I express my profound gratitude to my mother and my son for providing me with unfailing support and continuous encouragement throughout my years of study and through the process of researching and writing this thesis. This accomplishment would not have been possible without them. Thank you.

## RESUMO

Marcadores moleculares podem ser ferramentas diagnósticas importantes para apoiar a análise patológica em neoplasias da tireoide. No entanto, como os mesmos marcadores podem ser observados em algumas lesões tireodianas benignas, são necessárias abordagens adicionais para diferenciar os subtipos de tumores da tiróide, prevenir o tratamento excessivo e direcionar o tratamento clínico. Isto se aplica particularmente à variante recentemente descrita do câncer de tireoide, denominada Neoplasia folicular não-invasiva da tireoide com características nucleares papilífero-similar (do inglês, *Noninvasive Follicular Thyroid Neoplasm with Papillary-like Nuclear Features*, ou NIFTP). Esta variante tem uma prevalência mundial estimada de 4,4% a 9,1% de todos os carcinomas papilíferos da tireoide. Neste trabalho, utilizamos 60 lesões da tireoide no total: 20 de carcinoma papilífero de tireoide clássico (do inglês *Classic Papillary Thyroid Carcinoma*, ou CPTC), 20 amostras do subtipo folicular do carcinoma papilífero da tireoide encapsulado (do inglês, *Follicular Variant of Papillary Thyroid Carcinoma*, ou FVPTC) e 20 amostras do subtipo NIFTP. Examinamos características morfológicas e moleculares para identificar parâmetros que podem diferenciar o NIFTP dos outros subtipos de PTC. Ao investigar a arquitetura nuclear das neoplasias da tireoide, observamos que o NIFTP possui telômeros significativamente mais longos do que os subtipos CPTC e o FVPTC. A microscopia 3D de super-resolução (3D-SIM) demonstrou que o NIFTP é um subtipo heterogêneo e que seus núcleos contêm DNA mais densamente compactado e espaços intercromatina menores que os subgrupos de CPTC e o FVPTC, um padrão que se assemelha ao tecido tireoidiano normal. Estes dados são consistentes com o comportamento biológico indolente observado e o prognóstico favorável associado ao NIFTP, que não possui mutações $BRAF^{V600E}$. É importante ressaltar que as regiões “hot spot” sequenciadas e analisadas no nosso painel oncológico não contribuirão na distinção dos tipos histológicos do câncer de tireoide em nossa coorte de estudo. Em resumo, nossos dados sugerem que a arquitetura nuclear 3D pode ser uma poderosa ferramenta analítica para o diagnóstico e orientação clínica do NIFTP.

**Palavras-Chave**: Diferenciação de tipos histológicos, perfil 3D de telômeros, 3D-SIM, neoplasia folicular não-invasiva da tireoide com características nucleares papilífero-similares, sequenciamento de nova geração.

## ABSTRACT

Molecular markers can be diagnostic tools to support pathological analysis in thyroid neoplasms. However, because the same markers can be observed in some benign thyroid lesions, additional approaches are necessary to differentiate thyroid tumour subtypes, prevent overtreatment and tailor specific clinical management. This applies particularly to the recently described variant of thyroid cancer referred to as non-invasive follicular thyroid neoplasm with papillary-like nuclear features (NIFTP). This variant has an estimated prevalence of 4.4% to 9.1% of all papillary thyroid carcinomas worldwide. We studied 60 thyroid lesions: 20 classical papillary thyroid carcinoma (CPTC), 20 follicular variants of PTC (FVPTC) and 20 NIFTP. We examined morphological and molecular features to identify parameters that can differentiate NIFTP from the other PTC subtypes. When blindly investigating the nuclear architecture of thyroid neoplasms, we observed that NIFTP has significantly longer telomeres than CPTC and FVPTC. Super-resolved 3D-structured illumination microscopy demonstrated that NIFTP is heterogeneous and that its nuclei contain more densely packed DNA and smaller interchromatin spaces than CPTC and FVPTC, a pattern that resembles normal thyroid tissue. These data are consistent with the observed indolent biological behaviour and favourable prognosis associated with NIFTP, which lacks $BRAF^{V600E}$ mutations. Of note, next-generation thyroid oncological panel sequencing could not distinguish the thyroid cancer histotypes in our study cohort. In summary, our data suggest that 3D nuclear architecture can be a powerful analytical tool to diagnose and guide the clinical management of NIFTP.



**Keywords**: Histotypes differentiation, telomeres molecular profile, 3D-SIM, papillary thyroid carcinoma, Next generation sequencing.

## ABBREVIATIONS

3D: three-dimensional

3D-SIM: Three-dimensional structured illumination microscopy

BRAF: B-Raf proto-oncogene, serine/threonine kinase

CIN: chromosome instability

CPTC: classical papillary thyroid carcinoma

DAPI: 4',6-diamidino-2-phenylindole

FFPE: formalin-fixed paraffin-embedded

FVPTC: follicular variant of PTC

LN: lymph nodes.

MMR: DNA mismatch repair

NAT: normal adjacent thyroid tissue

NIFTP: noninvasive follicular thyroid neoplasm with papillary-like nuclear features

PPARγ: Peroxisome proliferator- activated receptor gamma

PTC: papillary thyroid carcinoma

Q-FISH: quantitative fluorescence *in situ* hybridization

RAS: Rat sarcoma virus

RET: Rearranged during Transfection

SSBs: DNA single-strand breaks

THADA: Thyroid adenoma-associated

## LISTA DE FIGURAS

## LISTA DE TABELAS

**SUMMARY**

# 1. INTRODUCTION

Thyroid carcinoma is the most common malignancy of the endocrine system in adult and pediatric populations. In adults, this type of cancer is increasing dramatically in both men and women, with an average annual percentage chance of 5.4% and 6.5%, respectively (RANGEL-POZZO et al., 2020b). It is projected to take the place of colon cancer and become the fourth leading cancer diagnosis in both sexes (second for women) by 2030 (FERLAY et al., 2019; RAHIB et al., 2014). Thyroid cancer presents with relatively stable mortality, but it has been increasing globally since the 1970s (DAVIES; WELCH, 2006; KEINAN-BOKER; SILVERMAN, 2016; LISE et al., 2012). It is estimated that by the end of the year 2030, thyroid cancer will claim the lives of 2,180 of the 52,890 new projected cases, corresponding to 0.4% of all cancer related deaths and 2.9% of new cancers throughout the world, respectively (RANGEL-POZZO et al., 2020b).

In most patients, the cause of thyroid cancer is unknown. Intensified surveillance has resulted in the detection of an increasing number of early thyroid cancers, especially papillary thyroid carcinoma (PTC), named for both its papillary architecture and nuclear morphology (ROSARIO; MOURÃO; CALSOLARI, 2019). Differentiated thyroid carcinoma (DTC) originates from the follicular cells of the thyroid and is the most common type (80-90%) of thyroid malignancy (TUTTLE et al., 2010). DTC is classified into follicular thyroid carcinoma (FTC) and papillary thyroid carcinoma (PTC) subtypes. This classification relies on histological differences and different metastatic dissemination routes between them. FTC accounts for 10% of all DTC and is characterized by the presence of small follicles and absence of ground-glass nuclei (characteristic of PTC). PTC encompasses the remaining 80-90% of all DTC and is characterized mainly by the presence of cells arranged into papillae, presenting clear or ground-glass nuclei. PTC is further subdivided based on histological variants as classic (CVPTC), follicular (FVPTC), solid (SVPTC), and diffuse sclerosing (DSVPTC) variants. Among these variants, children under age 10 seem to be unaffected by the most common type CVPTC found in adults (CORDIOLI et al., 2016).

The follicular variant of papillary thyroid carcinoma (FVPTC) is the most common variant of PTC (RANGEL-POZZO et al., 2020b). It is composed of neoplastic

follicles rather than papillae, but the cancer cells have nuclear features similar to those of PTC. Previously, most patients with FVPTC regardless of the subtype (unencapsulated and encapsulated FVPTC) were treated as PTC. Due to overdiagnosis and overtreatment, encapsulated FVPTC has since been reclassified and renamed as non-invasive follicular thyroid neoplasm with papillary-like nuclear features (NIFTP) (NIKIFOROV et al., 2016). The name “NIFTP" appropriately reflects the biological characteristics and clinical behavior of this subtype, which includes follicular growth pattern, presence nuclei morphologically similar to those of PTC and lack of capsular invasion.

## 1.1 Molecular profiling of NIFTP

From a molecular genomic standpoint NIFTP does not demonstrate the alterations associated with classic PTC, such as *BRAF*$^{V600E}$ mutations. Instead, it shows a high prevalence of mutations in the *RAS* gene as well as other mutations normally associated with follicular thyroid tumors including follicular adenoma, follicular thyroid carcinoma and invasive follicular-variant papillary thyroid cancer (ZHU et al., 2003). These molecular characteristics indicate that although most NIFTP lesions are driven by clonal genetic alterations and are therefore true neoplasms rather than hyperplastic proliferations, in most instances, they behave indolently. However, the general consensus of a low risk of an adverse outcome has been tempered by several studies demonstrating that among nodules diagnosed as NIFTP, there are some associated with metastatic disease, further emphasizing that NIFTP cannot always be considered benign (NIKIFOROV et al., 2016).

Recent studies have identified point mutations and/or gene fusions in 90% PTCs (AGRAWAL et al., 2014). Furthermore, a number of these tumors showed the *hTERT* promoter mutation associated with aggressive tumor behavior. The data also indicated a clear distinction between cases with *BRAF* mutations and those with *RAS* mutations suggesting that PTC could be sub-classified at the molecular level into *RAS*-like or *BRAF*$^{V600E}$-like tumors. Interesting, these two groups appeared to have specific morphological appearance: *BRAFV600E*-like PTCs were less differentiated than *RAS*-like tumors, with the latter tending to maintain differentiation closer to normal thyroid. A study

has also revealed that many of the tumors with *RAS* mutations were FVPTCs while classic variants of PTCs had *BRAF*$^{V600E}$ mutations (AGRAWAL et al., 2014). However, the genetic profiling of NIFTP is still evolving (SEETHALA et al., 2018). Initial studies showed an overlapping molecular profile with other thyroid neoplasms suggesting that the use of *BRAF*$^{V600E}$ alone to exclude the diagnosis of NIFTP is not clear cut, even though it is known that when papillary architecture is absent so is the *BRAFV*$^{600E}$ mutation. The earliest iterations of the criteria for NIFTP allowed the inclusion of isolated foci of papillary architecture in up to 1% of the tumor, but it is now believed that these foci result in the inclusion of the *BRAF*$^{V600E}$ mutation thereby causing more aggressive behavior. The data have suggested that more stringent criteria (i.e. no of papillae and no *BRAF* mutations) be applied (ALVES et al., 2018). Thus, if mutations characteristic of classic PTC or high-risk cancer are identified (*BRAF*$^{V600E}$, *RET/PTC*, or *ALK* and *TERT*), NIFTP should not be diagnosed.

The most recent literature indicates that NIFTPs belong to the *RAS*-like thyroid tumors and show a high prevalence of RAS mutations, as well as other mutations normally associated with follicular thyroid tumors, such as *PPARG*, *THADA* gene fusions with the absence of *BRAFV*$^{600E}$ (CHU; SADOW, 2020). These molecular characteristics indicate that most NIFTP lesions are driven by clonal genetic alterations indicating that they are true neoplasms and not hyperplastic proliferations. NIFTP lesions are considered as low risk for disease progression; however, several studies have demonstrated that among nodules diagnosed as NIFTP, there are some associated with metastatic disease, further emphasizing that NIFTP cannot always be considered benign (ZAJKOWSKA et al., 2020). From this, it is evident that stringent histopathological criteria alone are insufficient to predict the behavior of these lesions and that additional molecular approaches are needed. The elucidation of these findings highlight the limitations of relying solely on histopathological assessments to prognosticate NIFTP lesions, thereby advocating for the integration of molecular diagnostics as a complementary approach (ALVES et al., 2018). Incorporating such molecular markers into the diagnostic algorithm could not only refine the accuracy of NIFTP identification but also afford a more personalized approach to the

tumor prognosis and to the patient management, ultimately guiding the decision-making process regarding the necessity and extent of therapeutic interventions at the outset.

## 1.2. Genomic instability

Genomic instability is a complex phenomenon observed both at the DNA nucleotide level and at the chromosome level. However, the existence of genetic alterations in a tumor, even when frequent, does not mean that the tumor is genetically unstable (LENGAUER; KINZLER; VOGELSTEIN, 1998). Instability is, by definition, a matter of rate, whereas the existence of a mutation is a state, providing no information about the rate of its occurrence. In fact, instability is a process. Cells become prone to an increased propensity for genomic alterations, which accumulate during the cell division cycles. The presence of genomic instability can provide to cancer cells different types of advantages, from shorter cell cycle to the possibility of bypassing intracellular and immunological control systems, resulting in a growth advantage when compared to normal cells (YAO; DAI, 2014). Different are the known causes which lead to genomic instability. Physical stresses (like the UV light) and chemical stresses (like oxygen free radicals) can induce the formation of DNA-adducts which disturb nucleotide-pairing, blocking DNA replication and transcription, and leading to the formation of DNA single-strand breaks (SSBs) and double-strand breaks (DSBs) (JACKSON; BARTEK, 2009). To sense, signal and repair DNA damage, the cells have developed different mechanisms, known as DNA-damage response (DDR), where a major role in the DDR-signaling is played by the protein kinases ATM and ATR (HARPER; ELLEDGE, 2007; ROUSE; JACKSON, 2002). Defects in the DDR lead to tumor development (GORGOULIS et al., 2005).

Lack of accuracy during DNA replication has also been associated with genomic instability, since sequence changes at DNA base, i. e. substitutions or deletions or insertions of a few nucleotides as observed in numerous cancers which involve a missing or damaged *TP53* gene or damage mutations in the *ATM* gene (BAILEY et al., 2018; GREENMAN et al., 2007). Normally, DNA base mismatch would be corrected by different DNA mismatch repair (MMR) proteins, however, mutations in MMR genes have

been associated with cancer development, and loss of MMR is associated with a significant fraction of sporadic cancers (HSIEH; YAMANE, 2008).

Epigenetic changes can also lead to genomic instability, since DNA methylation has been implicated in affecting stability within the genomic microsatellites regions, which are particularly susceptible to length change alterations. Microsatellite repeat instability (MSI) is found in many diseases such as Huntington's, myotonic dystrophy, and cancer and is often associated with defects in the MMR machinery (PUTIRI; ROBERTSON, 2011).

Additionally, defects in the maintenance of chromosome ploidy and structure have been correlated with genomic instability and have been described as chromosome instability (CIN). CIN includes alterations in chromosome number (nCIN), which leads to aneuploidy and structural chromosome changes (sCIN), such as translocation, inversions and deletions, generate gene fusions (TAYLOR et al., 2018; ZHANG et al., 2018). Theodor Boveri was the first scientist who, by observing abnormal development of sea urchin and ascaris embryos in presence of aberrant chromosome number, suggested that chromosomes played a role in cellular cooperation, and supposed that disrupted (increased) growth patterns in human cancers may result from chromosomal aneuploidy (CHENG; LOEB, 1993; LAUBICHLER; DAVIDSON, 2008). As demonstrated by the presence of increased rate of CIN in transformed CHO cells with increased ploidy, the aneuploidy destabilizes the genome by unbalancing genes required for mitosis, resulting in the autocatalytic formation of randomly generated karyotypes due to recurrent segregation errors (DUESBERG et al., 1998). Defects in the mitotic spindle assembly checkpoint, result in numerical aneuploidy and CIN (KOPS; WEAVER; CLEVELAND, 2005). Deregulation of the expression of the mitotic checkpoint components MAD1, MAD2, or CENP-E leads to missegregation of one or more chromosomes per division, resulting in tumorogenesis, especially when coupled with other tumor-promoting activity, such as reduced rate of cell death (WEAVER; CLEVELAND, 2009). Interestingly, high rates of CIN caused by complete depletion of MAD2 or BUBR1 have been shown to cause rapid death in tumor cells (KOPS; FOLTZ; CLEVELAND, 2004; MICHEL et al., 2004).

Ongoing nCIN or sCIN lead to the production of genetically distinct populations of daughter cells (BAYANI et al., 2007; LEPAGE et al., 2019). CIN is responsible for the increased intratumoral heterogeneity which may confer a selective growth advantage to a subpopulation of cells like increased cell proliferation, metastatic potential, or intrinsic drug resistance (LEE et al., 2011). Selective pressures, like the one promoted by the chemotherapy, potentially induce unregulated proliferation of cells harboring specific growth advantages (such as drug resistance), producing a highly aggressive or drug-resistant tumor (GERLINGER; SWANTON, 2010).

### 1.3. Telomere related genomic instability and nuclear architecture.

Telomeres, tandem repeats (TTAGGG)n, ensure that the ends of chromosomes are not recognized as sites of DNA damage and processed by DNA repair pathways (CLEAL; NORRIS; BAIRD, 2018; MACIEJOWSKI; DE LANGE, 2017; RANGEL-POZZO et al., 2020b). Telomere function in humans depends on a cap of tightly bound proteins to repress DNA damage signaling, which includes the t-loop and the association of telomere-associated proteins, i.e, the shelterin complex - TRF1 and TRF2, POT1, TIN2, RAP1, and TPP1 (DE LANGE, 2005; RANGEL-POZZO et al., 2020b). Due to the inefficiency of the DNA replication machinery to replicate the chromosome ends, which is called the end replication problem, telomeres progressively shorten after each cell division (D'ADDA DI FAGAGNA, 2008; DE LANGE, 2009; RANGEL-POZZO et al., 2020b). During replication, DNA synthesis of the discontinued strand at a replication fork occurs with a mechanism that produces short DNA fragments. However, this process meets a problem when the replication fork reaches the end of a linear chromosome/DNA. The final RNA primer synthesized on the discontinued-strand template cannot be replaced and telomeres sequences are lost from the ends of all chromosomes each time a cell divide (D'ADDA DI FAGAGNA, 2008; DE LANGE, 2009; RANGEL-POZZO et al., 2020b).

It is noteworthy to mention that telomere shortening is an important tumor suppressor mechanism as it leads to cell replicative cellular senescence and cycle arrest in normal cells, thus preventing genome instability. However, cancer cells can elongate their telomeres and regain telomere stability by activating one of two known telomere

maintenance mechanisms (TMM): telomerase, which is activated in 85–90% of cancers; or the alternative lengthening of telomeres (ALT) mechanism (10–15% of cancers), which is often present in cancer cells that do not express telomerase (RANGEL-POZZO et al., 2020b; SOBINOFF; PICKETT, 2017).

However, even though *TERT* promoter mutation drives telomerase expression, it does not always prevent telomere shortening in PTC. This gave rise to the hypothesis that re-activated telomerase expression could only allow genetically unstable clones to maintain their telomeres barely above a critically short length, so that prevention of cellular senescence and apoptosis occur (CHIBA et al., 2017; RANGEL-POZZO et al., 2020b). Telomere shortening, genomic instability, and *TERT* activation are associated with PTC features and are the most frequent alterations observed in aggressive stages (GADJI; POZZO, 2019; MAI; GARINI, 2006; RANGEL-POZZO et al., 2020b). Therefore, telomere studies could provide additional information to predict metastasis and aggressive behavior of PTC tumors having poor biological characterization and very limited therapeutic options.

With the advances of 3D imaging analysis, it is now possible to analyze, on a single cell level, telomere length, telomere numbers, their spatial organization, and cell cycle dependency within interphase nuclei rather than using the classical metaphase chromosomes, polymerase chain reactions or DNA blotting techniques, which simply determine telomere length. For example, Caria et al. (2019), used a 3D imaging approach to reveal specific 3D telomeric signatures of PTC-derived cell lines. This was the first study using 3D telomere quantitative Fluorescence *in situ* hybridization and quantitative 3D imaging in PTC cells. Interesting, the authors demonstrated that thyroid cell lines BCPAP, K1, and TPC1 (all with *TERT* C228T mutation) have more telomere signals, more telomere aggregates and less average intensity (proportional to telomere length) than the control cell lines Nthy-ori 3-1 (CARIA et al., 2019). Telomere aggregates are fused telomeric signals or telomeres in close illegitimate proximity capable of engaging in recombination events. Short and unprotected telomeres are recognized as broken DNA ends and are eventually joined by the DNA repair proteins, which may likely generate deletions, duplication, non-reciprocal translocation, and most of the overall genetic

changes observed during tumor progression (GADJI; POZZO, 2019; MAI; GARINI, 2006). Additional studies have corroborated these findings (RANGEL-POZZO et al., 2021b; SISDELLI et al., 2021). However, the 3D nuclear organization from NIFTP, remains underexplored.

The nuclear architecture of cancer cells can also be analyzed in detail using 3D structured illumination microscopy (3D-SIM). The 3D-SIM is able to overcome the limits of conventional wide field fluorescence microscopy and reveal cellular structures that cannot be visualized directly by conventional microscopy (RANGEL-POZZO et al., 2020b; WEGEL et al., 2016). Shortly, 3D-SIM uses illumination patterns to excite the sample and the reconstruction software doubles the resolution in all three dimensions (GUSTAFSSON, 2000; GUSTAFSSON et al., 2008; RANGEL-POZZO et al., 2020b). Application of 3D-SIM has been geared to the study of biological structures, most importantly to analyze the chromatin present in cancer cells. Many authors have used this technology to examine the cancer cell genome, where the presence of DNA structure, along with DNA interchromatin spaces (spaces without of DNA structure) were quantified (AJAEZI et al., 2018; RANGEL-POZZO et al., 2020a; RIGHOLT et al., 2014; SATHITRUANGSAK et al., 2015). The biological significance of these interchromatin spaces still needs further investigation but have already been correlated with disease stage and tumor aggressiveness (AJAEZI et al., 2018; RANGEL-POZZO et al., 2020a; RIGHOLT et al., 2014; SATHITRUANGSAK et al., 2015).

Therefore, the genome of a normal cell is structurally different from that of a tumor cell. Recent quantitative measurements of the three-dimensional (3D) genome structure of normal *vs.* tumor cell nuclei have indicated that these differences lie in the way the genome is organized. Using centromeres, telomeres, chromosomes, and DNA as tools to measure the 3D organization order, distinct changes can be identified and quantitated (RIGHOLT et al., 2014; SCHMÄLTER et al., 2015; VERMOLEN et al., 2005; YU et al., 2019). These studies have shown that the genome structure can serve as an architectural biomarker of cancer stage and aggressiveness (BABU; FULLWOOD, 2015; GADJI et al., 2010; RANGEL-POZZO et al., 2021a). The 3D telomere organization in nuclei of cancer cells has enabled the distinction of stable or progressive disease in

myelodysplastic syndromes and acute myeloid leukemia (GADJI et al., 2012), time to progression in glioblastoma (GADJI et al., 2010), response to treatment in Hodgkin's lymphoma (KNECHT et al., 2012), segregation of patients into subgroups of disease aggressiveness in neuroblastoma (KUZYK; GARTNER; MAI, 2016), risk to progression in intermediate risk prostate cancer (DRACHENBERG et al., 2019), and risk to progression in multiple myeloma (RANGEL-POZZO et al., 2021a). Three-dimensional structured illumination microscopy (3D-SIM) imaging has enabled a closer look at the DNA organization in the nuclei of both normal and tumor cells. In previous publications, we have described quantitative measurements of DNA structure using 3D-SIM in normal and Hodgkin's Lymphoma cells, multiple myeloma and in neuroblastoma (RANGEL-POZZO et al., 2019; RIGHOLT et al., 2014; SATHITRUANGSAK et al., 2015).

Thus, in this project we decided to examine the spatial three-dimensional (3D) genome organization, in situ hybridization, pathological analysis and targeted sequencing of NIFTP, classical PTC and FVPTC. In the end, among other findings our results reinforced the idea that NIFTP is a lesion with a low risk of disease progression, underscore the existence of heterogeneity within the group.

## 2. RATIONALE AND HYPOTHESIS

### 2.1. Rationale

The challenges in the diagnosis of NIFTP clearly require both stringent histopathological criteria and molecular profiling to make an accurate diagnosis but there is still a need for better tools to refine these diagnostic criteria to more accurately predict the outcome of a given case and to determine what additional therapeutic measures might be implemented at the time of diagnosis. We hypothesized that an analysis of the spatial organization of the genome in the cancer cells might help to more clearly define NIFTP and predict its outcome.

Our preliminary findings suggest that while NIFTP has 3D telomere profiles and genomic spatial organizational features of a neoplasm, these parameters appear to be different from those seen in conventional thyroid neoplasms. These data suggest that this approach might have diagnostic utility and might provide additional objective prognostic parameters to guide clinical management. Further investigation of these findings is necessary to robustly conclude that there are significant and potentially diagnostically important differences between NIFTP and PTC and that these differences could serve to assign/stratify a patient with thyroid cancer at the time of diagnosis.

### 2.2. Hypothesis

NIFTP has characteristic features identifiable through 3D nuclear telomere profiling, SR genomic imaging and genetic profiling that differentiate this lesion from aggressive thyroid cancer.

# 3. OBJECTIVES

## 3.1. General Aims

Our goal was to stratify patients with PTC and NIFTP into structural genetic subgroups to enable personalized patient care. We focused on the structural characterization of NIFTP and compared our findings in this tumor with classical PTC and FVPTC.

**Aim 1.** To determine the 3D nuclear telomere architecture of retrospective tumor samples from patients with NIFTP, classical PTC and FVPTC. To this end, we have blindly examined retrospective samples from Dr. Pathak's database (with clinical follow-up) – University of Manitoba. The outcome of these analyses are the first ever definition of specific 3D telomeric signatures for NIFTP (as opposed to FVPTC and PTC) which lend themselves as future structural biomarkers for NIFTP.

**Aim 2**. To determine the super resolution (SR) DNA structure and that of DNA-interchromatin spaces in retrospective thyroid cancer samples. We have studied genomic structure by assessing the super-resolved DNA structure of the nuclei. SR analysis of the DNA structure as described below was carried out on all of the above samples and granulometry measurements will be performed to identify DNA structure and DNA interchromatin regions.

**Aim 3.** To investigate the mutational profiling in a set of thyroid-cancer associated genes using NGS and fluorescence *in situ* hybridization (FISH) for the gene fusions most frequently associated with PTC.

## 4. INNOVATIVE NATURE OF THE PROJECT.

To date, no studies have investigated the structural organization of the genome in thyroid cancer in order to stratify subtypes by this method. The combination of structural hallmarks of the genome with a thyroid-specific onco-panel has never been performed. These innovative approaches to thyroid cancer diagnosis allows a greater level of patient-specific tumor analyses that could potentially be applied to fine needle aspirates done before the tumor is resected. From our point of view, this project uses “transformative, paradigm-shifting research to alter current research or clinical practice approaches”, utilizes “novel theoretical concepts, approaches or methodologies, instrumentation, or interventions that may be exploited or adopted by several fields of research”, and applies “novel theoretical concepts, approaches or methodologies, instrumentation, or interventions (in ways that have not been previously proposed)”. The efficacy and feasibility of our project has been supported by our results and current publication.

## 5. MATERIALS AND METHODS

### 5.1. Patient cohort

Retrospective cases diagnosed as PTC, FVPTC and NIFTP were retrieved from the archives of the Anatomical Pathology Section of Max Rady College of Medicine (University of Manitoba, Winnipeg, Canada) for the interval 2018-2020. Each case was re-evaluated by two pathologists (Dr. John Gartner and Dr. Gabor Fisher) according to the World Health Organization classification (OSAMURA RY, KLÖPPEL G, ROSAI JLR, 2017). The tumor and normal adjacent tissue (NAT) of formalin-fixed paraffin-embedded (FFPE) sections (5 μm), were circled with a pen, after review of the corresponding hematoxylin and eosin-stained sections. In total, we analyzed sixty PTC: 20 CPTC (classic thyroid papillary carcinoma), 20 FVPTC and 20 NIFTP. For all PTC cases the following clinico-pathological characteristics were recorded: tumor size, presence of extrathyroidal extension, lymphovascular invasion, multifocality and American Joint Committee on Cancer T, N and M stages. This study was conducted in accordance with the institutional review board approval of the Health Research Ethics Board on human studies from University of Manitoba, Canada, (Ethnic number: HS21723; H2018:156). All experiments were performed blinded for the tumor characteristics and patient outcome. Our cohort was composed of 11 (18.3%) men and 49 (81.6%) women, ages 23-78 (median age of 50.6 years). Clinical and pathological characteristics of the sixty patients included in the study are shown in Table 1.

**Table 1**: Clinical information of the 60 patients examined in our study.

TABLE 1 Clinical information of the 60 patients examined in our study.

| Parameter | |
|---|---|
| Age (mean) | 50.6 years |
| Sex | |
| Male | 11 (18.3%) |
| Female | 49 (81.6%) |
| *CPTC* | 20 |
| Tumor size | |
| 0-4 cm | 18 |
| ≥4 cm | 2 |
| Focality | |
| Multifocal | 10 |
| Unifocal | 10 |
| Stage | |
| pT1a | 5 |
| pT1b | 7 |
| pT2 | 6 |
| pT3 | 2 |
| LN | 6 |
| *FVPTC* | 20 |
| Tumor size | |
| 0-4 cm | 16 |
| ≥4 cm | 4 |
| Focality | |
| Multifocal | 8 |
| Unifocal | 12 |
| Stage | |
| pT1a | 7 |
| pT1b | 4 |
| pT2 | 5 |
| pT3 | 4 |
| LN | 1 |
| *NIFTP* | 20 |
| Tumor size | |
| 0-4 cm | 18 |
| ≥4 cm | 2 |
| Focality | |
| Multifocal | 6 |
| Unifocal | 14 |

Abbreviations: CPTC, classic thyroid papillary carcinoma; FVPTC, follicular variant PTC; LN, lymph nodes; NIFTP, noninvasive follicular thyroid neoplasm with papillary-like nuclear features.

CPTC: classic thyroid papillary carcinoma; FVPTC: Follicular Variant PTC; LN: LN: lymph nodes; NIFTP: non-invasive follicular thyroid neoplasm with papillary-like nuclear features.

### 5.2. Three-dimensional (3D) nuclear telomere analysis.

Thyroid tissue samples were analyzed by 3D imaging using an AxioImager Z1 (Zeiss) following 3D quantitative FISH (Q-FISH). Forty *z* stacks were acquired using *x*, *y*: 102 nm and *z*: 200nm. Telomeres were labeled with a Cy3-tagged peptide nucleic acid telomere probe (DAKO), and nuclei was counterstained using 4',6-diamidino-2-phenylindole (DAPI). Image stacks were analyzed following constrained iterative deconvolution, and all 3D telomere parameters were measured using the TeloView® program (SCHAEFER; SCHUSTER; HERZ, 2001) (Telo Genomics Corp., Toronto, ON, Canada). One hundred nuclei were examined per sample. TeloView® determined the following 6 telomere parameters: telomere signal intensity (total and average), number of telomere signals, number of telomere aggregates (i.e., clusters of telomeres too close to be further resolved at an optical resolution limit of 200 nm), nuclear volume, *a/c* ratio (i.e., spatial distribution of the telomeres within the nucleus in a cell cycle-dependent manner), and distribution of telomeres relative to the nuclear periphery.

### 5.3. Telomere statistical analysis

The software package SAS × version 9.4 (SAS Institute Inc., Cary, NC, USA) was employed to perform nested factorial analysis of variance in the telomere parameters measured using TeloView®. Chi-square tests were used to compare the percentage of interphase telomere signals at each given intensity level at intervals of 1000 intensity units, ultimately divided into quartiles for analysis. Nested factorial analysis of variance was also used to compare the distribution of signal intensities across NIFTP, FVTPC, and PTC. A *p*-value of 0.05 or below was considered significant. If needed, multiple test corrections were applied using the False Discovery Rate (FDR) method.

### 5.4. Super-resolution imaging of nuclear DNA.

Formalin-fixed and paraffin-embedded patient thyroid sections (5 µm-thick) were treated with xylene (2x of 15min, Sigma-Aldrich) and tissues were rehydrated through incubation in solutions of descending concentration of ethanol: 100%, 90%, 70%, 5 min each. Subsequently, sections were incubated for 5 min in PBS and permeabilized

using 0.75% TX-100 in PBS for 30 min at 37ºC. Nuclear DNA was stained by overnight incubation with 50 µg/ml DAPI followed by 1 min wash in PBS. One hundred cells from tumor (50 cells) and normal adjacent tissue (50 cells) were imaged with a Zeiss Elyra PS1 SIM equipped with a Plan Apochromat 63×/1.40 Oil immersion objective using an And or EM-CCD iXon 885 camera and a 1.6× tube lens. The 3D-SIM images were reconstructed with ZEN 2012 black edition (Carl Zeiss, Jena, Germany) with the standard settings. The image processing and measurement steps were performed in Matlab (MathWorks, Natick, MA) with the toolbox DIPimage (RIGHOLT et al., 2014). The granulometry program which analyze the DNA structure and interchromatin spaces was used to measure morphological sieve applied to the error-function clipped images (RIGHOLT et al., 2014) and the two-sided, two-sample Kolmogorov–Smirnov (KS) tests were used to determine the significance between the differences observed, with a *p*-value below 0.05 indicating statistical significance..

**5.5. Genetic profile and analysis of thyroid-cancer associated genetic changes.**

DNA extraction was performed from 30 µm FFPE sections using the QIAamp® DNA FFPE Tissue Kit (QIAGEN, Gaithersburg, MD) according to the manufacturer's instructions. DNA concentration was assessed using Qubit dsDNA Assay kit on the Qubit 2.0 Fluorometer (Thermo Fisher Scientific, Waltham, MA). Targeted next-generation sequencing was performed on libraries prepared with the TruSeq Amplicon Cancer Panel (TSACP, Illumina) on the MiSeq sequencer (Illumina, San Diego, CA) to cover hotspot regions of 48 genes: *ABL1, AKT1, ALK, APC, ATM, BRAF, CDH1, CDKN2A, CSF1R, CTNNB1, EGFR, ERBB2, ERBB4, FBXW7, FGFR1, FGFR2, FGFR3, FLT3, GNA11, GNAQ, GNAS, HNF1A, HRAS, IDH1, JAK2, JAK3, KDR, KIT, KRAS, MET, MLH1, MPL, NOTCH1, NPM1, NRAS, PDGFRA, PIK3CA, PTEN, PTPN11, RB1, RET, SMAD4, SMARCB1, SMO, SRC, STK11, TP53,* and *VHL* (Https://Emea.Illumina.Com/Systems/Sequencing-Platforms.Html). To generate a consistent set of somatic mutations, we used two different established pipelines for variant calling and additional quality control pipelines, as follows. First, we used FASTQC (https://www.bioinformatics.babraham.ac.uk/projects/fastqc/) and TRIMMOMATIC to

check the sequenced reads quality and filter out adapters or low-quality reads (BOLGER; LOHSE; USADEL, 2014). Secondly, due to DNA quality, 12 tumor-normal pairs were excluded from further steps. Next, we used the Burrows-Wheeler Alignment tool (BWAMEN), specifically the maximal exact matches algorithm to align sequences from tumors and their normal adjacent tissue to human reference genome (build GRCh38/hg38). Somatic mutations were identified in the aligned data using BCFTOOLS CALL (DANECEK et al., 2021) and Genome Analysis Toolkit (GATK—v4.1.4.0) (VAN DER AUWERA BD, O'CONNOR GA, 2020). In the GATK front, we performed the marking of duplicate reads (Mark Duplicates—v1.114), base recalibration (Picard Toolkit 2019; all parameters default) and variant calling with the "Haplotype Caller" tool (all parameters default) (VAN DER AUWERA BD, O'CONNOR GA, 2020). Finally, we used ANNOVAR (WANG; LI; HAKONARSON, 2010) for the annotation of variants. In addition, SAMTOOLS (v1.13) was used in many steps, such as sorting, indexing, filtering and getting a number of basic statistics like coverage (DANECEK et al., 2021). Scripts in shell (Linux CentOS v8.5.2111), R (v4.1.0) (R Core Team) and Python (v3.6.15) were utilized in order to create and organize the entire pipeline.(FRED L, DRAKE GVR, 2009)

### 5.6. *RET and PPARγ rearrangements*.

Double-target FISH probes containing DNA sequences flanking the breakpoints of the *RET* and *PPARγ* genes (involved in *RET/PTC* and *PAX8* [or *CREB3L2*]/*PPARγ* gene fusions) were used to identify *RET* and *PPARγ* rearrangements. The analytical specificity (percentage of FISH signal located at the correct metaphase chromosome position of *RET* and *PPARγ* genes) and sensitivity (percentage of metaphases or nuclei with FISH signal pattern), and a cutoff value of the break-apart *RET* and *PPARγ* probes were previously demonstrated (CARIA et al., 2014). Briefly,100% specificity for both *RET* and *PPARγ* and 99.5% sensitivity for *RET* and 99.8% for *PPARγ* were established in metaphases and nuclei of lymphocytes. The cut-off value, established in nuclei from the apparently tumor-free contralateral thyroid lobe was calculated as the beta inverse function and was split FISH signals in 2.4% of cells for *RET* and 0% for *PPARγ*. Probe efficiency was confirmed on nuclei from PTCs and FTCs positive for

*RET/PTC* and *PAX8/PPARγ* alterations by conventional RT-PCR. On this basis, we studied from 150 to 200 nuclei per sample and considered a sample positive if a broken signal for *RET* or *PPARγ* was observed in ≥3% of nuclei (CARIA et al., 2014).

## 6. RESULTS

The flowchart methodology of this research is available in the Figure 1

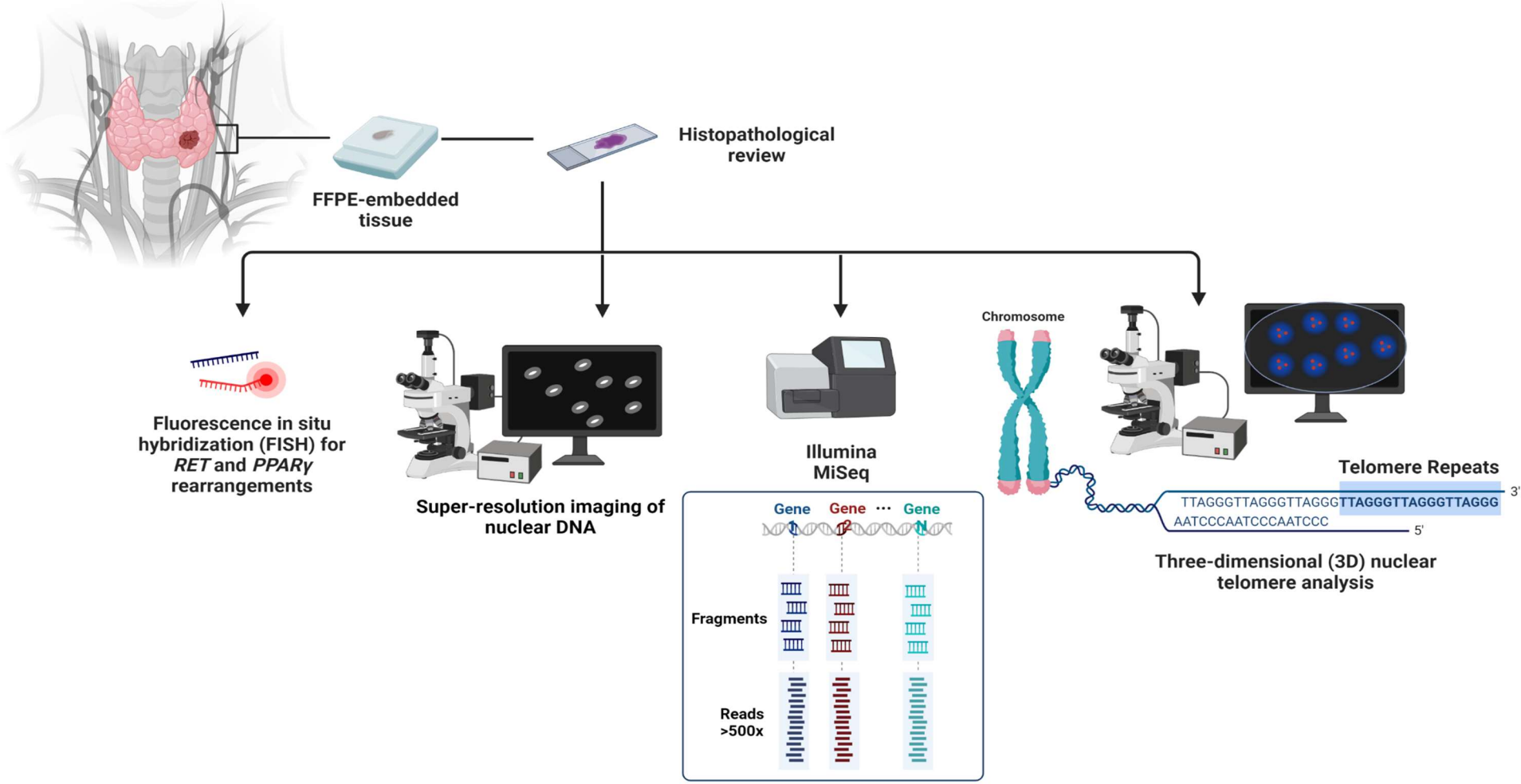

### 6.1. Low presence of RET and absence of PPARγ rearrangements in the study cohort

Somatic mutations in thyroid tumors such as *RET/PTC* and *PAX8/PPARγ* chromosomal rearrangements are frequently used in clinical mutation panels to detect malignant thyroid cancers. Among 60 cases analyzed in this work, a split-apart *RET* FISH signal was identified in 2 (3.3%) samples (one CPTC and one NIFTP), the percentage of positive nuclei was 38% (57/150) and 24% (36/150). No *PPARγ* rearrangements were found in our cohort (Figure 2 A,B). In addition, we haven't observed alterations in the normal adjacent tissue (NAT).

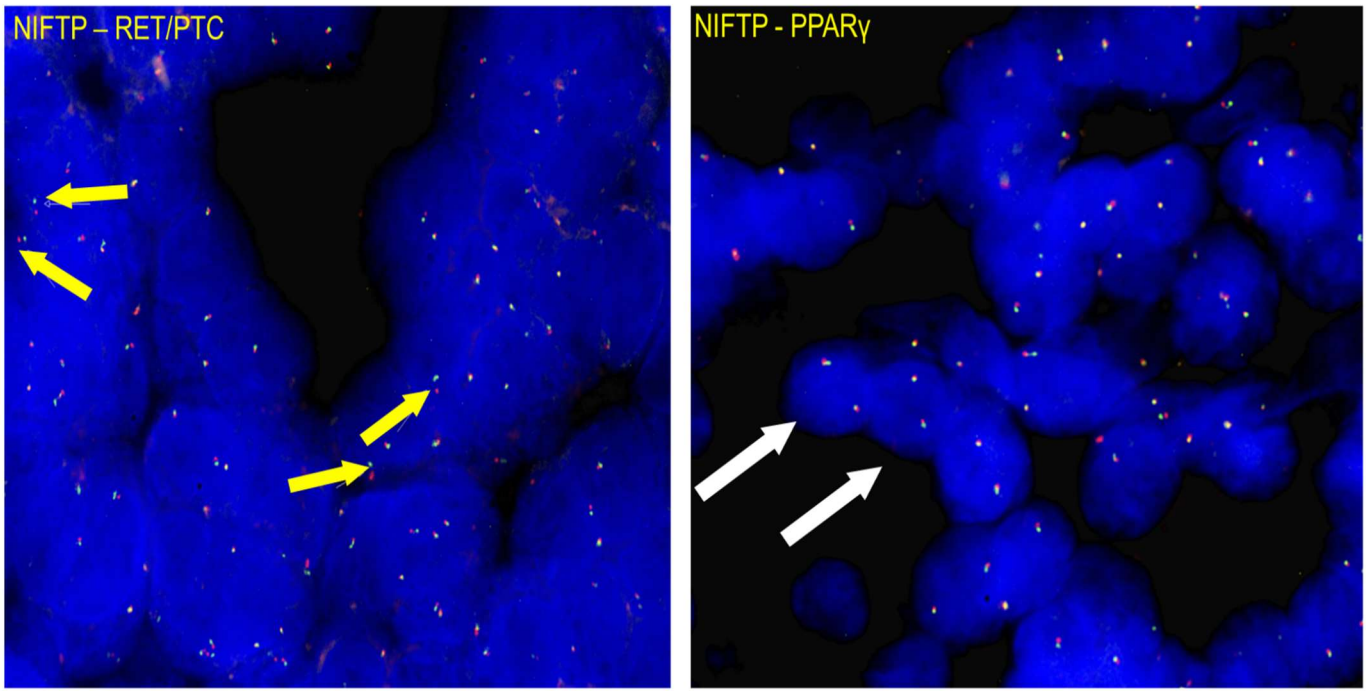


**Figure 2**: I-FISH with break-apart DNA probes specific for RET and PPARγ genes. **(A)** Yellow arrows show split of one red/green signal indicating disruption of RET gene copy. **(B)** Example of nuclei with two red/green fused signals indicates PPARγ gene integrity.

### 6.2. NIFTP has a higher frequency of long telomeres than CPTC and FVPTC

We investigated the 3D telomere profiles of three histotypes to determine whether or not there were thyroid histotype-specific profiles. We analyzed sixty paraffin embedded tissues of thyroid nodules at diagnosis (CPTC (20), FVPTC (20) and NIFTP (20) and their normal adjacent tissues (NAT). Five of six TeloView® telomeric parameters (number of telomeric signals, number of telomere aggregates, average intensity, total intensity, and nuclear volume) differentiated NAT from tumor tissues (Table 2).

**Table 2**: Statistical analysis of 3D telomere parameters of thyroid tumor vs normal to adjacent tumor tissue.

| Histotype | Number of telomere signals | Number of telomere aggregates | Average intensity | Total intensity | *a/c* ratio | Nuclear Volume |
|---|---|---|---|---|---|---|
| NIFTP | $P < .0001$ (↓ NTA vs T↑) | $P < .001$ (↓ NTA vs T↑) | $P < .001$ (↑ NTA vs T↓) | $P < .001$ (↑ NTA vs T↓) | ns | $P < .001$ (↓ NTA vs T↑) |
| CPTC | $P < .0001$ (↓ NTA vs T↑) | $P < .001$ (↓ NTA vs T↑) | $P < .001$ (↑ NTA vs T↓) | $P < .001$ (↑ NTA vs T↓) | ns | $P < .001$ (↓ NTA vs T↑) |
| FVPTC | $P < .0001$ (↓ NTA vs T↑) | $P < .001$ (↓ NTA vs T↑) | $P < .001$ (↑ NTA vs T↓) | $P < .001$ (↑ NTA vs T↓) | ns | $P < .001$ (↓ NTA vs T↑) |

Abbreviations: CPTC: classic thyroid papillary carcinoma; FVTPC: follicular variant of papillary thyroid carcinoma; NAT: normal adjacent tissue; NIFTP: non invasive follicular thyroid neoplasm with papillary-like nuclear features; T: tumor; ↓ decrease, ↑ increase, ns: not significant.

NIFTP could be differentiated from CPTC and FVPTC through the analysis of telomere signal intensities, subdivided into four quartiles (Figure 3). Relative telomere signal intensities measured in arbitrary units (a.u.) represent telomere length (Poon et al., 1999). Four cell subpopulations (quartiles) were examined, based on their telomeric signal intensities in arbitrary units (a.u.): cells with very short telomeres (≤ 5000 a.u.), cells with short telomeres (5001-9000 a.u), cell with medium telomeres (9001-16000 a.u), and cells with large telomeres (>16.000 a.u.). As shown in Figure 3, NIFTP had significantly longer telomeres (>16.000 a.u.) than the other histotypes. Significant differences were also found in the short (5001-9000 a.u.) and medium sized (9001-16000 a.u.) telomere quartiles. However, no significant difference was observed in the frequency distribution of very short telomeres (≤ 5000 a.u.). Thus, NIFTP cases present with longer telomeres than either

CPTC or FVPTC. Representative figures of the telomere staining are shown in Figure 3.1. A different representation of the same data is shown in Figure 3.2.

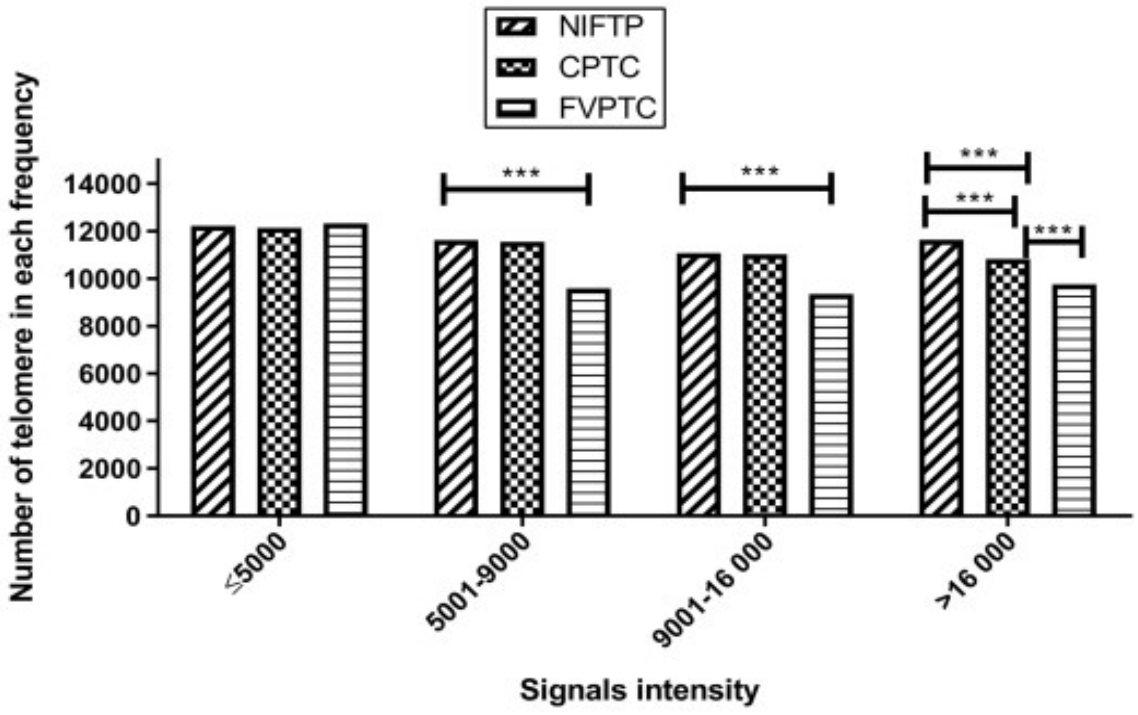


**Figure 3:** Bar plot of the differences among telomeric signal intensity (telomere length) differences in quartiles between CPTC, FVPTC and NIFTP. Nuclei with intensities of >16.000 a.u. represent very large telomeres. In the quartile analysis, <5000 a.u. represent very short, 5001 to 9000 a.u. short, 9001 to 16 000 a.u. mediumsized telomeres, respectively. The x-axis assigns one box for each cell population analyzed. The y-axis refers to the number of telomeres in different quartiles. We only show P values, *** P < .0001. CPTC, classic thyroid papillary carcinoma; FVTPC, follicular variant of papillary thyroid carcinoma; NIFTP, noninvasive follicular thyroid neoplasm with papillary-like nuclear features.

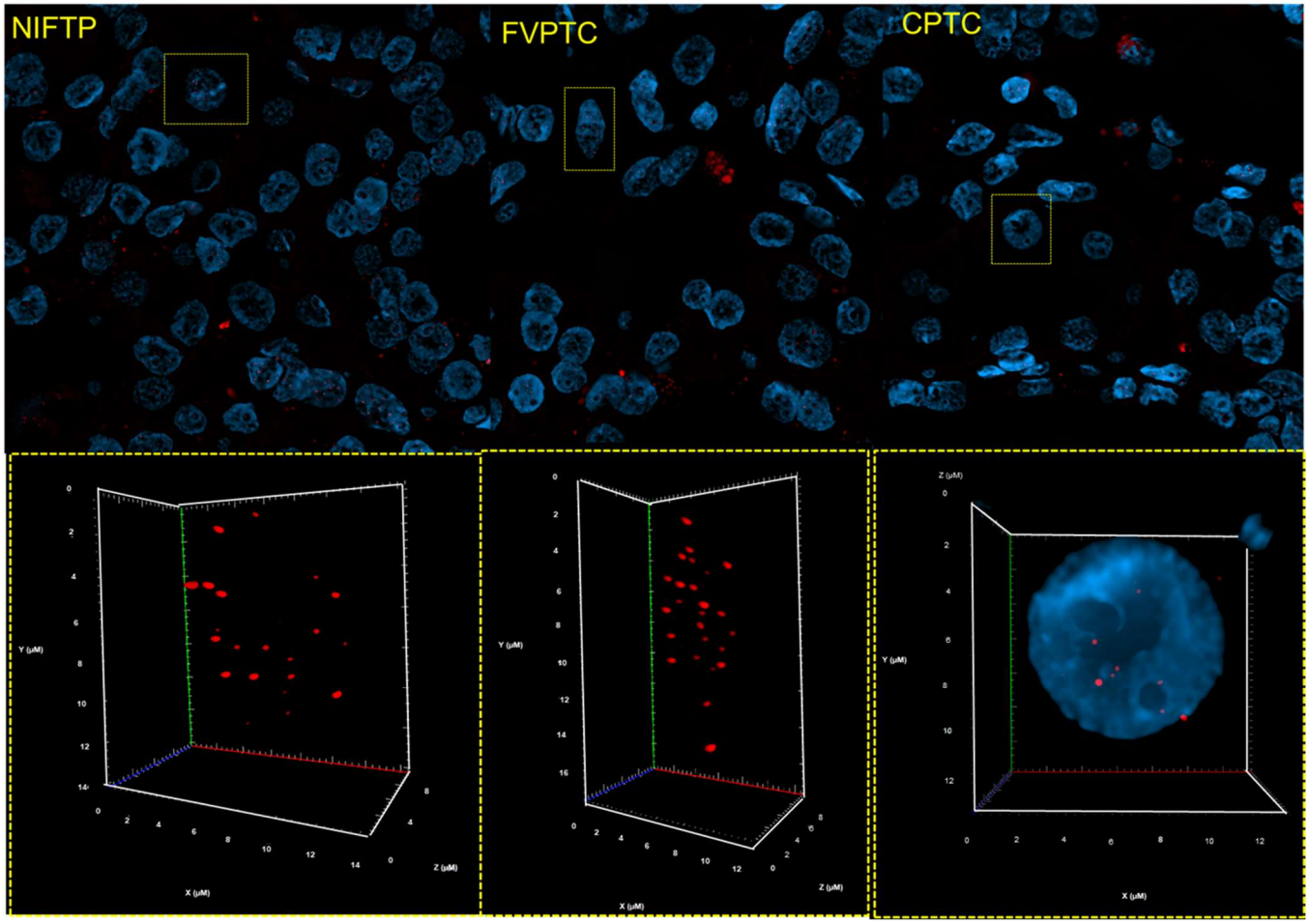


**Figure 3.1:** Differences in the 3D nuclear telomere architecture between NIFTP, FVPTC, and CPTC. Representative nuclei, counterstained with DAPI (blue), are shown for each histotype. Cy-3 labeled telomeres appear as red signals in the 3D figures in the enlarged box (lower panel). NIFTP: Non-invasive follicular thyroid neoplasm with papillary-like

nuclear features; FVPTC: Follicular variant papillary thyroid carcinoma; CPTC: Classical-papillary thyroid carcinoma; 3D: Three-dimensional.

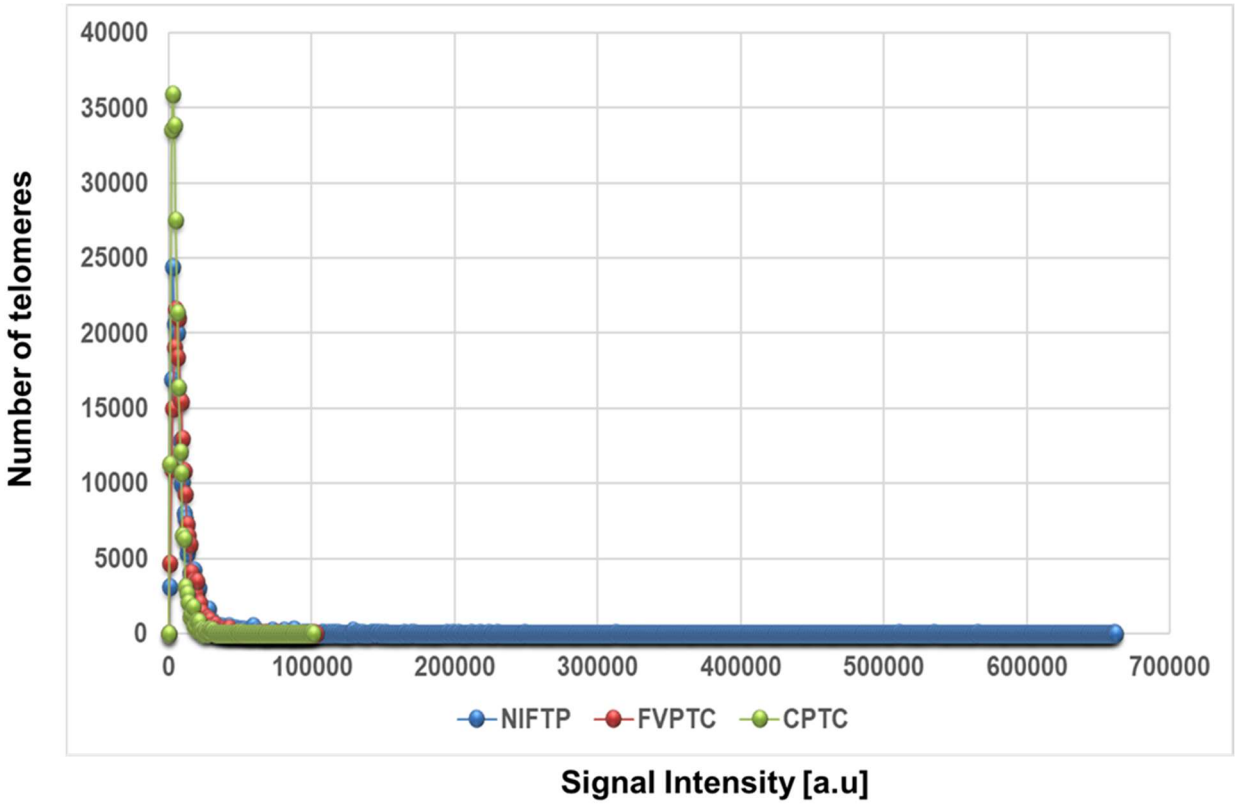


**Figure 3.2**: Representative examples of the 3D telomere profile for patient's samples classified as NIFTP, FVPTC and PTC. The X-axis shows the number of telomeres, and the Y-axis represents the telomere length in arbitrary units of fluorescence (a.u.). NIFTP: Non-invasive follicular thyroid neoplasm with papillary-like nuclear features; FVPTC: Follicular variant papillary thyroid carcinoma; CPTC: Classical-papillary thyroid carcinoma.

### 6.3. Chromatin de-condensation is a nuclear marker of PCT histotypes and could be used as a differential feature to exclude NIFTP.

Super-resolution imaging of the genome provides high resolution information about chromatin organization. Granulometry quantitatively assesses the DNA size distribution and the differences of the DNA structure and interchromatin spaces in normal and cancer cells (RIGHOLT et al., 2014). To determine whether chromatin organization

patterns allow for differentiation of thyroid cancer histotypes, we imaged and quantified pathological tissue (CPTC, FVPTC and NIFTP) and compared it to the corresponding normal adjacent tissue (NAT) for each different histotype. Using granulometry, we measured DNA granule sizes detected in the 3D-SIM images as well as the DNA-free spaces, which represent interchromatin spaces. Super-resolution imaging revealed significant differences in DNA decompaction among PTC histotypes. NATs samples have more densely packaged DNA followed by NIFTP, FVPTC and CPTC with high overall DNA de-condensation (Figure 4 A, C). Interestingly, the same pattern was observed for the size of the-interchromatin spaces: the interchromatin spaces increase starting from NAT/NIFTP followed by FVPTC and CPTC, with the largest interchromatin spaces in CPTC (Figure 4 B, D). There are no significant differences between NATs and NIFTP in relation to interchromatin spaces (Figure 4D (two blue lines) and Table 3). Figure 4.1 illustrates representative 3D-SIM images for DNA structure and interchromatin spaces.

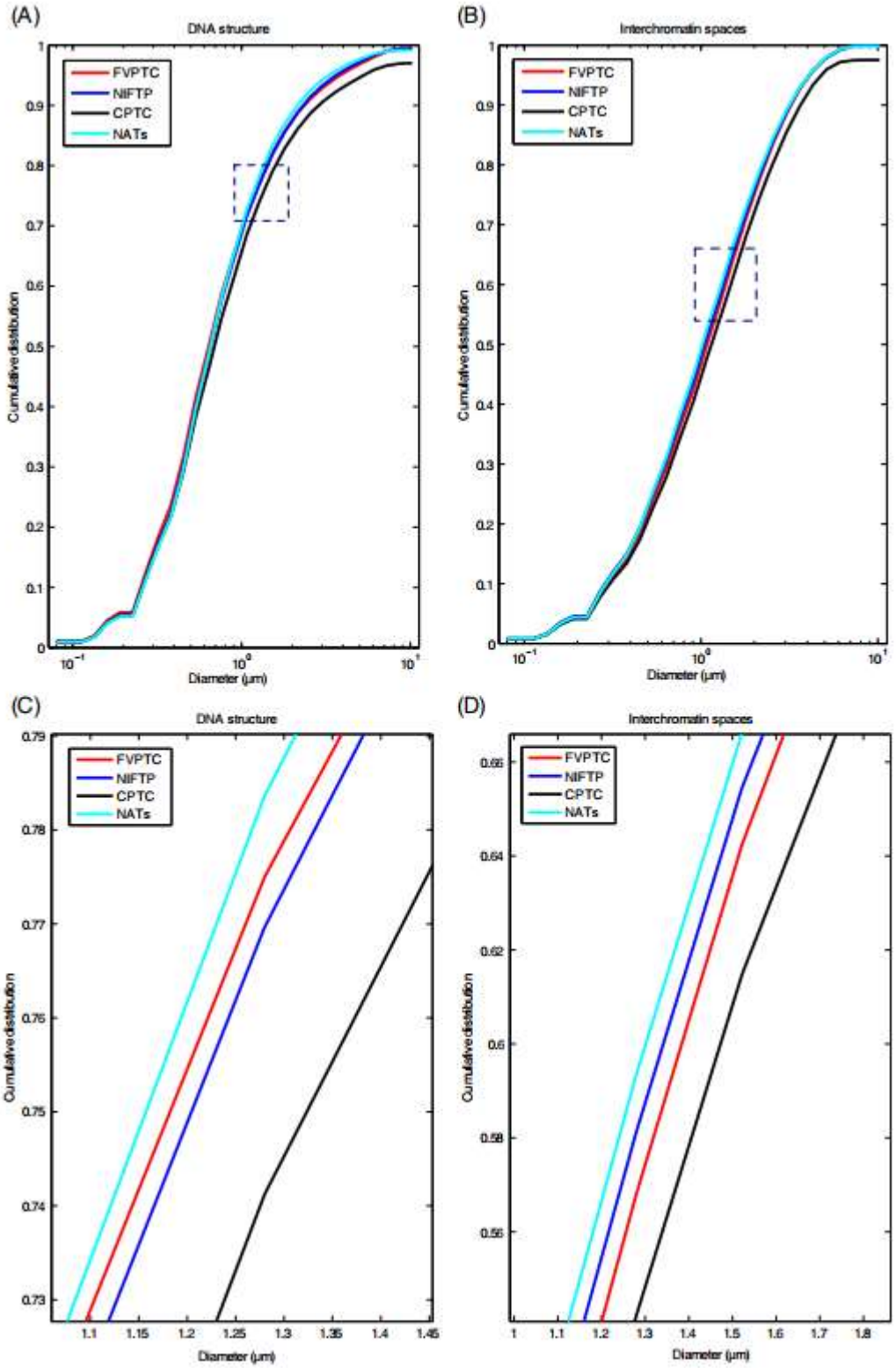
(A)
DNA structure
FVPTC
NIFTP
CPTC
NATs
Cumulative distribution
Diameter (µm)
(B)
Interchromatin spaces
FVPTC
NIFTP
CPTC
NATs
Cumulative distribution
Diameter (µm)
(C)
DNA structure
FVPTC
NIFTP
CPTC
NATs
Cumulative distribution
Diameter (µm)
(D)
Interchromatin spaces
FVPTC
NIFTP
CPTC
NATs
Cumulative distribution
Diameter (µm)

**Figure 4**: Three-dimensional (3D)-structured illumination microscopy (SIM) identify significant differences in DNA structure between normal adjacent tissue (NATs), noninvasive follicular thyroid neoplasm with papillary-like nuclear features (NIFTP), classic papillary thyroid carcinoma (CPTC), follicular variant of papillary thyroid carcinoma (FVPTC). (A) Cumulative distribution and diameter of DNA structure between PTC histotypes; (B) cumulative distribution and diameter of interchromatin spaces between PTC histotypes; (C,D) are enlarged versions from the boxes above.

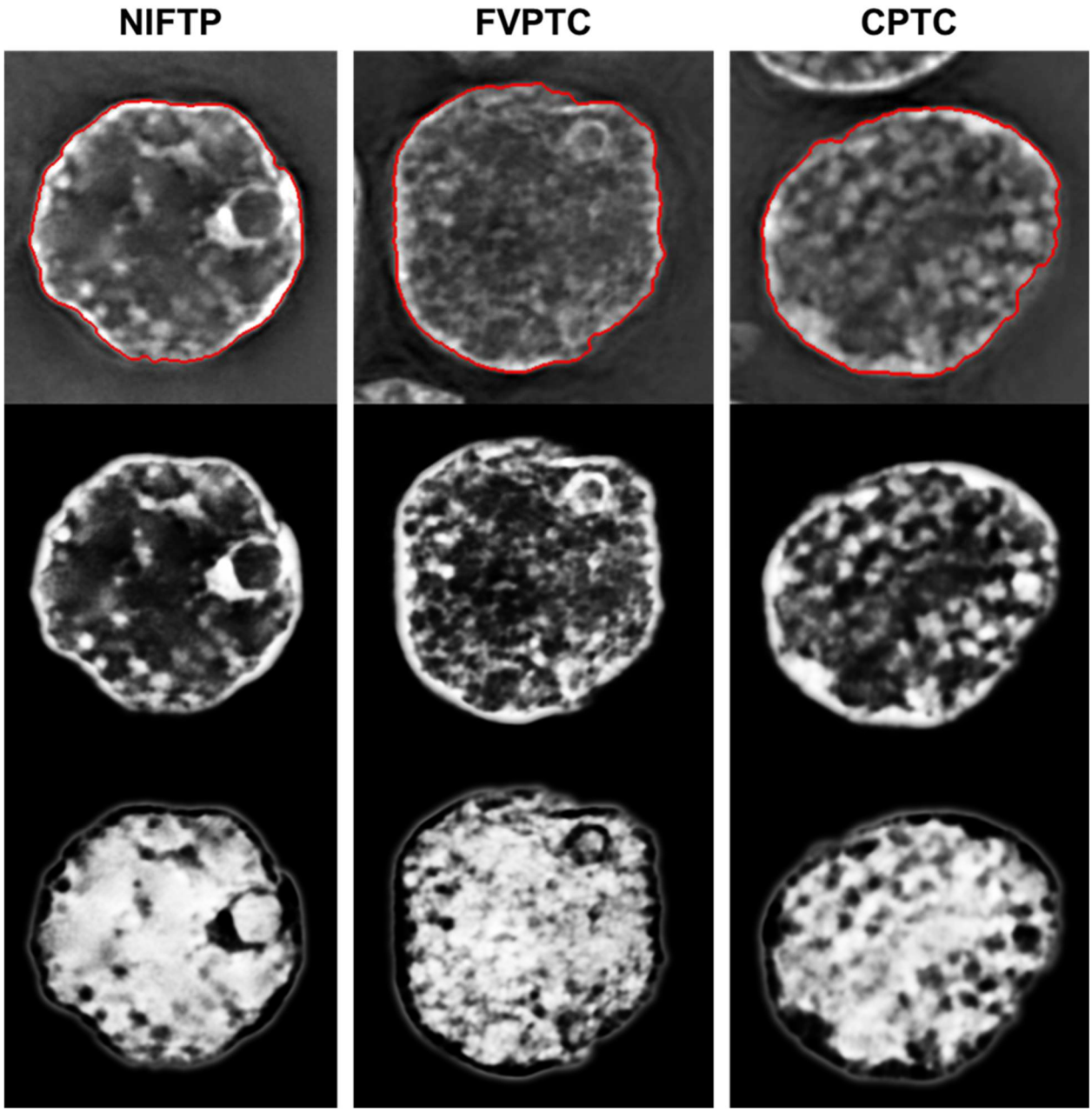


**Figure 4.1**: Representative Three-dimensional (3D)-SIM (Structured Illumination Microscopy) images of NIFTP, FVPTC and CPTC cells and their respective light and dark granulometry images. Top images: reconstructed 3D SIM images, middle images: DNA structure; bottom images: Interchromatin spaces. NIFTP: Non-invasive follicular thyroid neoplasm with papillary-like nuclear features; FVPTC: Follicular variant papillary thyroid carcinoma; CPTC: Classical-papillary thyroid carcinoma.

**Table 3:** Statistical analysis and *p*-values for the comparisons in Figure 4 A, B.

| Group 1 | Group 2 | P-value |
|---|---|---|
| *2-2-KS-test for light granulometries (DNA structure)* | | |
| NATs | FVPTC | <.0001 |
| NATs | NIFTP | .000260638 |
| NATs | CPTC | <.0001 |
| FVPTC | NIFTP | <.0001 |
| FVPTC | CPTC | <.0001 |
| NIFTP | CPTC | <.0001 |
| *2-2-KS-test for dark granulometries (Interchromatin spaces)* | | |
| NATs | FVPTC | <.0001 |
| NATs | NIFTP | .503796688 |
| NATs | CPTC | <.0001 |
| FVPTC | NIFTP | .000315958 |
| FVPTC | CPTC | <.0001 |
| NIFTP | CPTC | <.0001 |

Next, due to the unconfirm low-risk nature of NIFTP and observed heterogeneous patterns of this histotype described by Macerola et al., we used 3D-SIM to compare the measurements of individual NIFTP tissues within the group (Figure 5.1). As presented in Figure 5, the NATs measurements of DNA structure (light-blue line) clearly separate the NIFTP samples into two groups with more and less condensed chromatin (Figure 5A). The same is observed with the size of inter-chromatin spaces (Figure 5B). (MACEROLA; PROIETTI; BASOLO, 2020). In order to support the hypothesis that 3D chromatin architecture can be used to grade NIFTP lesions, we have used the grading information unifocal *vs* multifocal to demonstrate the potential of this parameter for thyroid lesions.

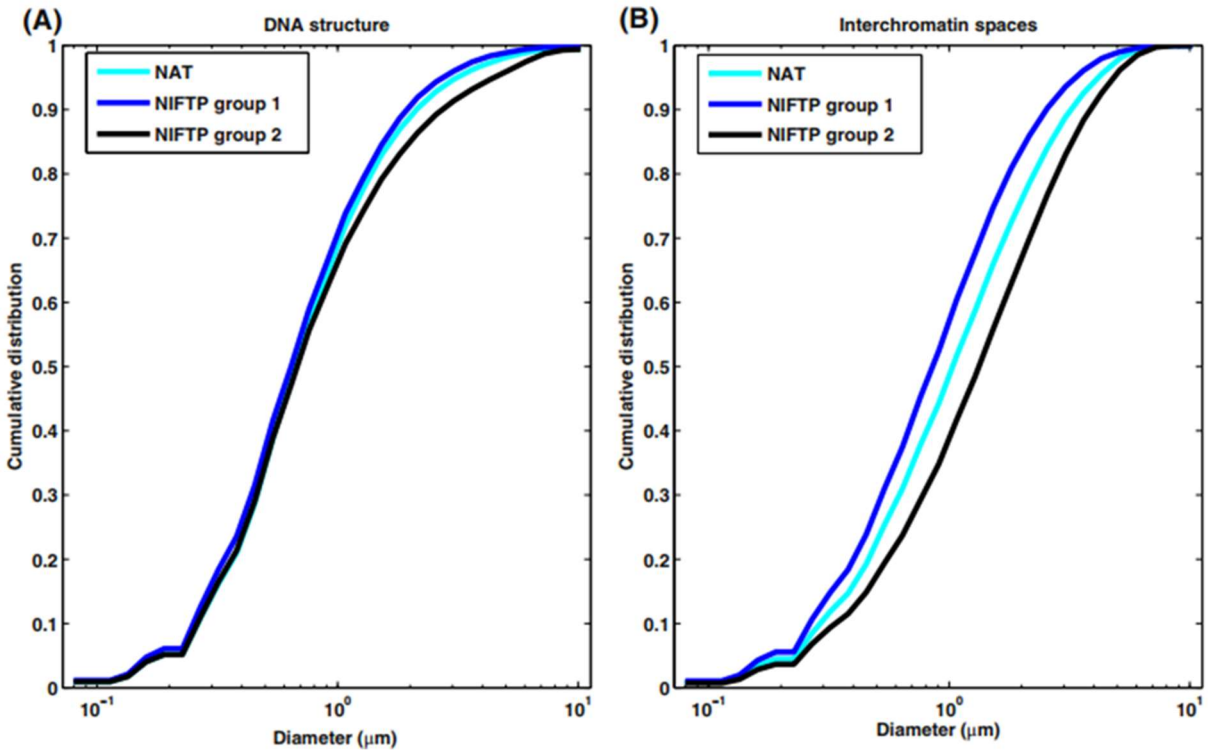


**Figure 5:** The 3D-SIM identifies two subgroups within noninvasive follicular thyroid neoplasm with papillary-like nuclear features (NIFTP) group. The two groups are compared to normal adjacent tissue (NATs). (A) Cumulative distribution and diameter of DNA structure. (B) Cumulative distribution and diameters of interchromatin spaces (Figure 4.2 and 4.3).

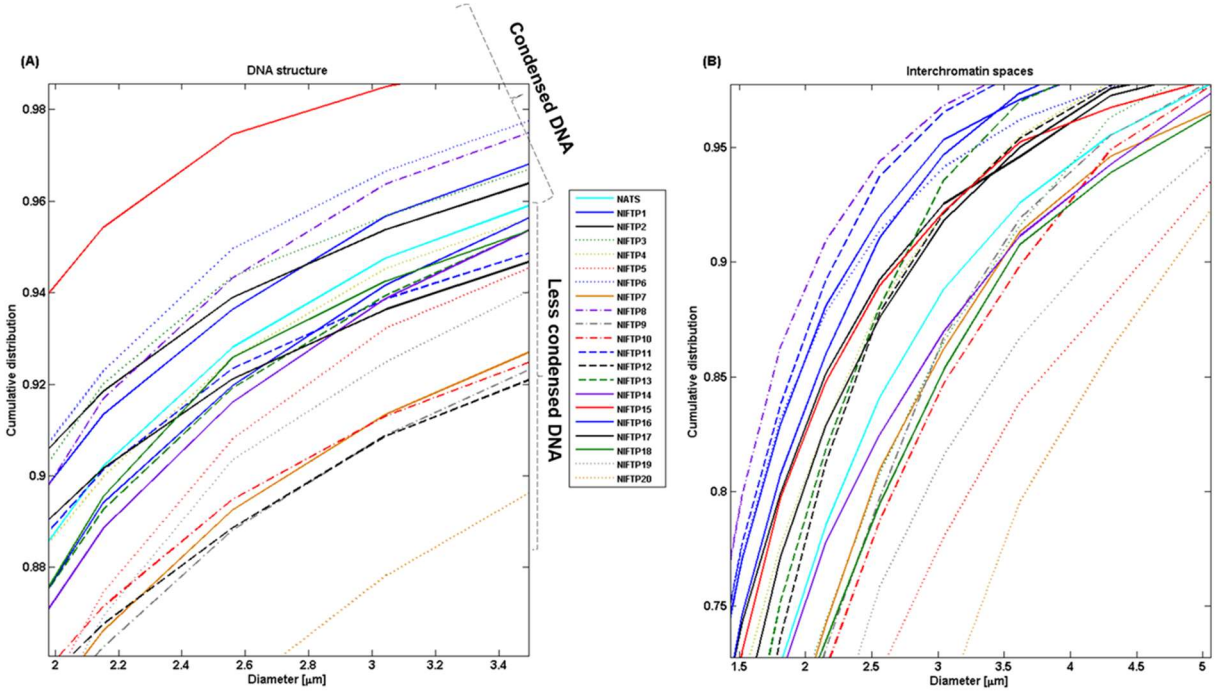


**Figure 5.1**: Three-dimensional (3D)-SIM (Structured Illumination Microscopy) identify heterogeneous patterns in DNA structure between Normal Adjacent Tissue (NATs) and individual tissue derived from Non-Invasive Follicular Thyroid neoplasm with Papillary-like nuclear features (NIFTP) patients. (A) Enlarged version of the cumulative distribution and diameter of DNA structure. (B) Enlarged version of the cumulative distribution and diameters of interchromatin spaces.

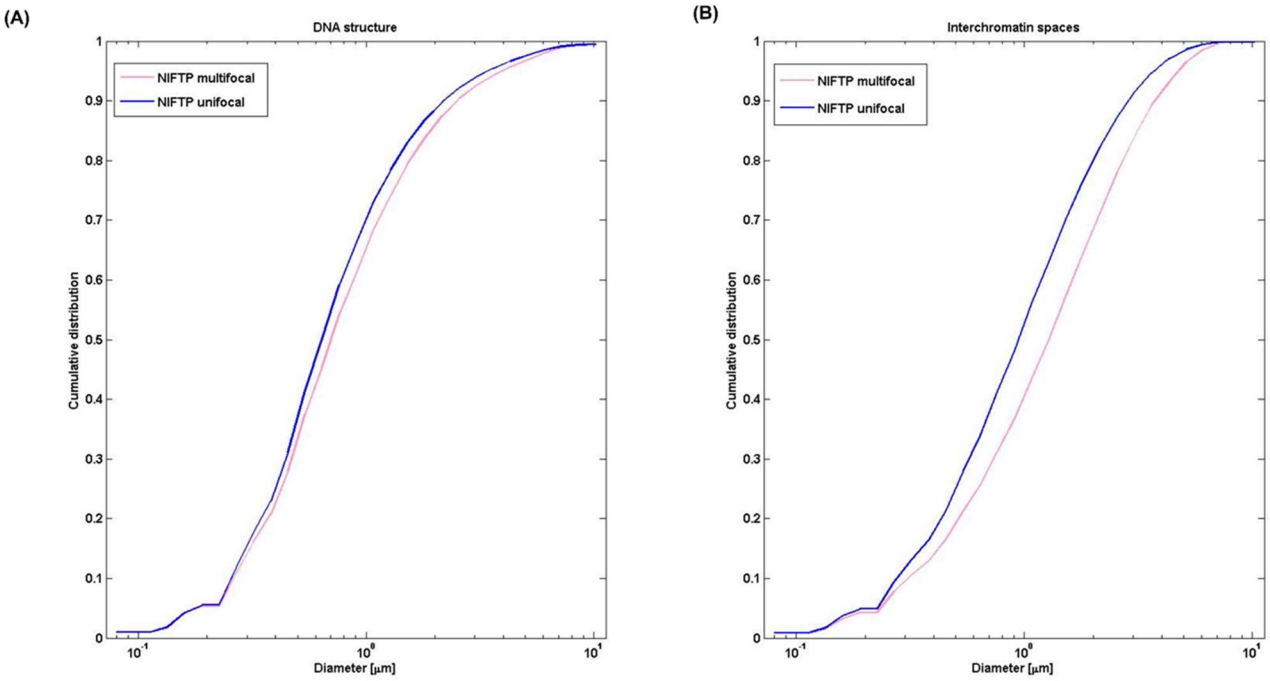


**Figure 5.2**: Comparison between NIFTP multifocal and unifocal groups in relation to DNA structure ($p$<0.001) and number and sizes of the interchromatin spaces (p<0.001) using three-dimensional (3D)-SIM (Structured Illumination Microscopy). NIFTP: Non-Invasive Follicular Thyroid neoplasm with Papillary-like nuclear features.

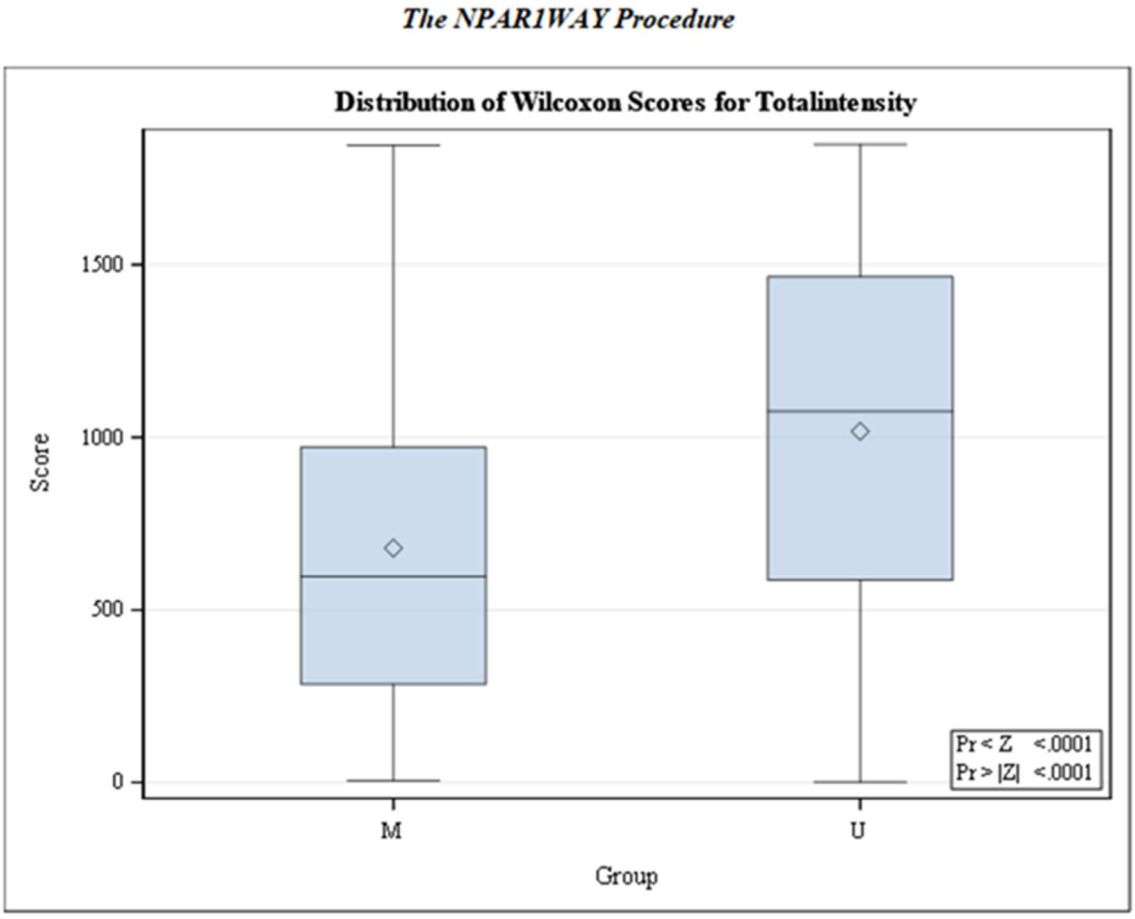


**Figure 5.3**: Differences in total intensity between NIFTP unifocal (U) and multifocal (M) groups. For total intensity, the position of each telomere is identified by using a threshold. Then, the center of gravity and the integrated intensity of each telomere is calculated as arbitrary units based on the number of sequences CCCTAA/probe intensity. The integrated intensity of each telomere is the appropriate parameter for determining the length of the telomere.

### 6.4. NIFTP, FVPTC and PTC have specific mutational profiles.

DNA extracted from tumor specimens and their respective normal adjacent tissues resulted in sufficient DNA amount and quality for downstream sequencing-analysis of 48 samples (CPTC = 17; FVPTC = 12; NIFTP = 19). Over 48 genes analyzed, we found alterations in 28 hotspot genes (Figure 6). The list of genes investigated, and targeted sequencing area is shown in Tables S1 to S3. Using matched adjacent normal tissue, we

distinguish between germline and somatic variations. SNVs or INDELs found in the NAT for each tumor were considered as germline and were excluded from the analysis. Figure 6 shows the results for all 48 patients analyzed, variation burden, altered genes and mutation type observed. Sixty percent (60%) (10 out of the 17 samples) of the CPTC samples harbored a $BRAF^{V600E}$ mutations. We observed *NRAS* mutations in one NIFTP case (1 out of 19, 5.2%). As expected, NIFTP was characterized by the lack of $BRAF^{V600E}$ mutation (Figure 6). In addition, tumor variation burden, which indicates the number of mutations seen in a section of DNA per mega base, was lower in NIFTP cases compared to CPTC and FVPTC.

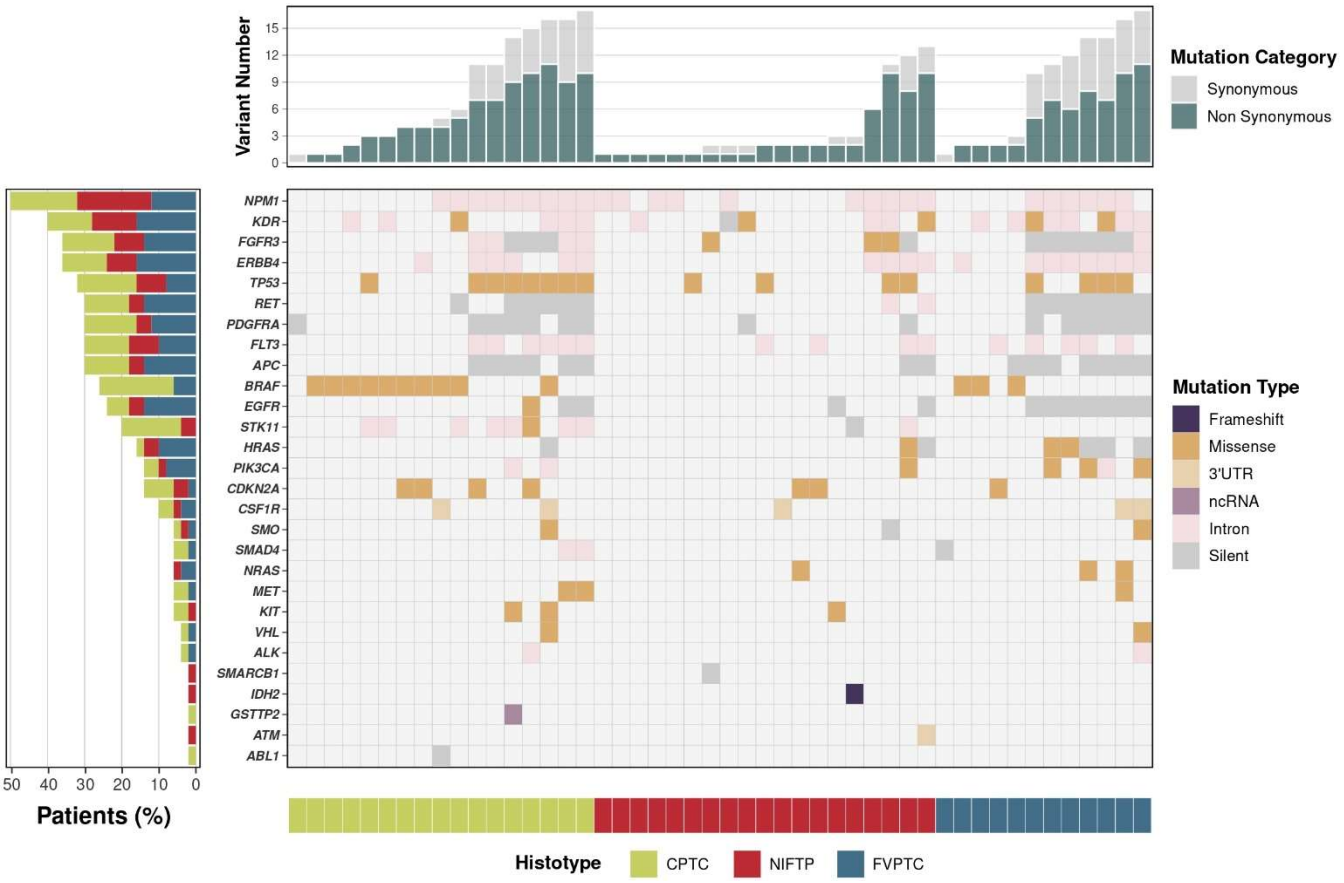


**Figure 6**: Summary of all somatic variants found in patients with thyroid cancer. CoMut Plot summarizing the main findings from the oncopanel regarding the mutational profile analysis. (Center panel) Plot showing all types of somatic mutations (shown with different colors) found for 28 protein-coding genes (sorted by number of alterations—see left graph) in our cohort of 48 samples (sorted by their respective histotypes—see bottom

graph—and, within each histotype, by variant number—see top graph). Unfilled boxes indicate the absence of alteration for a given set of gene/sample; (Bottom panel) bar indicating with different colors the histotype of the samples; (Top panel) Bar plot showing the total (synonymous and nonsynonymous) number of somatic variations for all samples, also ordered by histotype and, within each histotype, by number of variations; (Left panel) Horizontal bar plot showing the percentage of patients (each color represents their corresponding histotypes) containing somatic alterations in the genes shown, ordered from the most mutated to the least mutated. The complete list of variants and specific changes for all patients are described in Table S4. 3'UTR, 3 prime untranslated region; CPTC, classical papillary thyroid carcinoma; FVPTC, follicular variant of papillary thyroid carcinoma; ncRNA, noncoding RNA; NIFTP, non-invasive follicular thyroid neoplasm with papillary-like nuclear features.

## 7. DISCUSSION

It has long been recognized and accepted that histopathology is the "gold standard" for treatment decisions and evaluation of outcomes for thyroid neoplasms. However, there is considerable diagnostic variability among pathologists when examining follicular-patterned thyroid nodules (LIU; LIN, 2015). This particularly evident in follicular lesions where both benign and malignant lesions have similar architectural features, which leads to increasing diagnostic complexity. This aspect is even more challenging in accurately differentiating the recently recognized "non-invasive follicular thyroid neoplasm with papillary-like nuclear features" (NIFTP) from CPTC and FVPTC and its classification as a benign lesion. Outcome studies in patients with NIFTP have reported lymph node metastases in some patients (ROSARIO; MOURÃO; CALSOLARI, 2019). Therefore, the classification of this entity as a truly benign lesion continues to be controversial. To address this problem, molecular markers are being used to help delineate benign from malignant thyroid lesions, differentiate the various follicular neoplasms and provide potential prognostic biomarkers for treatment decisions (RANGEL-POZZO et al., 2020b). The large-scale study of The Cancer Genome Atlas (TCGA) identified a 71-gene signature that divided PTCs into $BRAF^{V600E}$-like and RAS-like tumors (AGRAWAL et al., 2014).

Although molecular profile analyses of NIFTP are limited, being considered helpful but not required for the diagnosis, there is an indication that they typically enter the RAS-like group (BRANDLER et al., 2018). This molecular approach is useful in most, but not all cases of NIFTP. This has been well documented in outcome studies in which patients with NIFTP have reported lymph node metastases in some nodules, which apparently met the stringent NIFTP classification criteria (CHO et al., 2017).

To overcome these limitations and add knowledge to NIFTP biology we have explored the potential of a single-cell approach to refine the diagnosis of this entity. Single-cell techniques, including telomere pattern analysis, have been shown to be a powerful tool for deciphering the cellular and molecular landscapes in cancers and elucidating cancer lesions' biological characteristics and dynamics (VERMOLEN et al., 2005). Telomere dysfunction is considered the primary mechanism for cancer survival and aggressiveness (DONATI; CIARROCCHI, 2019). The progressive telomere shortening is a rate limiting step for uncontrolled cell proliferation (RANGEL-POZZO et al., 2020b). As with other groups, we have reported a significantly higher frequency of short telomeres in thyroid cancers compared to normal thyroid tissue (RANGEL-POZZO et al., 2021b). However, in the present study, the various histotypes did not show significant differences in the number of short telomeres and other telomere features, preventing the use of these variables to differentiate nodules. In contrast and remarkably, the number of long telomeres was significantly different among histotypes, with NIFTP having the highest frequency of long telomeres (>16.000 a.u.) followed by CPTC and FVPTC (Figure 3). This was an encouraging result, indicating that this single cell approach could be used as a biomarker to distinguish NIFTP from CPTC and FVPTC.

The development of new microscopes and cutting-edge imaging-based methods, including three-dimensional and super-resolution microscopy has a crucial role in understanding chromatin and nuclear architecture. It has been suggested that the nuclear localization of genes might be dynamically regulated relative to their expression (MELDI; BRICKNER, 2011) and that, while active nuclear compartment has lower DNA density and active gene transcription, the inactive nuclear compartment has a high DNA density (CREMER et al., 2015). Indeed, cancer cells can reprogram the chromatin status

to increase chromatin accessibility by transcription factors and DNA repair machinery during damage (YU; YANG; SHEN, 2016). In this context, our 3D-SIM data highlight statistically significant differences in the DNA structure and interchromatin spaces among the thyroid cancer histotypes. A striking progression of DNA de-condensation was detected across histotypes, with the consistent progression of DNA de-condensation from more densely packaged DNA in normal thyroid tissue followed by NIFTP, FVPTC and CPTC (with overall high de-condensation of DNA). A similar trend was observed for the size of interchromatin spaces, which increased starting from NAT/NIFTP followed by FVPTC and CPTC (with the largest interchromatin spaces) (Figure 4). It seems that thyroid cells develop ways to impair heterochromatin structure during malignant transformation, which could trigger important signaling cascades that lead to tumorigenesis. Indeed, the presence of an aberrant 3D genome (high overall DNA decondensation and increase of interchromatin spaces) in PTC and FVPTC tumors compared to normal tissue and NIFTP could lead to promoting tumor cell aggressiveness. The clearcut 3D-SIM distinction between the thyroid subtypes, coupled with the above-mentioned observation that NIFTP has the highest frequency of long telomeres, may be used as a differentiating characteristic of NIFTP. To support the hypothesis that 3D chromatin architecture could be used to grade NIFTP lesions, we have used the grading information (unifocal *vs* multifocal) to show insights the potential of this parameter for thyroid lesions (Figures 5.2 and 5.3). However, due to the sample size, the prognostic significance and the biological importance of these findings deserve further studies.

The existing molecular panel for thyroid nodules is inconclusive, where the same markers are also prevalent in benign thyroid nodules. Up to 48% of benign thyroid lesions have *RAS* mutations, up to 68% have *RET/PTC* rearrangements and up to 55% of benign thyroid lesions have *PAX/PPARγ* rearrangements (RANGEL-POZZO et al., 2020b). Although, the prevalence of these markers is significantly higher in malignant lesions, relying upon their presence for differential diagnosis and clinical decision making for an indeterminate thyroid lesion might result in misclassification or overtreatment of potentially benign lesions. In our cohort, FISH analysis showed *RET/PTC* rearrangements in a few patients (3.3%) and *PPARγ* rearrangements in none of the patients. The

prevalence of RET rearrangements in sporadic PTC is highly heterogeneous (ranging from 2.5% to 73%), due to ethnicity, different geographical location, environmental exposure and the method used for their identification and genetic heterogeneity (LI et al., 2019). *PPARγ* rearrangements, which may be detected in typical follicular thyroid carcinoma (FTC), FVPTC, NIFTP and only in 0% to 1% of PTC were missing in our cohort (Figure 2), possibly due to the small number of cases.

The further molecular characterization of the samples through a custom-designed onco-panel showed a consistent presence of $BRAF^{V600E}$ in PTC and FVPTC, and its absence in NIFTP. The lack of $BRAF^{V600E}$ is a relevant secondary diagnostic criteria of NIFTP (NIKIFOROV et al., 2018). However, as shown in Figure 6, *TP53* variations were found in four NIFTP. The most frequent was *TP53* rs1042522 (Arg72Pro). This finding prompted us to conduct a pathological review of nodules carrying *TP53* variants since the presence of *TP53* mutations is a secondary exclusion criterion of the NIFTP classification (NIKIFOROV et al., 2018). The revision still met the revised NIFTP primary histological criteria, including encapsulation or clear demarcation from adjacent thyroid parenchyma, follicular growth pattern without well-formed papillae, absence of psammoma bodies and solid growth pattern <30% trabecular/insular. The confirmed diagnosis is in line with ongoing evidence that *TP53* coding region variants are far more prevalent than previously suspected. Hence, attention must be paid to “finding the needles in a haystack of pathogenic variants.” (SOUSSI, 2022). Evidence has been accumulated indicating that *TP53* variants may have implications other than in tumor suppression function. The arg allele of rs1042522 is slightly more active in inducing apoptosis49 and it has been associated with winter temperature. Indeed, this variant is considered benign in the ClinVar archive according to the American College of Medical Genetics and Genomics (ACMG) criteria, and recently the effect of *TP53*-rs1042522 variants on decreased risk of PTC, smaller tumor size and lower incidence of vascular invasion was described. Nevertheless, we observed that NIFTP nodules with these variants had significant differences in chromatin condensation ($p$ = .0002). Further study of cases with the same variant will clarify if this association may characterize a subtype of NIFTPs.

An important finding from the onco-panel is a low variation burden, defined as the number of somatic variations per mega base, found in NIFTP samples. However, due to differences in panel size, mutation types and bioinformatic platforms analysis, tumor burden analysis used as a predictive biomarker is not clear and requires further study.

Altogether our results indicate that, compared to the molecular approach, the single-cell approach achieved by the 3D-SIM examination has a much greater potential in identifying NIFTP-specific features (Figures 5 and 5.1). The NIFTP groups presented in Figure 4 do not show significant differences in telomere structure and/or number of SNVs. However, the prognostic significance of these features and their biological behavior clearly deserve additional further study.

In summary, this is the first study investigating the 3D structural organization of the genome to differentiate papillary and follicular thyroid cancer subtypes. Our data indicate that NIFTP has a specific 3D genome organization similar to normal thyroid tissue and that it is clearly different from that of classical and follicular variant PTC. These results, while reinforcing the idea that NIFTP is a lesion with a low risk of disease progression, underscore the existence of heterogeneity within the group (Figure 5). We will continue to explore this in a long-term follow-up study, confident that this innovative approach could also be applied to fine needle aspirates in the initial diagnosis of thyroid malignancy.

## 8. CONCLUSIONS

NIFTP requires additional precise and innovative markers in clinical practice. The differentiation of NIFTP from CPTC and FVPTC by onco-panel sequencing in our limited cohort did not yield useful molecular information that might be applied clinically. The 3D structural architecture of the genome revealed by super resolution imaging of nuclear DNA organization and 3D imaging of telomeres allowed for the robust and reliable differentiation of NIFTP from CPTC and FVPTC and distinguished all the histotypes from normal adjacent thyroid tissues. We conclude that the structural organization of the genome provides additional key data for each thyroid cancer subtype to enable its distinction from other morphologically similar thyroid cancer histotypes.

## 9. REFERENCES


AGRAWAL, N. et al. Integrated Genomic Characterization of Papillary Thyroid Carcinoma. Cell, v. 159, n. 3, p. 676–690, out. 2014.

AJAEZI, G. C. et al. Near-field infrared nanospectroscopy and super-resolution fluorescence microscopy enable complementary nanoscale analyses of lymphocyte nuclei. The Analyst, v. 143, n. 24, p. 5926–5934, 2018.

ALVES, V. A. F. et al. Noninvasive Follicular Thyroid Neoplasm With Papillary-Like Nuclear Features (NIFTP): Achieving Better Agreement By Refining Diagnostic Criteria. Clinics, v. 73, p. e576, 2018.

BABU, D.; FULLWOOD, M. J. 3D genome organization in health and disease: emerging opportunities in cancer translational medicine. Nucleus, v. 6, n. 5, p. 382–393, 3 set. 2015.

BAILEY, M. H. et al. Comprehensive Characterization of Cancer Driver Genes and Mutations. Cell, v. 173, n. 2, p. 371- 385.e18, 5 abr. 2018.

BAYANI, J. et al. Genomic mechanisms and measurement of structural and numerical instability in cancer cells. Seminars in Cancer Biology, v. 17, n. 1, p. 5–18, fev. 2007.

BOLGER, A. M.; LOHSE, M.; USADEL, B. Trimmomatic: a flexible trimmer for Illumina sequence data. Bioinformatics, v. 30, n. 15, p. 2114–2120, 1 ago. 2014.

BRANDLER, T. C. et al. Does Noninvasive Follicular Thyroid Neoplasm With Papillary-Like Nuclear Features (NIFTP) Have a Unique Molecular Profile? American Journal of Clinical Pathology, v. 150, n. 5, p. 451–460, 1 out. 2018.

CARIA, P. et al. Optimizing detection of RET and PPARg rearrangements in thyroid neoplastic cells using a home-brew tetracolor probe. Cancer Cytopathology, v. 122, n. 5, p. 377–385, maio 2014.

CARIA, P. et al. Characterizing the three-dimensional organization of telomeres in papillary thyroid carcinoma cells. Journal of Cellular Physiology, v. 234, n. 4, p. 5175–5185, abr. 2019.

CHENG, K. C.; LOEB, L. A. Genomic instability and tumor progression: mechanistic considerations. Advances in Cancer Research, v. 60, p. 121–156, 1993.

CHIBA, K. et al. Mutations in the promoter of the telomerase gene *TERT* contribute to tumorigenesis by a two-step mechanism. Science, v. 357, n. 6358, p. 1416–1420, 29 set. 2017.

CHO, U. et al. Molecular correlates and rate of lymph node metastasis of non-invasive follicular thyroid neoplasm with papillary-like nuclear features and invasive follicular variant papillary thyroid carcinoma: the impact of rigid criteria to distinguish non-invasive follicular thyroid neoplasm with papillary-like nuclear features. Modern Pathology, v. 30, n. 6, p. 810–825, jun. 2017.

CHU, Y.-H.; SADOW, P. M. Noninvasive follicular thyroid neoplasm with papillary-like nuclear features (NIFTP): Diagnostic updates and molecular advances. Seminars in Diagnostic Pathology, v. 37, n. 5, p. 213–218, set. 2020.

CLEAL, K.; NORRIS, K.; BAIRD, D. Telomere Length Dynamics and the Evolution of Cancer Genome Architecture. International Journal of Molecular Sciences, v. 19, n. 2, p. 482, 6 fev. 2018.

CORDIOLI, M. I. C. V. et al. Thyroid-Specific Genes Expression Uncovered Age-Related Differences in Pediatric Thyroid Carcinomas. International Journal of Endocrinology, v. 2016, p. 1956740, 2016.

CREMER, T. et al. The 4D nucleome: Evidence for a dynamic nuclear landscape based on co-aligned active and inactive nuclear compartments. FEBS Letters, v. 589, n. 20PartA, p. 2931–2943, 7 out. 2015.

D'ADDA DI FAGAGNA, F. Living on a break: cellular senescence as a DNA-damage response. Nature Reviews Cancer, v. 8, n. 7, p. 512–522, jul. 2008.

DANECEK, P. et al. Twelve years of SAMtools and BCFtools. GigaScience, v. 10, n. 2, p. giab008, 29 jan. 2021.

DAVIES, L.; WELCH, H. G. Increasing incidence of thyroid cancer in the United States, 1973-2002. JAMA, v. 295, n. 18, p. 2164–2167, 10 maio 2006.

DE LANGE, T. Shelterin: the protein complex that shapes and safeguards human telomeres. Genes & Development, v. 19, n. 18, p. 2100–2110, 15 set. 2005.

DE LANGE, T. How Telomeres Solve the End-Protection Problem. Science, v. 326, n. 5955, p. 948–952, 13 nov. 2009.

DONATI, B.; CIARROCCHI, A. Telomerase and Telomeres Biology in Thyroid Cancer. International Journal of Molecular Sciences, v. 20, n. 12, p. 2887, 13 jun. 2019.

DRACHENBERG, D. et al. Advancing Risk Assessment of Intermediate Risk Prostate Cancer Patients. Cancers, v. 11, n. 6, p. 855, 20 jun. 2019.

DUESBERG, P. et al. Genetic instability of cancer cells is proportional to their degree of aneuploidy. Proceedings of the National Academy of Sciences of the United States of America, v. 95, n. 23, p. 13692–13697, 10 nov. 1998.

FERLAY, J. et al. Estimating the global cancer incidence and mortality in 2018: GLOBOCAN sources and methods. International Journal of Cancer, v. 144, n. 8, p. 1941–1953, 15 abr. 2019.

FRED L, DRAKE GVR. Python 3 Reference Manual. CreateSpace. Scotts Valley, CA: Independent Publishing Platform;, 2009.

GADJI, M. et al. Three-dimensional Nuclear Telomere Architecture Is Associated with Differential Time to Progression and Overall Survival in Glioblastoma Patients. Neoplasia, v. 12, n. 2, p. 183–191, fev. 2010.

GADJI, M. et al. Profiling Three-Dimensional Nuclear Telomeric Architecture of Myelodysplastic Syndromes and Acute Myeloid Leukemia Defines Patient Subgroups. Clinical Cancer Research, v. 18, n. 12, p. 3293–3304, 15 jun. 2012.

GADJI, M.; POZZO, A. R. From cellular morphology to molecular and epigenetic anomalies of myelodysplastic syndromes. Genes, Chromosomes and Cancer, v. 58, n. 7, p. 474–483, jul. 2019.

GERLINGER, M.; SWANTON, C. How Darwinian models inform therapeutic failure initiated by clonal heterogeneity in cancer medicine. British Journal of Cancer, v. 103, n. 8, p. 1139–1143, 12 out. 2010.

GORGOULIS, V. G. et al. Activation of the DNA damage checkpoint and genomic instability in human precancerous lesions. Nature, v. 434, n. 7035, p. 907–913, abr. 2005.

GREENMAN, C. et al. Patterns of somatic mutation in human cancer genomes. Nature, v. 446, n. 7132, p. 153–158, 8 mar. 2007.

GUSTAFSSON, M. G. L. Surpassing the lateral resolution limit by a factor of two using structured illumination microscopy: SHORT COMMUNICATION. Journal of Microscopy, v. 198, n. 2, p. 82–87, maio 2000.

GUSTAFSSON, M. G. L. et al. Three-Dimensional Resolution Doubling in Wide-Field Fluorescence Microscopy by Structured Illumination. Biophysical Journal, v. 94, n. 12, p. 4957–4970, jun. 2008.

HARPER, J. W.; ELLEDGE, S. J. The DNA damage response: ten years after. Molecular Cell, v. 28, n. 5, p. 739–745, 14 dez. 2007.

HSIEH, P.; YAMANE, K. DNA mismatch repair: molecular mechanism, cancer, and ageing. Mechanisms of Ageing and Development, v. 129, n. 7–8, p. 391–407, 2008.

JACKSON, S. P.; BARTEK, J. The DNA-damage response in human biology and disease. Nature, v. 461, n. 7267, p. 1071–1078, 22 out. 2009.

KEINAN-BOKER, L.; SILVERMAN, B. G. Trends of Thyroid Cancer in Israel: 1980-2012. Rambam Maimonides Medical Journal, v. 7, n. 1, p. e0001, 28 jan. 2016.

KNECHT, H. et al. Three-dimensional Telomere Signatures of Hodgkin- and Reed-Sternberg Cells at Diagnosis Identify Patients with Poor Response to Conventional Chemotherapy. Translational Oncology, v. 5, n. 4, p. 269–277, ago. 2012.

KOPS, G. J. P. L.; FOLTZ, D. R.; CLEVELAND, D. W. Lethality to human cancer cells through massive chromosome loss by inhibition of the mitotic checkpoint. Proceedings of the National Academy of Sciences of the United States of America, v. 101, n. 23, p. 8699–8704, 8 jun. 2004.

KOPS, G. J. P. L.; WEAVER, B. A. A.; CLEVELAND, D. W. On the road to cancer: aneuploidy and the mitotic checkpoint. Nature Reviews. Cancer, v. 5, n. 10, p. 773–785, out. 2005.

KUZYK, A.; GARTNER, J.; MAI, S. Identification of Neuroblastoma Subgroups Based on Three-Dimensional Telomere Organization. Translational Oncology, v. 9, n. 4, p. 348–356, ago. 2016.

LAUBICHLER, M. D.; DAVIDSON, E. H. Boveri's long experiment: sea urchin merogones and the establishment of the role of nuclear chromosomes in development. Developmental Biology, v. 314, n. 1, p. 1–11, 1 fev. 2008.

LEE, A. J. X. et al. Chromosomal instability confers intrinsic multidrug resistance. Cancer Research, v. 71, n. 5, p. 1858–1870, 1 mar. 2011.

LENGAUER, C.; KINZLER, K. W.; VOGELSTEIN, B. Genetic instabilities in human cancers. Nature, v. 396, n. 6712, p. 643–649, 17 dez. 1998.

LEPAGE, C. C. et al. Detecting Chromosome Instability in Cancer: Approaches to Resolve Cell-to-Cell Heterogeneity. Cancers, v. 11, n. 2, p. 226, 15 fev. 2019.

LI, A. Y. et al. RET fusions in solid tumors. Cancer Treatment Reviews, v. 81, p. 101911, dez. 2019.

LISE, M. et al. Changes in the incidence of thyroid cancer between 1991 and 2005 in Italy: a geographical analysis. Thyroid: Official Journal of the American Thyroid Association, v. 22, n. 1, p. 27–34, jan. 2012.

LIU, H.; LIN, F. Application of Immunohistochemistry in Thyroid Pathology. Archives of Pathology & Laboratory Medicine, v. 139, n. 1, p. 67–82, 1 jan. 2015.

MACEROLA, E.; PROIETTI, A.; BASOLO, F. Noninvasive follicular neoplasm with papillary-like nuclear features (NIFTP): a new entity. Gland Surgery, v. 9, n. S1, p. S47–S53, jan. 2020.

MACIEJOWSKI, J.; DE LANGE, T. Telomeres in cancer: tumour suppression and genome instability. Nature Reviews Molecular Cell Biology, v. 18, n. 3, p. 175–186, mar. 2017.

MAI, S.; GARINI, Y. The significance of telomeric aggregates in the interphase nuclei of tumor cells. Journal of Cellular Biochemistry, v. 97, n. 5, p. 904–915, abr. 2006.

MELDI, L.; BRICKNER, J. H. Compartmentalization of the nucleus. Trends in Cell Biology, v. 21, n. 12, p. 701–708, dez. 2011.

MICHEL, L. et al. Complete loss of the tumor suppressor MAD2 causes premature cyclin B degradation and mitotic failure in human somatic cells. Proceedings of the National Academy of Sciences of the United States of America, v. 101, n. 13, p. 4459–4464, 30 mar. 2004.

NIKIFOROV, Y. E. et al. Nomenclature Revision for Encapsulated Follicular Variant of Papillary Thyroid Carcinoma: A Paradigm Shift to Reduce Overtreatment of Indolent Tumors. JAMA oncology, v. 2, n. 8, p. 1023–1029, 1 ago. 2016.

NIKIFOROV, Y. E. et al. Change in Diagnostic Criteria for Noninvasive Follicular Thyroid Neoplasm With Papillarylike Nuclear Features. JAMA oncology, v. 4, n. 8, p. 1125–1126, 1 ago. 2018.

OSAMURA RY, KLÖPPEL G, ROSAI JLR. WHO Classification of Tumours of Endocrine Organs. 4th ed. ed. Lyon, France: IARC, 2017.

PUTIRI, E. L.; ROBERTSON, K. D. Epigenetic mechanisms and genome stability. Clinical Epigenetics, v. 2, n. 2, p. 299–314, 1 ago. 2011.

RAHIB, L. et al. Projecting cancer incidence and deaths to 2030: the unexpected burden of thyroid, liver, and pancreas cancers in the United States. Cancer Research, v. 74, n. 11, p. 2913–2921, 1 jun. 2014.

RANGEL-POZZO, A. et al. MYCN overexpression is linked to significant differences in nuclear DNA organization in neuroblastoma. SPG BioMed, 2019.

RANGEL-POZZO, A. et al. p53 CRISPR Deletion Affects DNA Structure and Nuclear Architecture. Journal of Clinical Medicine, v. 9, n. 2, p. 598, 22 fev. 2020a.

RANGEL-POZZO, A. et al. Genetic Landscape of Papillary Thyroid Carcinoma and Nuclear Architecture: An Overview Comparing Pediatric and Adult Populations. Cancers, v. 12, n. 11, p. 3146, 27 out. 2020b.

RANGEL-POZZO, A. et al. Telomere Architecture Correlates with Aggressiveness in Multiple Myeloma. Cancers, v. 13, n. 8, p. 1969, 19 abr. 2021a.

RANGEL-POZZO, A. et al. Three-dimensional telomere profiles in papillary thyroid cancer variants: a pilot study. Bosnian Journal of Basic Medical Sciences, 8 dez. 2021b.

RIGHOLT, C. H. et al. Differences in Nuclear DNA Organization Between Lymphocytes, Hodgkin and Reed–Sternberg Cells Revealed by Structured Illumination Microscopy. Journal of Cellular Biochemistry, v. 115, n. 8, p. 1441–1448, ago. 2014.

ROSARIO, P. W.; MOURÃO, G.; CALSOLARI, M. R. Risk of recurrence in patients with papillary thyroid carcinoma and minimal extrathyroidal extension not treated with

radioiodine. Journal of Endocrinological Investigation, v. 42, n. 6, p. 687–692, jun. 2019.

ROUSE, J.; JACKSON, S. P. Interfaces Between the Detection, Signaling, and Repair of DNA Damage. Science, v. 297, n. 5581, p. 547–551, 26 jul. 2002.

SATHITRUANGSAK, C. et al. Quantitative Superresolution Microscopy Reveals Differences in Nuclear DNA Organization of Multiple Myeloma and Monoclonal Gammopathy of Undetermined Significance. Journal of Cellular Biochemistry, v. 116, n. 5, p. 704–710, maio 2015.

SCHAEFER, L. H.; SCHUSTER, D.; HERZ, H. Generalized approach for accelerated maximum likelihood based image restoration applied to three-dimensional fluorescence microscopy. Journal of Microscopy, v. 204, n. 2, p. 99–107, nov. 2001.

SCHMÄLTER, A.-K. et al. Changes in Nuclear Orientation Patterns of Chromosome 11 during Mouse Plasmacytoma Development. Translational Oncology, v. 8, n. 5, p. 417–423, out. 2015.

SEETHALA, R. R. et al. Noninvasive follicular thyroid neoplasm with papillary-like nuclear features: a review for pathologists. Modern Pathology, v. 31, n. 1, p. 39–55, jan. 2018.

SISDELLI, L. et al. A Multifocal Pediatric Papillary Thyroid Carcinoma (PTC) Harboring the AGK-BRAF and RET/PTC3 Fusion in a Mutually Exclusive Pattern Reveals Distinct Levels of Genomic Instability and Nuclear Organization. Biology, v. 10, n. 2, p. 125, 5 fev. 2021.

SOBINOFF, A. P.; PICKETT, H. A. Alternative Lengthening of Telomeres: DNA Repair Pathways Converge. Trends in Genetics, v. 33, n. 12, p. 921–932, dez. 2017.

SOUSSI, T. Benign SNPs in the Coding Region of *TP53* : Finding the Needles in a Haystack of Pathogenic Variants. Cancer Research, v. 82, n. 19, p. 3420–3431, 4 out. 2022.

TAYLOR, A. M. et al. Genomic and Functional Approaches to Understanding Cancer Aneuploidy. Cancer Cell, v. 33, n. 4, p. 676- 689.e3, 9 abr. 2018.

TUTTLE, R. M. et al. Thyroid Carcinoma. Journal of the National Comprehensive Cancer Network, v. 8, n. 11, p. 1228–1274, nov. 2010.

VAN DER AUWERA BD, O'CONNOR GA. Genomics in the Cloud. Sebastopol, CA: O'Reilly Media, Inc., 2020.

VERMOLEN, B. J. et al. Characterizing the three-dimensional organization of telomeres. Cytometry Part A, v. 67A, n. 2, p. 144–150, out. 2005.

WANG, K.; LI, M.; HAKONARSON, H. ANNOVAR: functional annotation of genetic variants from high-throughput sequencing data. Nucleic Acids Research, v. 38, n. 16, p. e164–e164, 1 set. 2010.

WEAVER, B. A. A.; CLEVELAND, D. W. The role of aneuploidy in promoting and suppressing tumors. The Journal of Cell Biology, v. 185, n. 6, p. 935–937, 15 jun. 2009.

WEGEL, E. et al. Imaging cellular structures in super-resolution with SIM, STED and Localisation Microscopy: A practical comparison. Scientific Reports, v. 6, n. 1, p. 27290, 6 jun. 2016.

YAO, Y.; DAI, W. Genomic Instability and Cancer. Journal of Carcinogenesis & Mutagenesis, v. 5, p. 1000165, 2014.

YU et al. Distinct Nuclear Organization of Telomeresand Centromeres in Monoclonal Gammopathyof Undetermined Significance and Multiple Myeloma. Cells, v. 8, n. 7, p. 723, 15 jul. 2019.

YU, S.; YANG, F.; SHEN, W. H. Genome maintenance in the context of 4D chromatin condensation. Cellular and Molecular Life Sciences, v. 73, n. 16, p. 3137–3150, ago. 2016.

ZAJKOWSKA, K. et al. Noninvasive follicular thyroid neoplasm with papillary-like nuclear features: a problematic entity. Endocrine Connections, v. 9, n. 3, p. R47–R58, mar. 2020.

ZHANG, C. et al. Long-Term In Vitro Expansion of Epithelial Stem Cells Enabled by Pharmacological Inhibition of PAK1-ROCK-Myosin II and TGF-β Signaling. Cell Reports, v. 25, n. 3, p. 598- 610.e5, 16 out. 2018.

ZHU, Z. et al. Molecular Profile and Clinical-Pathologic Features of the Follicular Variant of Papillary Thyroid Carcinoma: An Unusually High Prevalence of *ras* Mutations. American Journal of Clinical Pathology, v. 120, n. 1, p. 71–77, jul. 2003.

## 10. PUBLICATION



Received: 29 December 2022 | Revised: 30 June 2023 | Accepted: 4 July 2023

DOI: 10.1002/ijc.34667

IJC INTERNATIONAL JOURNAL of CANCER

RESEARCH ARTICLE

Tumor Markers and Signatures

# Three-dimensional nuclear architecture distinguishes thyroid cancer histotypes

Aline Rangel-Pozzo[1] | Filipe F. dos Santos[2,3] | Tinuccia Dettori[4] | Matteo Giulietti[5] | Daniela Virginia Frau[4] | Pedro A. F. Galante[2] | Roberta Vanni[6] | Alok Pathak[7] | Gabor Fischer[8] | John Gartner[8] | Paola Caria[4] | Sabine Mai[1]

[1]CancerCare Manitoba Research Institute, CancerCare Manitoba, University of Manitoba, Winnipeg, Canada

[2]Centro de Oncologia Molecular, Hospital Sirio-Libanes, Sao Paulo, Brazil

[3]Department of Biochemistry, Chemistry Institute, Universidade de Sao Paulo, Sao Paulo, Brazil

[4]Department of Biomedical Sciences, University of Cagliari, Monserrato, Italy

[5]Department of Specialistic Clinical and Odontostomatological Sciences, Polytechnic University of Marche, Ancona, Italy

[6]University of Cagliari, Department of Biomedical Sciences, University of Cagliari, Monserrato, Italy

[7]Department of Surgery, University of Manitoba, Winnipeg, Canada

[8]Department of Pathology, Max Rady College of Medicine, Rady Faculty of Health Sciences, University of Manitoba, Winnipeg, Canada

**Correspondence**
Paola Caria, Department of Biomedical Sciences, University of Cagliari, Monserrato, Italy.
Email: paola.caria@unica.it

Sabine Mai, CancerCare Manitoba Research Institute, CancerCare Manitoba, University of Manitoba, Winnipeg, Canada.
Email: sabine.mai@umanitoba.ca

**Abstract**

Molecular markers can serve as diagnostic tools to support pathological analysis in thyroid neoplasms. However, because the same markers can be observed in some benign thyroid lesions, additional approaches are necessary to differentiate thyroid tumor subtypes, prevent overtreatment and tailor specific clinical management. This applies particularly to the recently described variant of thyroid cancer referred to as noninvasive follicular thyroid neoplasm with papillary-like nuclear features (NIFTP). This variant has an estimated prevalence of 4.4% to 9.1% of all papillary thyroid carcinomas worldwide. We studied 60 thyroid lesions: 20 classical papillary thyroid carcinoma (CPTC), 20 follicular variant of PTC (FVPTC) and 20 NIFTP. We examined morphological and molecular features to identify parameters that can differentiate NIFTP from the other PTC subtypes. When blindly investigating the nuclear architecture of thyroid neoplasms, we observed that NIFTP has significantly longer telomeres than CPTC and FVPTC. Super-resolved 3D-structured illumination microscopy demonstrated that NIFTP is heterogeneous and that its nuclei contain more densely packed DNA and smaller interchromatin spaces than CPTC and FVPTC, a pattern that resembles normal thyroid tissue. These data are consistent with the observed indolent biological behavior and favorable prognosis associated with NIFTP, which lacks *BRAF*$^{V600E}$ mutations. Of note, next-generation thyroid oncopanel sequencing was unable to distinguish the thyroid cancer histotypes in our study cohort. In summary, our data suggest that 3D

**Abbreviations:** 3D, three-dimensional; 3D-SIM, three-dimensional structured illumination microscopy; *BRAF*, v-raf murine sarcoma viral oncogene homolog B1; CPTC, classical papillary thyroid carcinoma; DAPI, 4′,6-diamidino-2-phenylindole; FFPE, formalin-fixed paraffin-embedded; FVPTC, follicular variant of PTC; LN, lymph nodes; NAT, normal adjacent thyroid tissue; NIFTP, noninvasive follicular thyroid neoplasm with papillary-like nuclear features; *PPARγ*, peroxisome proliferator-activated receptor gamma; PTC, papillary thyroid carcinoma; Q-FISH, quantitative fluorescence in situ hybridization; *RAS*, rat sarcoma virus; *RET*, rearranged during transfection; *THADA*, thyroid adenoma-associated.

## 11. SUPPLEMENTARY MATERIAL

**Three-Dimensional Nuclear Architecture distinguishes thyroid cancer histotype**

**Aline Rangel-Pozzo, Filipe F dos Santos, Dettori Tinuccia, Matteo Giulietti, Daniela Virginia Frau, Pedro A.F. Galante, Roberta Vanni, Alok Pathak, Gabor Fischer, John Gartner, Paola Caria and Sabine Mai**

**Table of contents**

***Supplementary Table S1:*** *Summary of the targeted sequencing coverage and quality statistics*

| Sample ID | Total number of sequenced *reads* | Total number of uniquely mapped non-duplicate *reads* | Total number of covered targeted bases | Median coverage (and range) per targeted base | Percentage of targeted bases with coverage ≥200 |
|---|---|---|---|---|---|
| 11A_S22 | 530,418 | 530,023 | 22,027 (100%) | 1,948 (71 - 11,303) | 94.71% |
| 12A_S24 | 648,404 | 654,554 | 22,027 (100%) | 3,011 (66 - 9,792) | 95.35% |
| 13A_S38 | 1,122,254 | 1,149,125 | 22,027 (100%) | 4,780 (43 - 21,176) | 98.45% |
| 14A_S26 | 416,594 | 421,604 | 22,027 (100%) | 1,807 (62 - 5,796) | 94.64% |
| 14A_S28 | 583,172 | 589,798 | 22,027 (100%) | 2,493 (102 - 7,813) | 96.96% |
| 15A_S28 | 836,294 | 851,816 | 22,027 (100%) | 3,674 (108 - 11,898) | 98.37% |
| 17A_S31 | 685,530 | 733,048 | 22,027 (100%) | 3,075 (102 - 12,706) | 98.50% |
| 18A_S33 | 605,976 | 610,383 | 22,027 (100%) | 1,801 (45 - 11,025) | 96.63% |
| 27A_S34 | 624,858 | 627,687 | 22,027 (100%) | 2,239 (23 - 11,985) | 92.22% |
| 28A_S35 | 676,650 | 677,959 | 22,027 (100%) | 2,854 (157 - 9,868) | 99.98% |
| 29A_S37 | 711,732 | 721,674 | 22,027 (100%) | 3,067 (47 - 10,848) | 99.98% |
| 30A_S39 | 571,082 | 573,684 | 22,027 (100%) | 2,551 (138 - 8,919) | 99.50% |
| 32-1419T_S2 | 640,736 | 648,288 | 22,027 (100%) | 2,963 (77 - 8,647) | 99.48% |
| 32-1519T_S4 | 505,438 | 497,477 | 22,027 (100%) | 967 (26 - 21,516) | 93.01% |
| 3322-20-T_S8 | 676,518 | 665,418 | 22,027 (100%) | 1,012 (30 - 26,295) | 90.65% |
| 3324-20-1_S10/21 | 1,270,744 | 1,251,758 | 22,027 (100%) | 1,534 (14 - 34,674) | 89.20% |
| 3329-20-T_S12/23 | 1,244,162 | 1,240,339 | 22,027 (100%) | 3,164 (53 - 18,043) | 99.98% |
| 3330-20-T_S22 | 1,549,400 | 1,578,036 | 22,027 (100%) | 4,311 (55 - 40,593) | 98.90% |
| 3332-20-T_S1 | 706,050 | 674,126 | 22,027 (100%) | 1,035 (40 - 27,601) | 96.40% |
| 38A_S30 | 889,746 | 900,787 | 22,027 (100%) | 3,995 (310 - 11,322) | 100.00% |
| 38A_S41 | 693,548 | 702,266 | 22,027 (100%) | 3,086 (278 - 8,683) | 100.00% |
| 39A_S42 | 409,066 | 401,800 | 22,027 (100%) | 717 (34 - 14,644) | 90.63% |
| 41A_S42 | 879,386 | 894,152 | 22,027 (100%) | 3,517 (165 - 13,761) | 99.46% |
| 42A_S45 | 557,670 | 584,439 | 22,027 (100%) | 2,490 (77 - 7,920) | 99.98% |
| 43A_S32 | 814,406 | 817,358 | 22,027 (100%) | 2,917 (38 - 14,840) | 97.24% |
| 43A_S47 | 610,300 | 612,827 | 22,027 (100%) | 2,191 (30 - 10,942) | 95.53% |
| 45A_S33 | 669,732 | 675,827 | 22,027 (100%) | 2,892 (164 - 9,412) | 99.02% |
| 45A_S49 | 553,472 | 558,624 | 22,027 (100%) | 2,418 (114 - 7,820) | 97.83% |
| 47A_S36 | 1,034,180 | 1,048,601 | 22,027 (100%) | 3,399 (56 - 24,419) | 97.81% |
| 47A_S53 | 833,742 | 845,580 | 22,027 (100%) | 2,695 (47 - 20,060) | 96.74% |
| 48A_S43 | 601,422 | 624,578 | 22,027 (100%) | 2,551 (87 - 12,159) | 99.00% |
| 49A_S37 | 969,848 | 977,652 | 22,027 (100%) | 4,508 (56 - 15,595) | 95.91% |
| 49A_S54 | 733,048 | 739,215 | 22,027 (100%) | 3,312 (35 - 11,716) | 94.16% |
| 50A_S56 | 463,744 | 452,242 | 22,027 (100%) | 680 (2 - 21,454) | 87.12% |
| 54A-Undetermined_S0 | 1,966,002 | 872,240 | 22,027 (100%) | 1,587 (2 - 35,935) | 96.95% |
| 55A-Undetermined_S0 | 1,020,010 | 615,098 | 22,027 (100%) | 1,561 (94 - 12,298) | 97.83% |
| 57A_S63 | 694,276 | 701,090 | 22,027 (100%) | 3,123 (140 - 8,887) | 99.98% |
| 7A_S17 | 534,302 | 537,528 | 22,027 (100%) | 2,405 (117 - 8,953) | 97.42% |
| 8A_S19 | 432,354 | 430,905 | 22,027 (100%) | 1,713 (60 - 8,668) | 97.15% |
| 9A_S20 | 561,176 | 562,683 | 22,027 (100%) | 2,350 (82 - 9,445) | 96.38% |
| T1A_S5 | 409,152 | 413,505 | 22,027 (100%) | 1,667 (40 - 5,723) | 95.86% |
| T2A_S7 | 658,608 | 664,928 | 22,027 (100%) | 2,838 (228 - 9,244) | 100.00% |
| T3A_S9 | 548,016 | 551,849 | 22,027 (100%) | 2,344 (86 - 9,141) | 97.82% |
| T4A_S11 | 713,024 | 716,888 | 22,027 (100%) | 2,714 (230 - 10,796) | 100.00% |
| T5A_S13 | 568,170 | 567,297 | 22,027 (100%) | 2,282 (186 - 8,959) | 99.36% |
| T6A_S15 | 399,194 | 400,209 | 22,027 (100%) | 1,718 (90 - 6,629) | 96.71% |

Sequencing metrics of the data from samples with a median coverage >= 500x submitted to targeted NGS with amplicon libraries generated using multiplex PCR. HG38 (LiftOver) as the reference genome.

***Supplementary Table S2:*** *Cancer HotSpot sequences*

| Target ID | Upstream *Locus* -Specific Oligo Sequence | Downstream *Locus* -Specific Oligo Sequence | Gene ID |
|---|---|---|---|
| CHP2_MPL_1 | AGAGCGAACCAAGAATGCCTGTTTA | CACTAGATGCAGAGCGGTCACCAAG | MPL |
| CHP2_NRAS_3 | AACAAGTGTGATTTGCCAACAAGGA | GGTACAGCTTTCAGCATTTGTGCAA | NRAS |
| CHP2_NRAS_2 | ACACCCCCAGGATTCTTACAGAAAA | CCAATACATGAGGACAGGCGAAGGC | NRAS |
| CHP2_NRAS_1 | GGTTCTTGCTGGTGTGAAATGACTG | ATATGATCCCACCATAGAGGTGAGG | NRAS |
| CHP2_ALK_2 | CCCTGGAAGAGTGGCCAAGATTGGA | CTTACATCATCTCCTGGTACCCTGT | ALK |
| CHP2_ALK_1 | TTTGCCCAGACTCAGCTCAGTTAAT | CTCAAGTCCTTCCTCCGAGAGACCC | ALK |
| CHP2_IDH1_1 | GAAATCACCAAATGGCACCATACGA | ATGGGGATCAAGTAAGTCATGTTGG | IDH1 |
| CHP2_ERBB4_8 | TGGGAACTGATGACCTTTGGAGGAA | GACGTTTACATGGTCATGGTCAAAT | ERBB4 |
| CHP2_ERBB4_7 | CAGGGTCCTGACAACTGTACAAAGT | AAGGGTAAGCATTCTTGCTGGCCAA | ERBB4 |
| CHP2_ERBB4_6 | CTCAATCCCCTAACTCTGAGTCTTG | TCTTTCTAGTCACTGGTATTCATGG | ERBB4 |
| CHP2_ERBB4_5 | TGTTTTGAGCTTGTTTGCTGAATGT | TAAACCTTGCACTGACATTTGCCCA | ERBB4 |
| CHP2_ERBB4_4 | TGCAGGCCTGCATGAATTTCAATGA | GTCAAGAAATGTCCACGTAAGTAAC | ERBB4 |
| CHP2_ERBB4_3 | GTGACGGCAGATGCTACGGACCTTA | TCCTTTCCTTCCCTATTTGATTCAG | ERBB4 |
| CHP2_ERBB4_2 | GACACCATTCATTGGCAAGATATTG | AAATGTTCTACCCTATGTGGCGATG | ERBB4 |
| CHP2_ERBB4_1 | AACTTTGGACTTCAAGAACTTGGAT | TTGTTACATTGAGGAACACTCTAAG | ERBB4 |
| CHP2_VHL_1 | GCCCGTACCTCGGTAGCTGTGGATG | ATTGCAGAAGATGACCTGGGAGGGC | VHL |
| CHP2_VHL_2 | AACGTCAGTACCTGGCAGTGTGATA | AGCAAAGGTTGTTAAAGAGCCACAC | VHL |
| CHP2_VHL_3 | CTGACGATGTCCAGTCTCCTGTAAT | GAACGAACAAGAGGCTTTGCCAACA | VHL |
| CHP2_MLH1_1 | CCTGCCACTAGAAATATCTGTCTTA | CCAGAAGTAGAAGACGAGGTCAGAC | MLH1 |
| CHP2_CTNNB1_1 | CATCCTCTTCCTCAGGATTGCCTTT | TCCATCAAATCAGCTATAAATACGA | CTNNB1 |
| CHP2_PIK3CA_1 | AAGGGTTGAAAAAGCCGAAGGTCAC | TCTTGCTTCTTTAAATAGTTCATGC | PIK3CA |
| CHP2_PIK3CA_2 | TACGAAGGTATTGGTTTAGACAGAA | GCCTACTGGTTCAATTACTTTTAAA | PIK3CA |
| CHP2_PIK3CA_3 | ATCAGCATTTGACTTTACCTTATCA | GTGTAGCTGTGGAAATGCGTCTGGA | PIK3CA |
| CHP2_PIK3CA_4 | ATCAGCGGTATAATCAGGAGTTTTT | CATAATTCAGCCATTCATTCCACCT | PIK3CA |
| CHP2_PIK3CA_5 | AACAAGTTTATATTTCCCCATGCCA | AGGAAAATTCAACAATCATCTCTAT | PIK3CA |
| CHP2_PIK3CA_6 | TAAGAGAGAAGGTTTGACTGCCATA | AGGTACTGGCCAAAGATTCAAAGCC | PIK3CA |
| CHP2_PIK3CA_7 | GCACTTACCTGTGACTCCATAGAAA | TCATTGTCTCTAGCTAGTCTGTTAC | PIK3CA |
| CHP2_PIK3CA_8 | TTTGTGTTTCATCCTTCTTCTCCTG | TGTGCATCTCAGATCTAAAAGAATC | PIK3CA |
| CHP2_PIK3CA_9 | GAAAACCATTACTTGTCCATCGTCT | GTAAACAGGTCAATGGCTGCATCAT | PIK3CA |
| CHP2_PIK3CA_10 | GAAGATCCAATCCATTTTTGTTGTC | ATCAAAAGATTGTAGTTCTGGCATT | PIK3CA |
| CHP2_PIK3CA_11 | ATGCTGTTCATGGATTGTGCAATTC | ATGCTGTTTAATTGTGTGGAAGATC | PIK3CA |
| CHP2_FGFR3_1 | GGATGTGGGGCTGTGCGTCACTGTA | AGATGACGCTCAGGGGCCACCCCCT | FGFR3 |
| CHP2_FGFR3_2 | CGGTGGGGGAGCCCAGGCCTTTCTT | TCAGCCTCCACCAGCTCCTCCTCGG | FGFR3 |
| CHP2_FGFR3_3 | CGCCAGGCGTCCTACTGGCATGACC | ATCACGTTGTCCTCGGTCACCAGCA | FGFR3 |
| CHP2_FGFR3_4 | GGGATGCCACTCACAGGTCGTGTGT | AGCGTGAAGATCTCCCAGAGCAGGA | FGFR3 |
| CHP2_FGFR3_5 | GGCTGCTAGGGACCCCTCACATTGT | GGAGTACTGCTCGAAAGGCGCCGAC | FGFR3 |
| CHP2_PDGFRA_1 | CATCTCTTGGAAACTCCCATCTTGA | GTGAATTACCAAAGTCCCAGTGCAC | PDGFRA |
| CHP2_PDGFRA_2 | ACCACATGTGTCCAGTGAAAATCCT | CAGACATGAGAGCTTGTTTTTCACT | PDGFRA |
| CHP2_PDGFRA_3 | GTGTGCTTTCATCAGCAGGGTTCAA | TAAATGGGGCCTATGGGGACAAAAG | PDGFRA |
| CHP2_PDGFRA_4 | TTAAAGTGAAGGAGGATGAGCCTGA | AGATCACGGTGGACACACTGCATGG | PDGFRA |
| CHP2_KIT_1 | TCCATTTGACAAAGCCCGGATCAGT | TTGAGTATGATCTTCTTCCTTGGCG | KIT |
| CHP2_KIT_2 | GATATGGTAGACAGAGCCTAAACAT | TAAGCCTTACATTCAACCGTGCCAT | KIT |
| CHP2_KIT_3 | TGTCTCAGTCATTAGAGCACTCTGG | AAAGGAGTGAACAGGGTGTGGGGAT | KIT |
| CHP2_KIT_4 | TTTCATACTGACCAAAACTCAGCCT | GGAGAAAGGGAAAAATAGATCACCT | KIT |
| CHP2_KIT_5 | CTTGGACACGGCTTTACCTCCAATG | TTGGAAACATGCATTTTAGCAAAAA | KIT |
| CHP2_KIT_6 | TTGAACAAATAAATGAATCACGTTT | AAGCACATAAGAAAAGGTTAGAAAG | KIT |
| CHP2_KIT_7 | GGACAACATAAGAAACTCCAGGTTT | ATGGGTCATGCTCTACCTCCTCATC | KIT |
| CHP2_KIT_8 | TGTCAAGCAGAGAATGGGTACTCAC | ATGAGTAAGGAGGATATTTCTGGCT | KIT |
| CHP2_KIT_9 | CCTAAAGAGAACAGCTCCCAAAGAA | GTAGTCGAGCCTGTAATAGAAGCAC | KIT |
| CHP2_KDR_9 | ACCACCGTGTACTCCAGTGAGGAAG | CAACTCCTGGACATCACATGAGAGG | KDR |
| CHP2_KDR_8 | TGAGGGTAAAAAGCAAAAGAATTGT | ACTCCGATGACACAGACACCACCGT | KDR |
| CHP2_KDR_7 | TGAGCATGGAAGAGGATTCTGGACT | AGGTACTGTATATGGCCTAACATCC | KDR |
| CHP2_KDR_6 | CAGCATTCAGGAAGAAAGAGGCATT | TGGTGGAACATTTGGGAAATCTCTT | KDR |
| CHP2_KDR_5 | TGGAGCAATCCCTGTGGATCTGAAA | AGAGGAAGGTACTGGCTAGTGCTTC | KDR |
| CHP2_KDR_4 | GGGACCCCAATTATTGAAGGAAATG | CACCATCTCAATGTGGTCAACCTTC | KDR |
| CHP2_KDR_3 | GGCTGCGTTGGAAGTTATTTCTAAG | TACCCTTGTGAAGAATGGAGAAGTG | KDR |
| CHP2_KDR_2 | GCTTTGGAAGTTCAGTCAACTCTTT | CTTAACTATAGATGGTGTAACCCGG | KDR |
| CHP2_KDR_1 | TATCTGTTGGAGAAAAGCTTGTCTT | TGAAGTTTGCTTGAGAGATAGGGGC | KDR |
| CHP2_FBXW7_5 | TCTTGATACATCAATCCGTGTTTGG | TTGTCTCTGGGAATGCAGATTCTAC | FBXW7 |
| CHP2_FBXW7_4 | TCCCTCTGCAGAGTTGTTAGCGGTT | TATGATGGCAGGAGGGTTGTTAGTG | FBXW7 |
| CHP2_FBXW7_3 | TCATCACAAATGAGAGACAACATCA | GGGAAAATCTTGTCATGGTTGGGAC | FBXW7 |
| CHP2_FBXW7_2 | CATCTTTCTTATAGGTGCTGAAAGG | TAAAAGTTTGGTCAGCAGTCACAGG | FBXW7 |
| CHP2_FBXW7_1 | TCATTGATAGTTGTGAACCAACACA | AACAGCTACCACCTTTAAACATTGT | FBXW7 |
| CHP2_APC_1 | GTATGAATGGCTGACACTTCTTCCA | TAGACCAATTCCGCGTTCTCTCTCC | APC |
| CHP2_APC_2 | CATCTTCTTGACACAAAGACTGGCT | AACTTGAGGTGTTTATCATCAGTGC | APC |
| CHP2_APC_3 | GGATTTGGTTCTAGGGTGCTGTGAC | TTCAGCTGATGACAAAGATGATAAT | APC |
| CHP2_APC_4 | GTGAACTGACAGAAGTACATCTGCT | AACTAGAACCCTGCAGTCTGCTGGA | APC |
| CHP2_APC_5 | GACCCTCTGAACTGCAGCATTTACT | TATCTGGAAGATCACTGGGGCTTAT | APC |
| CHP2_APC_6 | GTCATTTTCCTGAACTGGAGGCATT | TGGAAGAACCTGGACCCTCTGAACT | APC |
| CHP2_APC_7 | TTACGTGATGACTTTGTTGGCATGG | TTTAGGCTGCTCTGATTCTGTTTCA | APC |
| CHP2_CSF1R_2 | AGAGCTCTAGTGAGCACCTGACCTG | AACTTCAACTCCTCCATGGATGGGG | CSF1R |
| CHP2_CSF1R_1 | TCTTCCCACTAATGCCAGATGCTTG | CTCAACCTCAAAGTCATGGTGGAGG | CSF1R |
| CHP2_NPM1_1 | CAGCCAGATATCAACTGTTACAGAA | AGGAACCACAACACTTCATAGACAT | NPM1 |
| CHP2_EGFR_1 | GTCCGGTTTTATTTGCATCATAGTT | ACTGTGTTGAGGGCAATGAGGACAT | EGFR |
| CHP2_EGFR_2 | CCCAAAGACTCTCCAAGATGGGATA | ACATCCATCTGGTACGTGGTGGGGT | EGFR |
| CHP2_EGFR_3 | ACTTCCAGACCAGGGTGTTGTTTTC | GTGGAGAAAAATGTTCATGCATGTC | EGFR |
| CHP2_EGFR_4 | CTGTGCCAGGGACCTTACCTTATAC | TGGGTGTAAGAGGCTCCACAAGCTG | EGFR |
| CHP2_EGFR_5 | TGGGCCTGAGGTTCAGAGCCATGGA | TGACAGAGAGAGAAGGAAGACGTTA | EGFR |

| | | | | |
|---|---|---|---|---|
| CHP2_EGFR_6 | GTTCCCGGACATAGTCCAGGAGGCA | GTCAGTGTGGCTTCGCATGGTGGCC | EGFR | |
| CHP2_EGFR_7 | ATATCCCCATGGCAAACTCTTGCTA | TCTTTGTGTTCCCGGACATAGTCCA | EGFR | |
| CHP2_EGFR_8 | CATGTGTTAAACAATACAGCTAGTG | ATCTGTGATCTTGACATGCTGCGGT | EGFR | |
| CHP2_MET_1 | AAAGAAGTTGATGAACCGGTCCTTT | GTGAACCTCCGACTGTATGTCAGCA | MET | |
| CHP2_MET_2 | AGACATCTCACATTGTTTTTGTTGA | ATCATTCAGGCTGGCTCCTATTTGT | MET | |
| CHP2_MET_3 | TTTTCAAAAGGCTTAAACACAGGAT | TCTCTGAATTAGAGCGATGTTGACA | MET | |
| CHP2_MET_4 | AGTCTACAGATTCATTTGAAACCAT | CTTGTTAAAGACGGCTATCATGGGC | MET | |
| CHP2_MET_5 | AAACCACAAAAGTATACTCCATGGT | AACTTGGTTAGCACTGCGTAACATT | MET | |
| CHP2_MET_6 | TGACTTGGTGGTAAACTTTTGAGTT | CTCTGGCAAGACCAAAATCAGCAAC | MET | |
| CHP2_SMO_1 | GCCGCGATGTAGCTGTGCATGTCCT | TTGATGTTCTGCACCTCATTCTGGC | SMO | |
| CHP2_SMO_2 | GCCAGGCATAGGTGAGGACCACAAA | TCACTCTGTACTCCCTCTACCTGGT | SMO | |
| CHP2_SMO_3 | CCTGGTCTTCACTCACCTCGGATGA | AAAACAAATCCCACTCACAGAGTCC | SMO | |
| CHP2_SMO_4 | TGCACCAGGTACGCCTCCAGATGAG | TTCTTGATCTCACAGTCAGGGATGG | SMO | |
| CHP2_SMO_5 | TCCTCCAGAAGCTTGAACTCTCATA | ATTGAGGTCAAAGGCCAAGCCCGCT | SMO | |
| CHP2_BRAF_2 | TGCTCTGATAGGAAAATGAGATCTA | ACAGTTGTCTGGATCCATTTTGTGG | BRAF | |
| CHP2_BRAF_1 | TCTTTTTCTGTTTGGCTTGACTTGA | AAGGGAAAGTGGCATGGTAAGTATG | BRAF | |
| CHP2_EZH2_1 | CTAGCATCTATTGCTGGCACCATCT | GATAACCTGTATTCAGGTGGCATTG | EZH2 | |
| CHP2_FGFR1_2 | CCACCCCTCTTTAGCCATGGCAAGG | TTCATGTGTAAGGTGTACAGTGACC | FGFR1 | |
| CHP2_FGFR1_1 | CTAGGGGTCCCTAGGAGGAACCTCA | TTCCTATCTTACTGCCCTTTGGGTC | FGFR1 | |
| CHP2_JAK2_1 | ACACTGACACCTAGCTGTGATCCTG | TTGCTCATCATACTTGCTGCTTCAA | JAK2 | |
| CHP2_CDKN2A_2 | CTTCCTGGACACGCTGGTGGTGCTG | AGTAACCATGCCCGCATAGATGCCG | CDKN2A | |
| CHP2_CDKN2A_1 | CCCACCCTGGCTCTGACCATTCTGT | TTCCTGGACACGCTGGTGGTGCTGC | CDKN2A | |
| CHP2_GNAQ_1 | TTGTTAACCTTGCAGAATGGTCGAT | AGTGTTCTTTAGACAGGCAATGGAT | GNAQ | |
| CHP2_ABL1_1 | ACCGTCAGGCTGTATTTCTTCCACA | AGTTGGGGGACACACCATAGACAGT | ABL1 | |
| CHP2_ABL1_2 | CAGCTTCTTTCAAGAACTCTTCCAC | ATGCAAAATGGAGCTTCAGCGCATA | ABL1 | |
| CHP2_ABL1_3 | GCCTGGCCAGGCCCCTACCTGTGGA | TGATATAGAACGGGGGCTCCCGGGT | ABL1 | |
| CHP2_ABL1_4 | CGGACTTGATGGAGAACTTGTTGTA | CTACCTTCACCAAGTGGTTCTCCCC | ABL1 | |
| CHP2_NOTCH1_3 | CCACCTGGGCCGGAGCTTCCTGAGT | TGACCGCAGCCCAGTTCCTGACGCC | NOTCH1 | |
| CHP2_NOTCH1_2 | GCTGCCTCACCATGTCCTGACTGTG | TTGACAACCGGCAGTGTGTGCAGGC | NOTCH1 | |
| CHP2_NOTCH1_1 | CGGGCTGGACTGTGCGGAGCATGTA | CAACGTGGTCTTCAAGCGTGACGCA | NOTCH1 | |
| CHP2_RET_1 | CCTCCCTTGTTGGGACCTCAGATGT | TGCCATAGCCAGCTTTAATCCCCCG | RET | |
| CHP2_RET_2 | ACTTGTGGTAGCAGTGGATGCAGAA | GGTACAGGCTGCGTATGCTCTGCCT | RET | |
| CHP2_RET_3 | GCAGGCCCCATACAATTTGATGACA | AAACGATCGCTCCTGGAAGCCCCTT | RET | |
| CHP2_RET_4 | GCCTGCCCCATGGTGCACCTGGGAT | CAAGTCCCGATGAACGAGCTGTGAG | RET | |
| CHP2_RET_5 | CTTTGCGTGGTGTAGATATGATCAA | ATCCCTGAGCTTTCAGTAACCAGAG | RET | |
| CHP2_PTEN_1 | GCAGCCGCAGAAATGGATACAGGTC | AAGAAAAAGGAGGAGAGAGATGGCA | PTEN | |
| CHP2_PTEN_2 | ACCTCACTCTAACAAGCAGATAACT | ACAAACAAACAAAAAGCCACCATTA | PTEN | |
| CHP2_PTEN_3 | GCCCCGATGTAATAAATATGCACAT | TTCTAGCTGTGGTGGGTTATGGTCT | PTEN | |
| CHP2_PTEN_4 | GCCACTGGTCTATAATCCAGATGAT | CTATGGTAACTGGGTCGTAGCCATT | PTEN | |
| CHP2_PTEN_5 | TCTTCACCTTTAGCTGGCAGACCAC | GGATTCTGTATCTGCAATCTTGATC | PTEN | |
| CHP2_PTEN_6 | ATTTCTCCCAATGAAAGTAAAGTAC | GTCCTGAATTGGAGGAATATATCTT | PTEN | |
| CHP2_PTEN_7 | CGCTCTATACTGCAAATGCTATCGA | TCCTGGTATGAAGAATGTATTTACC | PTEN | |
| CHP2_PTEN_8 | TCACATACATACAAGTCAACAACCC | TCATTATCTGCACGCTCTATACTGC | PTEN | |
| CHP2_FGFR2_4 | GATGAAGATGATTGGGAAACACAAG | TTTAGAAATGGCTGGGCTTCCAGAT | FGFR2 | |
| CHP2_FGFR2_3 | TTCCTCCTCCTGTGATCTGCAATCT | AATGAAGAACACGACCAAGAAGCCA | FGFR2 | |
| CHP2_FGFR2_2 | TCCAGTGGATCAAGCACGTGGAAAA | CCTGTTGGAGTTGAGAGAGGATGAT | FGFR2 | |
| CHP2_FGFR2_1 | TATTGGTCTCTCATTCTCCCATCCC | GTTTGTCTGCAAGGTTTACAGTGAT | FGFR2 | |
| CHP2_HRAS_2 | TCCTCCTGCAGGATTCCTACCGGAA | TTTGCCATCAACAACACCAAGTCTT | HRAS | |
| CHP2_HRAS_1 | CCTGAGGAGCGATGACGGAATATAA | ACTATAGAGGTGAGCCTGGCGCCGC | HRAS | |
| CHP2_ATM_1 | GAAATTTCTAAATGTGACATGACCT | TATGACTTATCTCATTCACTAGCAG | ATM | |
| CHP2_ATM_2 | AGATGAAAGGATTCCACTGAAAGTT | AAAATCATTCTGTGACTTCTGAAGG | ATM | |
| CHP2_ATM_3 | ATACCATTCTGGCACGCTTTGGAAA | AGAAGACCAAAAGCCATGTAAAGAA | ATM | |
| CHP2_ATM_4 | TCCAGGTTCGTTTGCATCACTAACA | CTCCACGGTCAAATGGCTTTTTGAT | ATM | |
| CHP2_ATM_5 | CATACCTGTTTTCCCAATAAGTTTT | TACAAGAATCTTTGGAAAGCAGTCT | ATM | |
| CHP2_ATM_6 | TCAGCATTATGAAGGTCCACTGAAG | CAGCTTCCAACAGCCTCTACATATA | ATM | |
| CHP2_ATM_7 | CTGTAGATAGGCCAGCATTGGATCT | ATTCAAATGCCTATCAAGTACACCA | ATM | |
| CHP2_ATM_8 | ATTTCACATTTTGTGCCTCCACTGT | ATCCAGGCCTTCAAAAGGGTTTTCT | ATM | |
| CHP2_ATM_9 | GCTGTAAAGTGAGCAGCACAAGACT | TGTTCCTGAAGAAGGTCTAAAGAAA | ATM | |
| CHP2_ATM_10 | AAGCGTTTACGATCCTCTTTCAGTG | CACAAAAGCCATGAACTTTAACAGA | ATM | |
| CHP2_ATM_11 | TAATTGCAAATTACCTTAATTTCCA | TCTGCTGGAATATTTATGCCTTCTG | ATM | |
| CHP2_ATM_12 | CTCACCTTAACAAGCTGTCTCCTCT | AGTCACCAGATTTCCATATTCTCCT | ATM | |
| CHP2_ATM_13 | TTTCCGTGTTTCTCTGCAGTAATGT | AAAAACACAGAGTCATCTGAGAATA | ATM | |
| CHP2_ATM_14 | ATCTTGGTAGGCAAACAACATTCCA | ATGTAACCAACTGGAGAAAAAAGAA | ATM | |
| CHP2_ATM_15 | ATACACAGTCTACCTGGTAAGAAAA | TTCTCACAGCATCTAGAGTCAAACA | ATM | |
| CHP2_ATM_16 | AAATTCACTTGTCCACCAACACTGA | AAAACACAAAGGTTTCAGTGAGGTG | ATM | |
| CHP2_ATM_17 | TGTTGGCAGGTTAAAAATAAAGGCT | TCTATGGCCTGCTGTATGAGCAAAT | ATM | |
| CHP2_KRAS_3 | CTCTGAAGATGTACCTATGGTCCTA | AGGTAAGTAACACTGAAATAAATAC | KRAS | |
| CHP2_KRAS_2 | AAGGTGCACTGTAATAATCCAGACT | AATGAGGGACCAGTACATGAGGACT | KRAS | |
| CHP2_KRAS_1 | GCCTGCTGAAAATGACTGAATATAA | ATATTACTGGTGCAGGACCATTCTT | KRAS | |
| CHP2_PTPN11_1 | TCTTTTAATTGCCCGTGATGTTCCA | AAATAGTCCATTGGAAAGGGAGGCA | PTPN11 | |
| CHP2_PTPN11_2 | CTGGTACCTGCTCTTCTTCAATCCT | GTCAACACCTACGAAGGAAACATCA | PTPN11 | |
| CHP2_HNF1A_1 | CTCGCTCCTCCTTGCTAGGGTTCTT | TCACCTGTGGGCTCTTCAATCAGCC | HNF1A | |
| CHP2_HNF1A_2 | GGGGGGGCCCGCTGTACGTGTCCAT | CCTGTGCCTGTGATGGGGACACCCC | HNF1A | |
| CHP2_FLT3_4 | CACCCACGGGAAAGTGGTGAAGATA | TTTTATACGGCTATTTTGTGTTGTG | FLT3 | |
| CHP2_FLT3_3 | GAGAGGCACTCATGTCAGAACTCAA | GTAGCTTGATGACAAAGAGGATGTT | FLT3 | |
| CHP2_FLT3_2 | ACTCATCATTTCATCTCTGAAGCAA | TAGAGTTTGGTAAGAATGGAATGTG | FLT3 | |
| CHP2_FLT3_1 | GAGCTTATTTCACACGTTCTTTTCT | AGTGTTCAGACAAGTCTCCCAAGTA | FLT3 | |
| CHP2_RB1_1 | ACCTTTCCAATTTGCTGAAGAGTGC | TATGGACACTACAAAGGAAAGAATA | RB1 | |
| CHP2_RB1_2 | CCAAGCAGAGAATGAGGGAGGAGTA | ATCCAAGAAACTTTTAGCACCAATG | RB1 | |
| CHP2_RB1_3 | TGTGCAATACCTGTCTATAGAATCA | TCCTTTACATGTCATTACATCTCTC | RB1 | |
| CHP2_RB1_4 | CTGGAGTGTGTGGAGGAATTACATT | AAAGCAGTATAATGCTTCTGTTGTC | RB1 | |

***Supplementary Table S3:*** *Cancer HotSpot targets*

| TargetA | TargetB | Chr | Start | End | Strand | Sequence |
|---|---|---|---|---|---|---|
| CHP2_MPL_1 | CHP2_MPL_1 | chr1 | 4.4E+07 | 4.4E+07 | + | CTGGGCCTCAGCGCCGTCCTGGGCCTGCTGCTGCTGAGGTGGCAGTTTCCTGCACACTACAGGTACCGCCCCCGCCAGGCAGGAGACTGGCGGTGGACCAGGTGGAGCCGAAGGCCTG |
| CHP2_NRAS_3 | CHP2_NRAS_3 | chr1 | 1.2E+08 | 1.2E+08 | + | ATACCTGTCTGGTCTTGGCTGAGGTTTCAATGAATGGAATCCCGTAACTCTTGGCCAGTTCGTGGGCTTGTTTTGTATCAACTG |
| CHP2_NRAS_2 | CHP2_NRAS_2 | chr1 | 1.2E+08 | 1.2E+08 | + | TCTCTCATGGCACTGTACTCTTCTTGTCCAGCTGTATCCAGTATGTCCAACAAACAGGTTTCACCATCTATAACCACTTG |
| CHP2_NRAS_1 | CHP2_NRAS_1 | chr1 | 1.2E+08 | 1.2E+08 | + | TCATCTACAAAGTGGTTCTGGATTAGCTGGATTGTCAGTGCGCTTTTCCCAACACCACCTGCTCCAACCACCACCAGTTTGTACT |
| CHP2_ALK_2 | CHP2_ALK_2 | chr2 | 2.9E+07 | 2.9E+07 | + | GGACAAGCAGCCACACCCCATTCTTGAGGGGCTGAGGTGGAAGAGACAGGCCCGGAGGGGTGAGGCAGTCTTTACTCACCTGTAGATGTCTCGGGCCATCCCGAAGTC |
| CHP2_ALK_1 | CHP2_ALK_1 | chr2 | 2.9E+07 | 2.9E+07 | + | GTCTCCCCCCGCCATGAGCTCCAGCAGGATGAACCGGGGCAGGGATTGCAGGCTCACCCCAATGCAGCGAACAATGTTCTGGTGGTTGAATTTGCTGCAGAGCAGAGAGGGATGTAACCAAA |
| CHP2_IDH1_1 | CHP2_IDH1_1 | chr2 | 2.1E+08 | 2.1E+08 | + | AAGCATGACGACCTATGATGATAGGTTTTACCCATCCACTCACAAGCCGGGGGATATTTTTGCAGATAATGGCTTCTCTGAAGACCGTGCCACCCAGAATATT |
| CHP2_ERBB4_8 | CHP2_ERBB4_8 | chr2 | 2.1E+08 | 2.1E+08 | + | AATAGTGCAGATGGGAGGCTGAGGCAAACGTTCTCCTTTCTCTAATAAATCAGGGATTTCTCGCGTTGGAATTCCATCATAGGGTT |
| CHP2_ERBB4_7 | CHP2_ERBB4_7 | chr2 | 2.1E+08 | 2.1E+08 | + | GGGTGCAGTTTGGATGGCATGGGTGGCACTCCCGATCTGGATCAGCATACTTGAAAATGAAACTGTTTGCCCCCTGTAAGCCATCTGGACATTTTTCCACACAGTTTGGGCCATCTTTAAAATGAGAGC |
| CHP2_ERBB4_6 | CHP2_ERBB4_6 | chr2 | 2.1E+08 | 2.1E+08 | + | TCAAATTCCCATTGATCTTGGTACAGTTTATGAATTTGTCAATGTTACTGGAATCCACAGTCTGAGCTGACATCAATGATCCTGTGCCAATGCCATCACAAGCTGTAGAAA |
| CHP2_ERBB4_5 | CHP2_ERBB4_5 | chr2 | 2.1E+08 | 2.1E+08 | + | CACATTTTAATCCCATTTTCTTCTACTTCCATCTTGGAACTAGGGCAGGCACGCACACAAGAACTGGAATCTACCACAAAGTTATCTGATTAAAAAAAAAAAAAAGGTAAAATAAGCATTAATGTTA |
| CHP2_ERBB4_4 | CHP2_ERBB4_4 | chr2 | 2.1E+08 | 2.1E+08 | + | ACAGAATGCTCCATATGTGTACTTTGCATTGAAATTGTGCTCCAGTTGAAAGGTGGTTGGATTGTAGACAAAGGTTTGGGGACACTGAGTAACACATGCTCCACTG |
| CHP2_ERBB4_3 | CHP2_ERBB4_3 | chr2 | 2.1E+08 | 2.1E+08 | + | GAGCAGGATAATAAAAGAGAGAAATCACAGACATACAAAGCAGTCTGTGTCCTTAGGTCCTGAGCAGCCTCCAGCACATTCTCGATGGCAGCAGTCACTGACG |
| CHP2_ERBB4_2 | CHP2_ERBB4_2 | chr2 | 2.1E+08 | 2.1E+08 | + | TGAGAAATTAAAAAGAATAATTCTACTTACATCCTGAACTACCATTTGTTGACACAAGAGTCAAGTTGGAAGGCCATGGGTTCCGAA |
| CHP2_ERBB4_1 | CHP2_ERBB4_1 | chr2 | 2.1E+08 | 2.1E+08 | + | ATATGACAGTAACCCTACATATACAATTGCCTTATATTGATAATGAAAGCATATTTGCCATTTTGGATATATTCCTTACCTGTCAAGTTCTTTA |
| CHP2_VHL_1 | CHP2_VHL_1 | chr3 | 1E+07 | 1E+07 | + | CGCAGTCCGCGCGTCGTGCTGCCCGTATGGCTCAACTTCGACGGCGAGCCGCAGCCCTACCCAACGCTGCCGCCTGGCACGGGCCGCCG |
| CHP2_VHL_2 | CHP2_VHL_2 | chr3 | 1E+07 | 1E+07 | + | TGTCCCGATAGGTCACCTTTGGCTCTTCAGAGATGCAGGGACACACGATGGGCTTCTGGTTAACCAAACTGAATTATTTGTGCCATCTCTCAATGTTGACGGACAGCCTATTTTTGCCAA |
| CHP2_VHL_3 | CHP2_VHL_3 | chr3 | 1E+07 | 1E+07 | + | CTTGTACTGAGACCCTAGTCTGCCACTGAGGATTTGGTTTTTGCCCTTCCAGTGTATACTCTGAAAGAGCGATGCCTCCAGGTTGTCCGGAGCCTAGTCAAGCCTGAGA |
| CHP2_MLH1_1 | CHP2_MLH1_1 | chr3 | 3.7E+07 | 3.7E+07 | + | AAGTAGTGATAAGGTCTATGCCCACCAGATGGTTCGTACAGATTCCCGGGAACAGAAGCTTGATGCATTTCTGCAGCCTCTGAGCAAACCCCTGTCCAGTCAGCCCCAGGCCATTGTCACAGAGGA |
| CHP2_CTNNB1_1 | CHP2_CTNNB1_1 | chr3 | 4.1E+07 | 4.1E+07 | + | GTTGGACATGGCCATGGAACCAGACAGAAAAGCGGCTGTTAGTCACTGGCAGCAACAGTCTTACCTGGACTCTGGAATCCATTCTGGTGCCACTACCACAGCTCCTTCTCTGAGTGGT |
| CHP2_PIK3CA_1 | CHP2_PIK3CA_1 | chr3 | 1.8E+08 | 1.8E+08 | + | AAATACCCCCTCCATCAACTTCTTCAAGATGAATCTTCTTACATTTTCGTAAGTGTTACTCAAGAAGCAGAAAGGGAAGAATTTTTTGATGAAACAAGACGACTTT |
| CHP2_PIK3CA_2 | CHP2_PIK3CA_2 | chr3 | 1.8E+08 | 1.8E+08 | + | AACCGTGAAGAAAAGATCCTCAATCGAGAAATTGGTATGATACAATATCCTATTCTAAAATGCAAATAACCATAAAGCTTAACTGTTGTCCCTTTCTAAAATAT |
| CHP2_PIK3CA_3 | CHP2_PIK3CA_3 | chr3 | 1.8E+08 | 1.8E+08 | + | CATATATGAATGGAGAAACATCTACAAAATCCCTTTGGGTTATAAATAGTGCACTCAGAATAAAAATTCTTTGTGCAACCTACGTGAATGTAAATATTCGAGACAT |
| CHP2_PIK3CA_4 | CHP2_PIK3CA_4 | chr3 | 1.8E+08 | 1.8E+08 | + | ATATATACATTCCTGATCTTCCTCGTGCTGCTCGACTTTGCCTTTCCATTTGCTCTGTTAAAGGCCGAAAGGGTGCTAAAGAGGTAAAGTATTTCAGAAGGAACAATTATGTTTACCTTT |
| CHP2_PIK3CA_5 | CHP2_PIK3CA_5 | chr3 | 1.8E+08 | 1.8E+08 | + | TTTGGGGAAGAAAAGTGTTTTGAAATGTGTTTTATAATTTAGACTAGTGAATATTTTTCTTGTTTTTTAAGGAACACTGTCCAT |
| CHP2_PIK3CA_6 | CHP2_PIK3CA_6 | chr3 | 1.8E+08 | 1.8E+08 | + | CATGGATTAGAAGATTTGCTGAACCCTATTGGTGTTACTGGATCAAATCCAAATAAAGTAAGGTTTTTATTGTCATAAATTAGATATTTTT |
| CHP2_PIK3CA_7 | CHP2_PIK3CA_7 | chr3 | 1.8E+08 | 1.8E+08 | + | ATTAAGGGAAAATGACAAAGAACAGCTCAAAGCAATTTCTACACGAGATCCTCTCTCTGAAATCACTGAGCAGGAGAAAGAT |
| CHP2_PIK3CA_8 | CHP2_PIK3CA_8 | chr3 | 1.8E+08 | 1.8E+08 | + | ATAAAACAGTTAGCCAGAGGTTTGGCCTGCTTTTGGAGTCCTATTGTCGTGCATGTGGGATGTATTTGAAGCACCTGAATAGGCAAGTCGAGGCAATGGAAAAGCTCATTAACTTAACTGACATTCTCAAA |
| CHP2_PIK3CA_9 | CHP2_PIK3CA_9 | chr3 | 1.8E+08 | 1.8E+08 | + | ACGTTCATGTGCTGGATACTGTGTAGCTACCTTCATTTTGGGAATTGGAGATCGTCACAATAGTAACATCATGGTGAA |
| CHP2_PIK3CA_10 | CHP2_PIK3CA_10 | chr3 | 1.8E+08 | 1.8E+08 | + | GACATTGCATACATTCGAAAGACCCTAGCCTTAGATAAAACTGAGCAAGAGGCTTTGGAGTATTTCATGAAACAAATGAATGATGCACATCATGGTGGCTG |
| CHP2_PIK3CA_11 | CHP2_PIK3CA_11 | chr3 | 1.8E+08 | 1.8E+08 | + | GCATTGAACTGAAAAGATAACTGAGAAAATGAAAGCTCACTCTGGATTCCACACTGCACTGTTAATAACTCTCAGCAGGCAAAGACCGATTGCATAG |
| CHP2_FGFR3_1 | CHP2_FGFR3_1 | chr4 | 1803527 | 1803678 | + | GCCCCCACAGAGCGCTCCCCGCACCGGCCCATCCTGCAGGCGGGGCTGCCGGCCAACCAGACGGCGGTGCTGGGCAGCGACGTGGAGTTCCACTGCAAGGTG |
| CHP2_FGFR3_2 | CHP2_FGFR3_2 | chr4 | 1806057 | 1806212 | + | CGAGGCGGGCAGTGTGTATGCAGGCATCCTCAGCTACGGGGTGGGCTTCTTCCTGTTCATCCTGGTGGTGGCGGCTGTGACGCTCTGCCGCCTGCGCAGCCCCCCC |
| CHP2_FGFR3_3 | CHP2_FGFR3_3 | chr4 | 1807809 | 1807955 | + | GAAGATCGCAGACTTCGGGCTGGCCCGGGACGTGCACAACCTCGACTACTACAAGAAGACGACCAACGTGAGCCCGGCCCTGGGGTGCGGGGGTGGG |
| CHP2_FGFR3_4 | CHP2_FGFR3_4 | chr4 | 1808287 | 1808424 | + | GGGGGGCTCCCCGTACCCCGGCATCCCTGTGGAGGAGCTCTTCAAGCTGCTGAAGGAGGGCCACCGCATGGACAAGCCCGCCAACTGC |
| CHP2_FGFR3_5 | CHP2_FGFR3_5 | chr4 | 1808857 | 1809031 | + | CCGGGTGGCCAGGACACCCCCAGCTCCAGCTCCTCAGGGGACGACTCCGTGTTTGCCCACGACCTGCTGCCCCCGGCCCCACCCAGCAGTGGGGGCTCGCGGACGTGAAGGGCCACTGGTCCCCA |
| CHP2_PDGFRA_1 | CHP2_PDGFRA_1 | chr4 | 5.5E+07 | 5.5E+07 | + | CAGTTACCTGTCCTGGTCATTTATAGAAACCGAGGTATGAAATTCGCTGGAGGGTCATTGAATCAATCAGCCCAGATGGACATGAATATATTTATGTGGACCCGATGCAGCTGCCTTATGAC |
| CHP2_PDGFRA_2 | CHP2_PDGFRA_2 | chr4 | 5.5E+07 | 5.5E+07 | + | AACTGAAGATAATGACTCACCTGGGGCCACATTTGAACATTGTAAACTTGCTGGGAGCCTGCACCAAGTCAGGTGGGCTCACTGACCTGGAGTG |
| CHP2_PDGFRA_3 | CHP2_PDGFRA_3 | chr4 | 5.5E+07 | 5.5E+07 | + | CATCATCACAGAGTATTGCTTCTATGGAGATTTGGTCAACTATTTGCATAAGAATAGGGATAGCTTCCTGAGCCACCACCCAGAGAAGCCAAAGAAAGAGCTGGATATCTTTGGA |
| CHP2_PDGFRA_4 | CHP2_PDGFRA_4 | chr4 | 5.5E+07 | 5.5E+07 | + | GGCTGCTCGCAACGTCCTCCTGGCACAAGGAAAAATTGTGAAGATCTGTGACTTTGGCCTGGCCAGAGACATCATGCATGATTCGAACTATGTGTCGAAAGGCAGTGTACGTCCTCACTTCCCTCACTGG |
| CHP2_KIT_1 | CHP2_KIT_1 | chr4 | 5.6E+07 | 5.6E+07 | + | CACGATTCTGTTTTTCTTGGCAGGCTCTTCTCAACCATCTGTGAGTCCAGGGGAACCGTCTCCACCATCCATCCATCCAGGAAAATCAGACTTAATAGTCCGCGTGGGCGACGAGATTAGGCTGTTATGC |
| CHP2_KIT_2 | CHP2_KIT_2 | chr4 | 5.6E+07 | 5.6E+07 | + | CAACGATGTGGGCAAGACTTCTGCCTATTTTAACTTTGCATTTAAAGGTAACAACAAAGGTATATTTCTTTTTAATCCAATTTAAGGGG |
| CHP2_KIT_3 | CHP2_KIT_3 | chr4 | 5.6E+07 | 5.6E+07 | + | GCTGATTGGTTTCGTAATCGTAGCTGGCATGATGTGCATTATTGTGATGATTCTGACCTACAAATATTTACAGGTAACCATTTATTTGTTCTCTCT |
| CHP2_KIT_4 | CHP2_KIT_4 | chr4 | 5.6E+07 | 5.6E+07 | + | CCACAGAAACCCATGTATGAAGTACAGTGGAAGGTTGTTGAGGAGATAAATGGAAACAATTATGTTTACATAGACCCAACACAACTTCCTTATGATCACAAATGGGAGTTTCCCAGAAAC |
| CHP2_KIT_5 | CHP2_KIT_5 | chr4 | 5.6E+07 | 5.6E+07 | + | TTTTAGCGAGTGCCCATTTGACAGAACGGGAAGCCCTCATGTCTGAACTCAAAGTCCTGAGTTACCTTGGTAATCACATGAATATTGTGAATCTACTTGGAGCCTGCAC |
| CHP2_KIT_6 | CHP2_KIT_6 | chr4 | 5.6E+07 | 5.6E+07 | + | TTAGGGCCCACCCTGGTCATTACAGAATATTGTTGCTATGGTGATCTTTTGAATTTTTTGAGAAGA |
| CHP2_KIT_7 | CHP2_KIT_7 | chr4 | 5.6E+07 | 5.6E+07 | + | GAGTGCCCTTCTACATGTCCCACTTGATTCAGTCATGACTTGTTTCATCTCTCCCAGCAGCGATAGTACTAATGAGTACATGGACATG |
| CHP2_KIT_8 | CHP2_KIT_8 | chr4 | 5.6E+07 | 5.6E+07 | + | GGTCGGATCACAAAGATTTGTGATTTTGGTCTAGCCAGAGACATCAAGAATGATTCTAATTATGTGGTTAAAGGAAAC |
| CHP2_KIT_9 | CHP2_KIT_9 | chr4 | 5.6E+07 | 5.6E+07 | + | CTGTGAAGTGGATGGCACCTGAAAGCATTTTCAACTGTGTATACACGTTTGAAAGTGACGTCTGGTCCTATGGGATTT |
| CHP2_KDR_9 | CHP2_KDR_9 | chr4 | 5.6E+07 | 5.6E+07 | + | GGGGTGTGGATGCTTCCTTTTAAACAGGAGGAGAGCTCAGTGTGGTCCCCGAGTCAGGCTGGAGAATCTGGGCTGTGCTACCGGTTTGCACTCCAATCTCTATCAGCTTTAAAAGTTCTG |
| CHP2_KDR_8 | CHP2_KDR_8 | chr4 | 5.6E+07 | 5.6E+07 | + | GATATCCGGACTGGTAGCCGCTTGTCTGGTTTGAGCCTTCAGATGCCACAGACTCCCTGCTTTTGCTGGGCACCATTCCACTGCAGAAGAATGGCAAACAAAGGAGTTGGCAGAGAGAAG |
| CHP2_KDR_7 | CHP2_KDR_7 | chr4 | 5.6E+07 | 5.6E+07 | + | GATTCCTGCTGTGTTGTCATAATGGAATTTGGGGTCACATACTTCCTCCTCCTCCATACAGGAAACAGGTGAGGTAGGCAGAGAG |
| CHP2_KDR_6 | CHP2_KDR_6 | chr4 | 5.6E+07 | 5.6E+07 | + | ACTCTGAAAACGTGGGTCTCTGACTGGGCTCCCCGTGCCAGCAGTCCAGCATGGTCTGGTACCTAGAGAAGCAAAACACTGATTTCATTA |
| CHP2_KDR_5 | CHP2_KDR_5 | chr4 | 5.6E+07 | 5.6E+07 | + | TCTTCTACATCACTGAGGGACTTCTCCTCCACAAATCCAGAGCTGGCTGAGCTCTGGCTACTGGTGATGCTGTCCAAGCGCCG |
| CHP2_KDR_4 | CHP2_KDR_4 | chr4 | 5.6E+07 | 5.6E+07 | + | ACCAATATGAATGAGGATCTTGAGTTCAGACATGAGAGCTCGATGCTCACTGTGTGTTGCTCCTTCTACAAATACAGTACAAAGAGGGAAATCATAGGTATGGA |
| CHP2_KDR_3 | CHP2_KDR_3 | chr4 | 5.6E+07 | 5.6E+07 | + | TGGGTTTGTCACTGAGACAGCTTGGCTATAAGAAAGAGATAACAGCGCATATTATGATTTAATTTTTCTTTAATTAGAGTCAAGAGTAAGGAAAAGATTCAGACTTTGGTTATTCTGTT |
| CHP2_KDR_2 | CHP2_KDR_2 | chr4 | 5.6E+07 | 5.6E+07 | + | GTGCTCAAAAATTTCTTCATCTCACTCCCAGACTGGGTTTTTAGGTCTCGGTTTACAAGTTTCTTATGCTGATGCTGAAAA |
| CHP2_KDR_1 | CHP2_KDR_1 | chr4 | 5.6E+07 | 5.6E+07 | + | CTGGGGCTTATTATCTAAGTATTTGGAGGTCTGGCTTTGAATCATTAGCGTTACCTTCGAAGAAGGGTATTCCCAGTTGAAGTCAATCCCCACATTTAGTTCAGTTCTTGCTGTACAATTT |
| CHP2_FBXW7_5 | CHP2_FBXW7_5 | chr4 | 1.5E+08 | 1.5E+08 | + | GAATATTGTCTTTGAGTTCCATTCCACTTGTTAACGACTGGTGCCCTGTTAACGTGTGAATGCAATTCCCTGTCTCCACATC |
| CHP2_FBXW7_4 | CHP2_FBXW7_4 | chr4 | 1.5E+08 | 1.5E+08 | + | TTGAACACAGCGGACTGCTGCAACATGACCCATCAAAACATGTAAACACTGGCCTGTCTCAATATCCCAAACCCTAAGAGTGGCATCTCGAG |
| CHP2_FBXW7_3 | CHP2_FBXW7_3 | chr4 | 1.5E+08 | 1.5E+08 | + | TTACCTTTTTTCATGAAGATGCATACAACGCACAGTGGAAGTATGCCCATATAAGGTGTGTATACATTCTCCAGTCTCTGCATTCCACACTTTGAGTGTCCGATCTGTAGATCCACTAATGA |
| CHP2_FBXW7_2 | CHP2_FBXW7_2 | chr4 | 1.5E+08 | 1.5E+08 | + | AAGTGTTGTCATCAGAACCACTAACTATTCGGTTACCACAAAACTGTAAGCATGTGATCACATGATCATCATGT |
| CHP2_FBXW7_1 | CHP2_FBXW7_1 | chr4 | 1.5E+08 | 1.5E+08 | + | GAGTTATATATTCAAATAACACCCAATGAAGAATGTAATTGATAATCTTTACCTCTTTAGGGAGCAATGAAATGAAGTCTCGTTGAAACTGGGGTTCTATCACTTGCATCATATGTTTTACT |
| CHP2_APC_1 | CHP2_APC_1 | chr5 | 1.1E+08 | 1.1E+08 | + | GGCAACTACCATCCAGCAACAGAAAATCCAGGAACTTCTTCAAAGCGAGGTTTGCAGATCTCCACCACTGCAGCCCAGATTGCCAAAGTCA |
| CHP2_APC_2 | CHP2_APC_2 | chr5 | 1.1E+08 | 1.1E+08 | + | CCAACCACATTTTGGACAGCAGGAATGTGTTTCTCCATACAGGTCACGGGGAGCCAATGGTTCAGAAACAAATCGAGTGGGTTCTAATCATGGAATTAATCAAAATGTA |
| CHP2_APC_3 | CHP2_APC_3 | chr5 | 1.1E+08 | 1.1E+08 | + | GATGAAATAGGATGTAATCAGACGACACAGGAAGCAGATTCTGCTAATACCCTGCAAATAGCAGAAATAAAAGAAAAGATTGGAACTAGGTCAGCTGAAGATCCTGTGAGCGAAGTTCCAGCAGT |
| CHP2_APC_4 | CHP2_APC_4 | chr5 | 1.1E+08 | 1.1E+08 | + | TATCTTCAGAATCAGCCAGGCACAAAGCTGTTGAATTTTCTTCAGGAGCGAAATCTCCCTCCAAAAGTGGTGCTCAGACACCCAAAAGTCCACCTGAACACTATGTTCAGGAGACCCCACTCATGTTT |
| CHP2_APC_5 | CHP2_APC_5 | chr5 | 1.1E+08 | 1.1E+08 | + | CTGGACAAACCATGCCACCAAGCAGAAGTAAAACACCTCCACCACCTCCTCAAACAGCTCAAACCAAGCGAGAAGTACCTAAAAATAAAGCACCTACTGCTGAAAAGAGAGAGAGTGGACCTAAGCAAGCTGC |
| CHP2_APC_6 | CHP2_APC_6 | chr5 | 1.1E+08 | 1.1E+08 | + | GATGCTGATACTTTATTACATTTTGCCACGGAAAGTACTCCAGATGGATTTTCTTGTTCATCCAGCCTGAGTGCTCTGAGCCTCGATGAGCCATTTATACAGAAAGATGTGGAATTAAGAAT |
| CHP2_APC_7 | CHP2_APC_7 | chr5 | 1.1E+08 | 1.1E+08 | + | GAATCAAATGAAAACCAAGAGAAAGAGGCAGAAAAAACTATTGATTCTGAAAAGGACCTATTAGATGATTCAGATGATGATGATATTGAAATACTAGAAGAATGTATTATTTCTG |
| CHP2_CSF1R_2 | CHP2_CSF1R_2 | chr5 | 1.5E+08 | 1.5E+08 | + | TGTGGGAGGGGAGAGTGGTACTCCCTGTCGTCAACTCCTCAGCAGAACTGATAGTTGTTGGGCTGCAGCAAGGGCTGGGCGATATCCCCTTGCTCGCAG |
| CHP2_CSF1R_1 | CHP2_CSF1R_1 | chr5 | 1.5E+08 | 1.5E+08 | + | CCCCTCCCCCACGGTCACCTCCTGGATGAGGTTCTGCTCAGAGCTCAAGTTCAAGTAGGCACTCTCTGGAAAGCAGAACACA |
| CHP2_NPM1_1 | CHP2_NPM1_1 | chr5 | 1.7E+08 | 1.7E+08 | + | TAACCACATTTCTTTTTTTTTTTTTCCAGGCTATTCAAGATCTCTGGCAGTGGAGGAAGTCTCTTTAAGAAAATAGTTTAAACAATTTGTTAAAAAATTTTCCGTCTTATTTCAT |
| CHP2_EGFR_1 | CHP2_EGFR_1 | chr7 | 5.5E+07 | 5.5E+07 | + | GGAGCGAATTCCTTTGGAAAACCTGCAGATCATCAGAGGAAATATGTACTACGAAAATTCCTATGCCTTAGCAGTCTTATCT |
| CHP2_EGFR_2 | CHP2_EGFR_2 | chr7 | 5.5E+07 | 5.5E+07 | + | GAACCCCGAGGGCAAATACAGCTTTGGTGCCACCTGCGTGAAGAAGTGTCCCCGTGAGTCCTCCTCTGTGGGCCCTCTAACTGGTCAGGCATCCTTGTCCCGCTCTGTCTCCTGCTGAGCCCTGGAG |
| CHP2_EGFR_3 | CHP2_EGFR_3 | chr7 | 5.5E+07 | 5.5E+07 | + | CTTGGTGCAGGGACCAGACAACTGTATCCAGTGTGCCCACTACATTGACGGCCCCCACTGCGTCAAGACCTGCCCGGCAGGAGTCATGGGA |
| CHP2_EGFR_4 | CHP2_EGFR_4 | chr7 | 5.5E+07 | 5.5E+07 | + | GTGGAGAAGCTCCCAACCAAGCTCTCTTGAGGATCTTGAAGGAAACTGAATTCAAAAAGATCAAAGTGCTGGGCTCCGGTGCGTTCGGCACGGT |
| CHP2_EGFR_5 | CHP2_EGFR_5 | chr7 | 5.5E+07 | 5.5E+07 | + | TAGGGACTCTGGATCCCAGAAGGTGAGAAAGTTAAAATTCCCGTCGCTATCAAGGAATTAAGAGAAGCAACATCTCCGAAAGCCAACAAGGAAATCCTCGATGTGAGTTTCTGCTTTGCTGTGTGGGGG |
| CHP2_EGFR_6 | CHP2_EGFR_6 | chr7 | 5.5E+07 | 5.5E+07 | + | GTGCCTCTCCCTCCCTCCAGGAAGCCTACGTGATGGCCAGCGTGGACAACCCCCACGTGTGCCGCCTGCTGGGCATCTGCCTCACCTCCACCGTGCAGCTCATCACGCAGCTCATGCCCTTCGGC |
| CHP2_EGFR_7 | CHP2_EGFR_7 | chr7 | 5.5E+07 | 5.5E+07 | + | CAATATTGGCTCCCAGTACCTGCTCAACTGGTGTGTGCAGATCGCAAAGGTAATCAGGGAAGGGAGATACGGGGAGGGGAGATAAGGAGCCAGGATCCTCACATGCGGTCTGCGCTCCTGGGA |
| CHP2_EGFR_8 | CHP2_EGFR_8 | chr7 | 5.5E+07 | 5.5E+07 | + | TTTGGGCTGGCCAAACTGCTGGGTGCGGAAGAGAAAGAATACCATGCAGAAGGAGGCAAAGTAAGGAGGTGGCTTTAGGTCAGCCAGCATTTTCCTGACACCAGGGACCAGGCTGCCTTCC |
| CHP2_MET_1 | CHP2_MET_1 | chr7 | 1.2E+08 | 1.2E+08 | + | TGCATATTCTCCCCACAGATAGAAGAGCCCAGCCAGTGTCCTGACTGTGTGGTGAGCGCCCTGGGAGCCAAAGTCCTTTCATCTGT |
| CHP2_MET_2 | CHP2_MET_2 | chr7 | 1.2E+08 | 1.2E+08 | + | GACATTCTTTTCGGGGTGTTCGCACAAAGCAAGCCAGATTCTGCCGAACCAATGGATCGATCTGCCATGTGTGCATTCCCTATCAAATATGTCAACGACTTCTTCAACAAGATCG |
| CHP2_MET_3 | CHP2_MET_3 | chr7 | 1.2E+08 | 1.2E+08 | + | TAATCTGTTGTACCACTCCTTCCCTGCAACAGCTGAATCTGCAACTCCCCCTGAAAACCAAAGCCTTTTTCATGTTAGATGGGATCCTTTCCAAATACTTTGATCTCATTTATGTACATA |
| CHP2_MET_4 | CHP2_MET_4 | chr7 | 1.2E+08 | 1.2E+08 | + | CTCTTTCTTTCTCTCTGTTTTAAGATCTGGGCAGTGAATTAGTTCGCTACGATGCAAGAGTACACACTCCTCATTTGGATAGGCTTGTAAGTGCCCGAAGTGTAAGCCCAACTACAGAA |
| CHP2_MET_5 | CHP2_MET_5 | chr7 | 1.2E+08 | 1.2E+08 | + | CTTTCTTTTGCACAGGGCATTTTGGTTGTGTATATCATGGGACTTTGTTGGACAATGATGGCAAGAAAATTCACTGTGCTGTGAAATCCTTGAACAGTAAGTGGCATTTTATTTA |
| CHP2_MET_6 | CHP2_MET_6 | chr7 | 1.2E+08 | 1.2E+08 | + | ACATGTATGATAAAGAATACTATAGTGTACACAACAAAACAGGTGCAAAGCTGCCAGTGAAGTGGATGGCTTTGGAAAGTCTGCA |
| CHP2_SMO_1 | CHP2_SMO_1 | chr7 | 1.3E+08 | 1.3E+08 | + | GTTCAACAGTTCAGGCCAGTGCGAAGTGCCCTTGGTTCGGACAGACAACCCCAAGAGCTGGTACGAGGACGTGGAGGGCTGCGGCATCCAGTGCCAGAACCCGCTCTTCACAGAGGCTGAGCACC |
| CHP2_SMO_2 | CHP2_SMO_2 | chr7 | 1.3E+08 | 1.3E+08 | + | CCGCCTCAAGTGACACCTCACCTCTCTGCACAGCTCCAATGAGACTCTGTCCTGCGTCATCATCTTTGTCATCGTGTACTACGCCCTGATGGCTGGTGTGGTTTGG |
| CHP2_SMO_3 | CHP2_SMO_3 | chr7 | 1.3E+08 | 1.3E+08 | + | GTGGGCTACAAGAACTACCGATACCGTGCGGGCTTCGTGCTGGCCCCAATCGGCCTGGTGCTCATCGTGGGAGGCTACTTCC |
| CHP2_SMO_4 | CHP2_SMO_4 | chr7 | 1.3E+08 | 1.3E+08 | + | TCGCCCGAGCCTTCTGGTGGAGAAGATCAACCTGTTTGCCATGTTTGGAACTGGCATCGCCATGAGCACCTGGGTCTGGACCAAGGCCACGCTG |
| CHP2_SMO_5 | CHP2_SMO_5 | chr7 | 1.3E+08 | 1.3E+08 | + | GAGCCCTCAGCTGATGTCTCCTCTGCCTGGGCCCAGCATGTCACCAAGATGGTGGCTCGGAGAGGAGCCATACTGCCCCAGGATATTTCTGTCACCCCTGTGGCAACTCCAGG |
| CHP2_BRAF_2 | CHP2_BRAF_2 | chr7 | 1.4E+08 | 1.4E+08 | + | TCAAACTGATGGGACCCACTCCATCGAGATTTCACTGTAGCTAGACCAAAATCACCTATTTTTACTGTGAGGTCTTCATGAAGAAATATATCTGAGGTGTAGTAAGTAAAGGAAAACAG |
| CHP2_BRAF_1 | CHP2_BRAF_1 | chr7 | 1.4E+08 | 1.4E+08 | + | GTAGACTGTTCCAAATGATCCAGATCCAATTCTTTGTCCCACTGTAATCTGCCCATCAGGAATCTCCCAATCATCACTCGAGTCCCGTCTACCAAGTGTTTTCTTGATAAAAACAGTAAAAAAG |
| CHP2_EZH2_1 | CHP2_EZH2_1 | chr7 | 1.5E+08 | 1.5E+08 | + | AGTGCCTTACCTCTCCACAGTATTCTGAGATGAATTCATTTTTCTGCACAGGATCTTTGATAAAAATCCCCCAGCCTGCCACGTC |
| CHP2_FGFR1_2 | CHP2_FGFR1_2 | chr8 | 3.8E+07 | 3.8E+07 | + | CTCCACGTTGCTACCCAGGGCCACTGTTTTGTTGGCGGGCAACCCTGCTTGCAGGATGGGCCGGTGAGGGGACCGCTCTGTGGAAGATGGGAGAGGAGGCACTTGTCATGGGGA |
| CHP2_FGFR1_1 | CHP2_FGFR1_1 | chr8 | 3.8E+07 | 3.8E+07 | + | ACAGTGTCTCACGCATACGGTTTGGTTTGGTGTTATCTGTTTCTTTCTCCTCTGAAGAGGAGTCATCATCATCATCATCATCCTCCGAGGAGGGGAGAGCATCTATGGAAGAAGAAGGGGCAC |
| CHP2_JAK2_1 | CHP2_JAK2_1 | chr9 | 5073705 | 5073882 | + | GCTTTCTCACAAGCATTTGGTTTTAAATTATGGAGTATGTGTCTGTGGAGACGAGAGTAAGTAAAACTACAGGCTTTCTAATGCCTTTCTCAGAGCATCTGTTTTTGTTTATATAGAAAATTCAGTTT |
| CHP2_CDKN2A_2 | CHP2_CDKN2A_2 | chr9 | 2.2E+07 | 2.2E+07 | + | GCCTCTGGTGCCCCCCGCAGCCGCGCGCAGGTACCGTGCGACATCGCGATGGCCCAGCTCCTCAGCCAGGTCCACGGGCAGACGGCCCCAGGCATCGCGCACGTCCAGCCGCGCCCCGGCCCGGTG |
| CHP2_CDKN2A_1 | CHP2_CDKN2A_1 | chr9 | 2.2E+07 | 2.2E+07 | + | GCCCTCCCGGGCAGCGTCGTGCACGGGTCGGGTGAGAGTGGCGGGGTCGGCGCAGTTGGGCTCCGCGCCGTGGAGCAGCAGCAGCTCCGCCACTCGGGCGCTGCCCATCATCATGACCTGCCAGAGAGA |
| CHP2_GNAQ_1 | CHP2_GNAQ_1 | chr9 | 8E+07 | 8E+07 | + | TACCTCATTGTCTGACTCCACGAGAACTTGATCATATTCACTAAGCGCTACTAGAAACATGATAGAGGTGACATTTTCAAAGCAGTGTATCCATTTTCTTCTCTCTGACCTTTGGCCCCCTAC |
| CHP2_ABL1_1 | CHP2_ABL1_1 | chr9 | 1.3E+08 | 1.3E+08 | + | ACGACAAGTGGGAGATGGAACGCACGGACATCACCATGAAGCACAAGCTGGGCGGGGGCCAGTACGGGGAGGTGTACGAGGGCG |
| CHP2_ABL1_2 | CHP2_ABL1_2 | chr9 | 1.3E+08 | 1.3E+08 | + | TAACTAGTCAAGTACTTACCCACTGAAAAGCACTTCCTGAAATAATTTCACCTTCGTTTTTTTCCTTCTGCAGGAGGACACCATGGAG |
| CHP2_ABL1_3 | CHP2_ABL1_3 | chr9 | 1.3E+08 | 1.3E+08 | + | TGAGTTCATGACCTACGGGAACCTCCTGGACTACCTGAGGGAGTGCAACCGGCAGGAGGTGAACGCCGTGGTGCTGCTGTACATGGCCACTCAGATCTCGTCAGCCATGGAGTACCTGGAGAAGAAAAACTTCA |
| CHP2_ABL1_4 | CHP2_ABL1_4 | chr9 | 1.3E+08 | 1.3E+08 | + | CTGATTTTGGCCTGAGCAGGTTGATGACAGGGGACACCTACACAGCCCATGCTGGAGCCAAGTTCCCCATCAAATGGACTGCACCCGAGAGCCTGGCC |
| CHP2_NOTCH1_3 | CHP2_NOTCH1_3 | chr9 | 1.4E+08 | 1.4E+08 | + | CGGGTGGGACCAGCGAGGATGGCAGCGACGTGGGCAGGGCGGGGCTCTCCTGGGGCAGAATAGTGTGCACCGCCAGGCTGCTGGGGCCCAGTGGCTGCACGTCTGCCTGGCTCGGCTCTCC |
| CHP2_NOTCH1_2 | CHP2_NOTCH1_2 | chr9 | 1.4E+08 | 1.4E+08 | + | TCTCCAGGTAGACGATGGAGCTGGGCGGACAATCAGAGAGGGGCTGGGACCCGAGGCTTCCTCCTCCCCCGCCCACCGGCCAGGGATGCTGCCGCAGGACACTGAGGCCCATGACGC |
| CHP2_NOTCH1_1 | CHP2_NOTCH1_1 | chr9 | 1.4E+08 | 1.4E+08 | + | GTGTGCAGCACGCGGCTGAGCTCCCGCAGGAAGTGGAAGGAGCTGTTGCGCAGCTGCTCCGGCGGCATCAGCACCACCACCACCAGCGTGCCGGCCGCCAGCCTCTCGGG |
| CHP2_RET_1 | CHP2_RET_1 | chr10 | 4.4E+07 | 4.4E+07 | + | CCTGCAACTGCTTCCCTGAGGAGGAGAAGTGCTTCTGCGAGCCCGAAGACATCCAGGGTGAGTGGGTGGCGGCCGGGACCACCACCACCTCCCAGCCCCACAGAGGTCTCAACAGC |
| CHP2_RET_2 | CHP2_RET_2 | chr10 | 4.4E+07 | 4.4E+07 | + | GTGGTGCCGAGCCTCTGGCGGTGCCAAGCCTCACACCACCCCCACCCACAGATCCACTGTGCGACGAGCTGTGCCGCACGGTGATCGCAGCCGCTGTCCTCTTCTCCTTCATCGTCTCGGTGCTGCTGTCTGCC |
| CHP2_RET_3 | CHP2_RET_3 | chr10 | 4.4E+07 | 4.4E+07 | + | GCAACCTGCTCTGTGCTGCATTTCAGAGAACGCCTCCCCGAGTGAGCTGCGAGACCTGCTGTCAGAGTTCAACGTCCTGAAGCAGGTCAACCACCCACA |
| CHP2_RET_4 | CHP2_RET_4 | chr10 | 4.4E+07 | 4.4E+07 | + | CAGAAACATCCTGGTAGCTGAGGGGCGGAAGATGAAGATTTCGGATTTCGGCTTGTCCCGAGATGTTTATGAAGAGGATTCCTACGTGAAGAGGAGCCAGGTGCCCAGTCCCGGGGATGAGGCGGGGCTCCCAGGG |
| CHP2_RET_5 | CHP2_RET_5 | chr10 | 4.4E+07 | 4.4E+07 | + | AGGGCCTGGCCTTCTCCTTTACCCCTCCTTCCTAGAGAGTTAGAGTAACTTCAATGTCTTTATTCCATCTTCTCTTTAGGGTCGGATTCCAGTTAAATGGATGGCAATTGAATCCCTTT |
| CHP2_PTEN_1 | CHP2_PTEN_1 | chr10 | 9E+07 | 9E+07 | + | CAGCCACAGGCTCCCAGACATGACAGCCATCATCAAAGAGATCGTTAGCAGAAACAAAAGGAGATATCAAGAGGATGGATTCGACTTAGACTT |
| CHP2_PTEN_2 | CHP2_PTEN_2 | chr10 | 9E+07 | 9E+07 | + | TTTGTTTTAAGGTTTTTGGATTCAAAGCATAAAAACCATTACAAGATATACAATCTGTAAGTATGTTTTCTTATTTGTATGCTTGCAAATATCTTCTAAAACAACTATTAAGTGAA |
| CHP2_PTEN_3 | CHP2_PTEN_3 | chr10 | 9E+07 | 9E+07 | + | CTTATCAAACCCTTTTGTGAAGATCTTGACCAATGGCTAAGTGAAGATGACAATCATGTTGCAGCAATTCACTGTAAAGCTGGAAAGGGACGAACTGGTGTAATGAT |
| CHP2_PTEN_4 | CHP2_PTEN_4 | chr10 | 9E+07 | 9E+07 | + | CAATTTAGTGAAATAACTATAATGGAACATTTTTTTTCAATTTGGCTTCTCTTTTTTTTCTGTCCACCAGGGAGTAACTATTCCCAGTCAGAGGCGCTATGTGTATTATTATAGCTACCTGTTAAAGA |
| CHP2_PTEN_5 | CHP2_PTEN_5 | chr10 | 9E+07 | 9E+07 | + | ATATTTCGTGTATATTGCTGATATTAATCATTAAAATCGTTTTTGACAGTTTGACAGTTAAAGGCATTTCCTGTGAAATAATACTGGTATGTATTTAACCATGCAGATCCTCAGTTT |
| CHP2_PTEN_6 | CHP2_PTEN_6 | chr10 | 9E+07 | 9E+07 | + | CCACACGACGGGAAGACAAGTTCATGTACTTTGAGTTCCCTCAGCCGTTACCTGTGTGTGGTGATATCAAAGTAGAGTTCTTCCACAAACAGAACAAGATGCTAAAAAAGGTTT |
| CHP2_PTEN_7 | CHP2_PTEN_7 | chr10 | 9E+07 | 9E+07 | + | CCAGAGGAAACCTCAGAAAAAGTAGAAAATGGAAGTCTATGTGATCAAGAAA |
| CHP2_PTEN_8 | CHP2_PTEN_8 | chr10 | 9E+07 | 9E+07 | + | CAAGGAATATCTAGTACTTACTTTAACAAAAAATGATCTTGACAAAGCAAATAAAGACAAAGCCAACCGATACTTTTCTCCAAATTTTAAGGTCAGTTAAATTAAACATTTTGTGG |
| CHP2_FGFR2_4 | CHP2_FGFR2_4 | chr10 | 1.2E+08 | 1.2E+08 | + | ATGATTCAATCAAACTGCAGAGTATTTGGGCGAATGCAGTTTTTCCTCCTACTCACCATCCTGTGTGCAGGCTCCAAGAAGATTTATGATATT |
| CHP2_FGFR2_3 | CHP2_FGFR2_3 | chr10 | 1.2E+08 | 1.2E+08 | + | CGGCACAGGATGACTGTTACCACCATACAGGCGATTAAGAAGACCCCTATGCAGTAAATGGCTATCTCCAGGTAGTCTGGGGAAGCTGTAATCTCCTTTTCTCTTCCAGGCGCT |
| CHP2_FGFR2_2 | CHP2_FGFR2_2 | chr10 | 1.2E+08 | 1.2E+08 | + | AAATCAAAGAACCTGTGGCCAAACCCATGAAGGAGACCCCAGTTGTGGGTACCTTTAGATTCAGAAAGTCCTCACCTTGAGAACCTTGAGGTAGGGCAGCCCGTCGGGCCCGTATTTACTGCCGTTC |
| CHP2_FGFR2_1 | CHP2_FGFR2_1 | chr10 | 1.2E+08 | 1.2E+08 | + | TCTACGTCTCCTCCGACCACTGTGGAGGCATTTGCCGGCAGTCCGGCTTGGAGGATGGGCCGGTGAGGCGATCGCTCTGGTGGAGAGAGGGAAGAAAGGAGGAGTG |
| CHP2_HRAS_2 | CHP2_HRAS_2 | chr11 | 533788 | 533955 | + | CACACACAGGAAGCCCTCCCCGGTGCGCATGTACTGGTCCCGCATGGCGCTGTACTCCTCCTGGCCGGCGGTATCCAGGATGTCCAACAGGCACGTCTCCCCATCAATGACCACCTGC |
| CHP2_HRAS_1 | CHP2_HRAS_1 | chr11 | 534196 | 534333 | + | GGGGTCGTATTCGTCCACAAAATGGTTCTGGATCAGCTGGATGGTCAGCGCACTCTTGCCCACACCGCCGGCGCCCACCACCACCAGC |
| CHP2_ATM_1 | CHP2_ATM_1 | chr11 | 1.1E+08 | 1.1E+08 | + | TAGGAAGTAGAGGAAAGTATTCTTCAGGATTTCGTAATATTGCCGTCAAAGAAAATTTGATTGAATTGATGGCAGATATCTGTCACCAGGTACAGTAAGT |
| CHP2_ATM_2 | CHP2_ATM_2 | chr11 | 1.1E+08 | 1.1E+08 | + | GATCTTGTGCCTTGGTAAAGTGTTACCATTTTCTCATTCAGTGTCATTTTAATCTCTTGTATGTTATTTTTCAGAA |
| CHP2_ATM_3 | CHP2_ATM_3 | chr11 | 1.1E+08 | 1.1E+08 | + | AAGTGAAGCTTTTTGTTTTTCTTTGTAGTAATTTTCCTCATCTTGTACTGGAGAAAATTCTTGTGAGTCTCACTATGAAAAACTGTAAAGCTGCAATGAATTT |
| CHP2_ATM_4 | CHP2_ATM_4 | chr11 | 1.1E+08 | 1.1E+08 | + | AAGTAGAATCAATGGAAGATGATACTAATGGAAATCTAATGGAGGTGGAGGATCAGTCATCCATGAATCTATTTAACGATTACCCTGATAGTAG |
| CHP2_ATM_5 | CHP2_ATM_5 | chr11 | 1.1E+08 | 1.1E+08 | + | AATATTCTTCCTTATTTTGCCTATGAGGGTACCAGAGACAGTGGGATGGCACAGCAAAGAGAGACTGCTACCAAGGTCTATGATATGCTTAAAAGTG |
| CHP2_ATM_6 | CHP2_ATM_6 | chr11 | 1.1E+08 | 1.1E+08 | + | CTTGGGAGAAGTGGGTCCTATAGATTTCTCTACCATAGCTATACAACATAGTAAAGATGCATCTTATACCAAGGCCCTTAAGTTATTTGAAGATAAAGAA |
| CHP2_ATM_7 | CHP2_ATM_7 | chr11 | 1.1E+08 | 1.1E+08 | + | TGTTTTTTTCAGTGTCAAAGTTCGATCAGCAGCTGTTACCTGTTTGAAAAACATTTTAGCCACAAAGACTGGACATAGTTTCTGGGAGATTTATAAGATGACAAC |
| CHP2_ATM_8 | CHP2_ATM_8 | chr11 | 1.1E+08 | 1.1E+08 | + | GATATAAATCTGTGGATTCCTCTAAGTGAAAATCATGACATTTGGATAAAGACACTGACTTGTGCTTTTTGG |
| CHP2_ATM_9 | CHP2_ATM_9 | chr11 | 1.1E+08 | 1.1E+08 | + | ATTTTTAATGATGCTTTCTGGCTGGATTTAAATTATCTAGAAGTTGCCAAGGTAGCTC |
| CHP2_ATM_10 | CHP2_ATM_10 | chr11 | 1.1E+08 | 1.1E+08 | + | TTTTACCTTAATTATTCTATGCAAGATACACAGTAAAGGTTCAGCGAGAGCTGGAGTTGGATGAATTAGCCCTGCGTG |
| CHP2_ATM_11 | CHP2_ATM_11 | chr11 | 1.1E+08 | 1.1E+08 | + | CCAGCCAATTACTAAACTTAAGAATTTAGAAGATGTTGTTGTCCCTACTA |
| CHP2_ATM_12 | CHP2_ATM_12 | chr11 | 1.1E+08 | 1.1E+08 | + | ATACAGTCATTTAAAGCAGAATTTCGCTTAGCAGGAGGTGTAAATTTACCAAAAATAATAGATTGTGTAGGTTCCGATGGCAAGG |
| CHP2_ATM_13 | CHP2_ATM_13 | chr11 | 1.1E+08 | 1.1E+08 | + | ATAATAAAATAAACTGTACTTGTTTATTCATGCTTAATTATTCTGAAGGGCCGTGATGACCTGAGACAAGATGCTGTCATGCAACAGGTCTTCCAGATGTGTAAT |
| CHP2_ATM_14 | CHP2_ATM_14 | chr11 | 1.1E+08 | 1.1E+08 | + | ACTTGGACTTGGTGATAGACATGTACAGAATATCTTGATAAATGAGCAGTCAGCAGAACTTGTACATATAGATCTAGGTAAGTAATAAAATCTATGTATCTATTCTTTTTAGTAAATATTTGGTCATCA |
| CHP2_ATM_15 | CHP2_ATM_15 | chr11 | 1.1E+08 | 1.1E+08 | + | AACCATGGAAGTGATGAGAAACTCTCAGGAAACTCTGTTAACCATTGTAGAGGTAAAGTATTTTATAAGGAAGACTTTATTTT |
| CHP2_ATM_16 | CHP2_ATM_16 | chr11 | 1.1E+08 | 1.1E+08 | + | TGTCCTTAGTGATATTGACCAGAGTTTCAACAAAGTAGCTGAACGTGTCTTAATGAGACTACAAGAGAAACTGAAAGGAGTGGAAGAAGGCACTGTGC |
| CHP2_ATM_17 | CHP2_ATM_17 | chr11 | 1.1E+08 | 1.1E+08 | + | CCCCAAAAATCTCAGCCGACTTTTCCCAGGATGGAAAGCTTGGGTGTGATCTTCAGTATATGAATTACCCTTTCATTCAGCCTTTAGAAATTATATTTT |
| CHP2_KRAS_3 | CHP2_KRAS_3 | chr12 | 2.5E+07 | 2.5E+07 | + | GTCTTGTCTTTGCTGATGTTTCAATAAAAGGAATTCCATAACTTCTTGCTAAGTCCTGAGCCTGTTTTGTGTCTACTGTTCTAGAAGGCAAATCACATTTATTTCCTAC |
| CHP2_KRAS_2 | CHP2_KRAS_2 | chr12 | 2.5E+07 | 2.5E+07 | + | GCACTGTACTCCTCTTGACCTGCTGTGTCGAGAATATCCAAGAGACAGGTTTCTCCATCAATTACTACTTGCTTCCTGTAGGAATCCTGAGAAGGGAGAAACAC |

| | | | | | | |
|---|---|---|---|---|---|---|
| CHP2_KRAS_1 | CHP2_KRAS_1 | chr12 | 2.5E+07 | 2.5E+07 | + | GCATATTAAAACAAGATTTACCTCTATTGTTGGATCATATTCGTCCACAAAATGATTCTGAATTAGCTGTATCGTCAAGGCACTCTTGCCTACGCCACCAGCTCCAACTACCACAAGT |
| CHP2_PTPN11_1 | CHP2_PTPN11_1 | chr12 | 1.1E+08 | 1.1E+08 | + | TAGAAGAAATGGAGCTGTCACCCACATCAAGATTCAGAACACTGGTGATTACTATGACCTGTATGGAGGGGAGAAATTTGCCACTTTGGCTGAGTTGGTCCAGTATTACA |
| CHP2_PTPN11_2 | CHP2_PTPN11_2 | chr12 | 1.1E+08 | 1.1E+08 | + | TGCGATATTGACGTTCCCAAAACCATCCAGATGGTGCGGTCTCAGAGGTCAGGGATGGTCCAGACAGAAGCACAGTACCGATTTATCTATATGGCGGTCCAGCATTATATTGAAACACTACAGCGC |
| CHP2_HNF1A_1 | CHP2_HNF1A_1 | chr12 | 1.2E+08 | 1.2E+08 | + | TGAGCTACCAACCAAGAAGGGGCGGAGGAACCGTTTCAAGTGGGGCCCAGCATCCCAGCAGATCCTGTTCCAGGCCTATGAGAGGCAG |
| CHP2_HNF1A_2 | CHP2_HNF1A_2 | chr12 | 1.2E+08 | 1.2E+08 | + | GGCTGGGCTCCAACCTCGTCACGGAGGTGCGTGTCTACAACTGGTTTGCCAACCGGCGCAAAGAAGAAGCCTTCCGGCACAAGCTGGCC |
| CHP2_FLT3_4 | CHP2_FLT3_4 | chr13 | 2.9E+07 | 2.9E+07 | + | ATAAGTAGGAAATAGCAGCCTCACATTGCCCCTGACAACATAGTTGGAATCACTCATGATATCTCGAGCCAATCCAAAGTCACA |
| CHP2_FLT3_3 | CHP2_FLT3_3 | chr13 | 2.9E+07 | 2.9E+07 | + | AGTCTTTTTGATGAGGTGATTTTCGTGGAAGTGGGTTACCTGACAGTGTGCACGCCCCCAGCAGGTTCACAATATTCTCGTGGCTTCCCAGCTGGGTCATCATC |
| CHP2_FLT3_2 | CHP2_FLT3_2 | chr13 | 2.9E+07 | 2.9E+07 | + | AATTTTCTCTTGGAAACTCCCATTTGAGATCATATTCATATTCTCTGAAATCAACGTAGAAGTACTCATTATCTGAGGAGCCGGTCACCTGTACCATCTGTAGCTGGCTTTCATACCTAAA |
| CHP2_FLT3_1 | CHP2_FLT3_1 | chr13 | 2.9E+07 | 2.9E+07 | + | TCTTCCAGGTCCAAGATGGTAATGGGTATCCATCCGAGAAACAGGACGCCTGACTTGCCGATGCTTCTGCGAGCACTTGAGGTTTCCCTAT |
| CHP2_RB1_1 | CHP2_RB1_1 | chr13 | 4.9E+07 | 4.9E+07 | + | AATTCTTTAACTTACTAAAAGAAATTGATACCAGTACCAAAGTTGATAATGCTATGTCAAGACTGTTGAAGAAGTATGATGTATTGTTT |
| CHP2_RB1_2 | CHP2_RB1_2 | chr13 | 4.9E+07 | 4.9E+07 | + | CACATTTTATTAGCTAAAGGTAAGTTCATTATATTTATTAAATGCTAATATTTCAAATGTAATAATTAAATTGGCATTCCTTTGGACTAAATTCCCCAATTTTTATTGAGTAATG |
| CHP2_RB1_3 | CHP2_RB1_3 | chr13 | 4.9E+07 | 4.9E+07 | + | TAATTGTCAGTGACTTTTTTCTTTCAAGGTTGAAAATCTTTCTAAACGATACGAAGAAATTTATCTTAAAAATAAAGATCTAGATGCAAGATTATTTTTGGATCATGATAAAACTCTTCAGAC |
| CHP2_RB1_4 | CHP2_RB1_4 | chr13 | 4.9E+07 | 4.9E+07 | + | TTTGATGCATAAAGCACAAATTGTAAATTTTCAGTATGTGAATGACTTCACTTATTGTTATTTAGTTTTGAAACACAGAGAACACCACGAAAAAGTAACCTTGATGAAGAGGTG |
| CHP2_RB1_5 | CHP2_RB1_5 | chr13 | 4.9E+07 | 4.9E+07 | + | TATTACCGAGTAATGGAATCCATGCTTAAATCAGTAAGTTAAAAACAATATAAAAAAATTTCAGCCGGGCGCGGTGGCTCACGCCTGCAATCCCAGCACTTTGGGAGGCCGAGGTGGGCAG |
| CHP2_RB1_6 | CHP2_RB1_6 | chr13 | 4.9E+07 | 4.9E+07 | + | AAACATTTAGAACGATGTGAACATCGAATCATGGAATCCCTTGCATGGCTCTCAGTAAGTAGCTAAATAATTGAAGAAAT |
| CHP2_RB1_7 | CHP2_RB1_7 | chr13 | 4.9E+07 | 4.9E+07 | + | TAATTTCATCATGTTTCATATAGGATTCACCTTTATTTGATCTTATTAAACAATCAAAGGACCGAGAAGGACC |
| CHP2_RB1_8 | CHP2_RB1_8 | chr13 | 4.9E+07 | 4.9E+07 | + | TCGGCTAGCCTATCTCCGGCTAAATACACTTTGTGAACGCCTTCTGTCTGAGCACCCAGAATTAGAACATATCATCTGGACCCTTTTCCAGCACACCCTGCAGAATG |
| CHP2_RB1_9 | CHP2_RB1_9 | chr13 | 4.9E+07 | 4.9E+07 | + | TACATCAATTTATTTACTAGATTATGATGTGTTCCATGTATGGCATATGCAAAGTGAAGAATATAGACCTTAAATTCAAAATCATT |
| CHP2_RB1_10 | CHP2_RB1_10 | chr13 | 4.9E+07 | 4.9E+07 | + | TGATCAAAGAAGAGGAGTATGATTCTATTATAGTATTCTATAACTCGGTCTTCATGCAGAGACTGAAAACAAATATTTTGCAG |
| CHP2_AKT1_2 | CHP2_AKT1_2 | chr14 | 1.1E+08 | 1.1E+08 | + | CTTGAGGATCTTCATGGCGTAGTAGCGGCCTGTGGCCTTCTCCTTCACCAGGATCACCTTGCCGAAAGTGCCCTTGCCCAGCAGCT |
| CHP2_AKT1_1 | CHP2_AKT1_1 | chr14 | 1.1E+08 | 1.1E+08 | + | GAGCCTCACGTTGGTCCACATCCTGCGGCCGCTCCTTGTAGCCAATGAAGGTGCCATCATTCTTGAGGAGGAAGTAGCGTGGCCGCCAGGTCTTGATGTACTCCCCTACAGACGTGCGGGTGGTGAGAGCCACGC |
| CHP2_IDH2_1 | CHP2_IDH2_1 | chr15 | 9.1E+07 | 9.1E+07 | + | GCCATGGGCGTGCCTGCCAATGGTGATGGGCTTGGTCCAGCCAGGGACTAGGCGTGGGATGTTTTTGCAGATGATGGGCTCCCGGAAGACAGTCCCCCCCAGGATGTTCCGGATAGTTCCATTGGGACTT |
| CHP2_CDH1_1 | CHP2_CDH1_1 | chr16 | 6.9E+07 | 6.9E+07 | + | GGACAGCCTATTTTTCCCTCGACACCCGATTCAAAGTGGGCACAGATGGTGTGATTACAGTCAAAAGGCCTCTACGGTTTCATAACCCACAGATC |
| CHP2_CDH1_2 | CHP2_CDH1_2 | chr16 | 6.9E+07 | 6.9E+07 | + | GATCTCTCTGCAGAGTTTCCCTACGTATACCCTGGTGGTTCAAGCTGCTGACCTTCAAGGTGAGGGGTTAAGCACAACAGCAACAGCTGTGATCACAGTCACTGACACCAACGATAATCCTCCGATC |
| CHP2_CDH1_3 | CHP2_CDH1_3 | chr16 | 6.9E+07 | 6.9E+07 | + | TCTCTTTGCTCTGCAGTACAAGGGTCAGGTGCCTGAGAACGAGGCTAACGTCGTAATCACCACACTGAAAGTGACTGATGCTGATGCCCCCAATACCCCAGCG |
| CHP2_TP53_8 | CHP2_TP53_8 | chr17 | 7573899 | 7574060 | + | CACCTGGAGTGAGCCCTGCTCCCCCCTGGCTCCTTCCCAGCCTGGGCATCCTTGAGTTCCAAGGCCTCATTCAGCTCTCGGAACATCTCGAAGCGCTCACGCCCACGGATCT |
| CHP2_TP53_7 | CHP2_TP53_7 | chr17 | 7576991 | 7577176 | + | CCTCGCTTAGTGCTCCCTGGGGGCAGCTCGTGGTGAGGCTCCCCTTTCTTGCGGAGATTCTCTTCCTCTGTGCGCCGGTCTCTCCCAGGACAGGCACAAACACGCACCTCAAAGCTGTTCCGTCCCAGTAGATT |
| CHP2_TP53_6 | CHP2_TP53_6 | chr17 | 7577484 | 7577637 | + | CCAGTGTGATGATGGTGAGGATGGGCCTCCGGTTCATGCCGCCCATGCAGGAACTGTTACACATGTAGTTGTAGTGGATGGTGGTACAGTCAGAGCCAACCTAG |
| CHP2_TP53_5 | CHP2_TP53_5 | chr17 | 7578156 | 7578323 | + | GGCGGCTCATAGGGCACCACCACACTATGTCGAAAAGTGTTTCTGTCATCCAAATACTCCACACGCAAATTTCCTTCCACTCGGATAAGATGCTGAGGAGGGGCCAGACCTAAGAGCA |
| CHP2_TP53_4 | CHP2_TP53_4 | chr17 | 7578328 | 7578508 | + | CAGCCCCAGCTGCTCACCATCGCTATCTGAGCAGCGCTCATGGTGGGGGCAGCGCCTCACAACCTCCGTCATGTGCTGTGACTGCTTGTAGATGGCCATGGCGCCGGACGCGGGTGCCGGGCGGGGGTGTG |
| CHP2_TP53_3 | CHP2_TP53_3 | chr17 | 7578492 | 7578626 | + | GCCAGTTGGCAAAACATCTTGTTGAGGGCAGGGGAGTACTGTAGGAAGAGGAAGGAGACAGAGTTGAAAGTCAGGGCACAAGTGA |
| CHP2_TP53_2 | CHP2_TP53_2 | chr17 | 7579326 | 7579510 | + | AGACGGAAACCGTAGCTGCCCTGGTAGGTTTTCTGGGAAGGGACAGAAGATGACAGGGGCCAGGAGGGGGCTGGTGCAGGGGCCGCCGGTGTAGGAGCTGCTGGTGCAGGGGCCACGGGGGGAGCAGCCTC |
| CHP2_TP53_1 | CHP2_TP53_1 | chr17 | 7579829 | 7579985 | + | GAAAATGTTTCCTGACTCAGAGGGGCTCGACGCTAGGATCTGACTGCGGCTCCTCCATGGCAGTGACCCGGAAGGCAGTCTGGCTGCTGCAAGAGGAAAAGTGGGG |
| CHP2_ERBB2_1 | CHP2_ERBB2_1 | chr17 | 3.8E+07 | 3.8E+07 | + | AAAGTGTTGAGGGAAAACACATCCCCCAAAGCCAACAAAGAAATCTTAGACGTAAGCCCCTCCACCCTCTCCTGCTAGGAGGACAGGAAGGACCCCATGGCTGCAGGTCTGGGCTCTGGTCTCTCTTC |
| CHP2_ERBB2_2 | CHP2_ERBB2_2 | chr17 | 3.8E+07 | 3.8E+07 | + | CCTCTCAGCGTACCCTTGTCCCCAGGAAGCATACGTGATGGCTGGTGTGGGCTCCCCATATGTCTCCCGCCTTCTGGGCATCTGCCTGACATCCACGGTGCAGCTGGT |
| CHP2_ERBB2_3 | CHP2_ERBB2_3 | chr17 | 3.8E+07 | 3.8E+07 | + | GCGGCTCGTACACAGGGACTTGGCCGCTCGGAACGTGCTGGTCAAGAGTCCCAACCATGTCAAAATTACAGACTTCGGGCTGGCTCGGCTGCTGGACATTGACGAGACAGAGTACCATGCAGATGGGGG |
| CHP2_SMAD4_1 | CHP2_SMAD4_1 | chr18 | 4.9E+07 | 4.9E+07 | + | CTGGAGGTGGCCTGATCTTCACAAAAATGAACTAAAACATGTTAAATATTGTCAGTATGCGTTTGACTTAAAATGTGATAGTGTCTGTGTGAATCCATATCACTACGAACGAGT |
| CHP2_SMAD4_2 | CHP2_SMAD4_2 | chr18 | 4.9E+07 | 4.9E+07 | + | TGAACTTTTGTAATCTTTGGTTTAAATTTACATTCTCTGTTTTTAAATGGAAAAATACTTTCATTGTAATGATTAATGTTTCATTTGTTTTCCCCTTTAAACAATTAAGATCTCTCAGGATT |
| CHP2_SMAD4_3 | CHP2_SMAD4_3 | chr18 | 4.9E+07 | 4.9E+07 | + | CTTTGAGGGACAGCCATCGTTGTCCACTGAAGGACATTCAATTCAAACCATCCAGCATCCACCAAGTAATCGTGCATCGACAGAGACATACAGCACCCCAGCTCTGTTAGCC |
| CHP2_SMAD4_4 | CHP2_SMAD4_4 | chr18 | 4.9E+07 | 4.9E+07 | + | CAGGGCCTCAGCCAGGACAGCAGCAGAATGGATTTACTGGTCAGCCAGCTACTTACCATCATAGTATGTACATACTTTAAAAAATCTTTTAAATAGTTGAGAAAAAAGTAGGCAGCCTTTATAAAAG |
| CHP2_SMAD4_5 | CHP2_SMAD4_5 | chr18 | 4.9E+07 | 4.9E+07 | + | GCTTGCATTCCAGCCTCCCATTTCCAATCATCCTGGTAAGTGTATTTCAAAATTGATTTCCTGTATTTAGATTGATTTAGTGGTGATTGAAACGCACAAACACAGGCTTT |
| CHP2_SMAD4_6 | CHP2_SMAD4_6 | chr18 | 4.9E+07 | 4.9E+07 | + | TGCTTACTTTGAAATGGATGTTCAGGTAGGAGAGACATTTAAGGTTCCTTCAAGCTGCCCTATTGTTACTGTTGATGGATACGTGGACCCTTCTGGAGGAGATCGCTTTTGTTTGGG |
| CHP2_SMAD4_7 | CHP2_SMAD4_7 | chr18 | 4.9E+07 | 4.9E+07 | + | GCAAAGGTGTGCAGTTGGAATGTAAAGGTGAAGGTGATGTTTGGGTCAGGTGCCTTAGTGACCACGCGGTCTTTGTACAGAGTTACTACTTAGACAGAGAAGCTGGGCGTGCACCTGGAG |
| CHP2_SMAD4_8 | CHP2_SMAD4_8 | chr18 | 4.9E+07 | 4.9E+07 | + | CATCGACAGATGCAGCAGCAGGCGGCTACTGCACAAGCTGCAGCAGCTGCCCAGGCAGCAGCCGTGGCAGGAAACATCCCTGGCCCAGGAT |
| CHP2_SMAD4_9 | CHP2_SMAD4_9 | chr18 | 4.9E+07 | 4.9E+07 | + | ACCTTCGTCGCTTATGCATACTCAGGATGAGTTTTGTGAAAGGCTGGGGACCGGATTACCCAAGACAGAGCATCAAAGAAACACCTTGCTGGATTGAAATTCACTTACACCGGGCC |
| CHP2_STK11_1 | CHP2_STK11_1 | chr19 | 1206953 | 1207129 | + | GGACACGTTCATCCACCGCATCGACTCCACCGAGGTCATCTACCAGCCGCCGCCGCAAGCGGGCCAAGCTCATCGGCAAGTACCTGATGGGGGACCTGCTGGGGGAAGGCTCTTACGGCAAGGTGAAG |
| CHP2_STK11_2 | CHP2_STK11_2 | chr19 | 1220286 | 1220475 | + | ACCCCTGTGAGGGGCAGGGAGGCCTCGGCCCCAGGACGGGTGTGTGCTGCCCGCAGGTACTTCTGTCAGCTGATTGACGGCCTGGAGTACCTGCATAGCCAGGGCATTGTGCACAAGGACATCAAGCCGGGGAAC |
| CHP2_STK11_3 | CHP2_STK11_3 | chr19 | 1220456 | 1220628 | + | ATCTCCGACCTGGCGTGCCCGAGGTAGGCACGTGCTAGGGGGGGCCCTGGGGCGCCCCCTCCCGGGCACTCCCTGAGGGCTGCACGGCACCGCCACAGGCACTGCACCCGTTCGCGGCGGAC |
| CHP2_STK11_4 | CHP2_STK11_4 | chr19 | 1221212 | 1221357 | + | CCCTTCGAAGGGCACAACATCTACAAGTTGTTTGAGAACATCGGGAAGGGGAGCTACGCCATCCCGGGCGACTGTGCGCCCCCCGCTCTCTGACCTG |
| CHP2_STK11_5 | CHP2_STK11_5 | chr19 | 1222990 | 1223169 | + | CACCAGTGCCCATCCCACCGAGCCCAGACACCAAGGACCCGTGCCGCAGCATGACTGTGGTGCCGTACTTGGAGGACCTGCACGGCGCCGACGAGGACGAGGACCTCTTCGACATCGAGGATGACATCA |
| CHP2_GNA11_1 | CHP2_GNA11_1 | chr19 | 3118857 | 3118998 | + | GGGCGCCAGGTGGCTGAGTCCTGGCGCTGTGTCCTTCAGGATGGTGGATGTGGGGGGCCAGCGGTCGGAGCGGAGGAAGTGGATCCACTGC |
| CHP2_JAK3_3 | CHP2_JAK3_3 | chr19 | 1.8E+07 | 1.8E+07 | + | CAAAGTGGGGGTTCGGAGACCGATGCCCGGTGAGGGGCTCTGACCTTAGCAGGATCCAGGGCACTGATGGGCATGGTGACGCCACTAAACACTTCCCAGACCGTGGCGCCGAAGCCCC |
| CHP2_JAK3_2 | CHP2_JAK3_2 | chr19 | 1.8E+07 | 1.8E+07 | + | CACTTGGCTCATCAAGCTCGCTGCTTCCAGGAATGACTGGGGAAGGTGGGAAGGGAGAGAAGATGCCTGGGTTTCTTCCACTCCAATA |
| CHP2_JAK3_1 | CHP2_JAK3_1 | chr19 | 1.8E+07 | 1.8E+07 | + | ATGTTGCCCCTTGGACCCCCAACCCCCTGGGTCAAACCCCAGGCAGAACCCCACCTGGGCAAAGAGGTGCTCCAGGACTGGCAGGTCAAGG |
| CHP2_SRC_1 | CHP2_SRC_1 | chr20 | 3.6E+07 | 3.6E+07 | + | GCCAGTGCTGGCGGAAGGAGCCTGAGGAGCGGCCCACCTTCGAGTACCTGCAGGCCTTCCTGGAGGACTACTTCACGTCCACCGAGCCCCAGTACCAGCCCGG |
| CHP2_GNAS_1 | CHP2_GNAS_1 | chr20 | 5.7E+07 | 5.7E+07 | + | TGTTTCAGGACCTGCTTCCGCTGCCGTGTCCTGACTTCTGGAATCTTTGAGACCAAGTTCCAGGTGGACAAAGTCAACTTCCAGTAAGCCAACTGTTACCTTTTTATAT |
| CHP2_GNAS_2 | CHP2_GNAS_2 | chr20 | 5.7E+07 | 5.7E+07 | + | TCCTCCCCACCAGCATGTTTGACGTGGGTGGCCAGCGCGATGAACGCCGCAAGTGGATCCAGTGCTTCAACGGTAGGATGCTGTGGGCTTGGCTGTTCGTAAAGAACGCT |
| CHP2_SMARCB1_1 | CHP2_SMARCB1_1 | chr22 | 2.4E+07 | 2.4E+07 | + | CCTCCGTATGTTCCGAGGTTCTCTGTACAAGAGATACCCCTCACTCTGGAGGCGACTAGCCACTGTGGAAGAGAGGAAGAAAATAGTTGCATCGTCACATGGTAAAAAAAC |
| CHP2_SMARCB1_2 | CHP2_SMARCB1_2 | chr22 | 2.4E+07 | 2.4E+07 | + | GTGCCATGCTCCACAACCATCAACAGGAACCGATGGGCCGAGACAAGAAGAGAACCTTCCCCCTTTGGTGTGGATGCATCGCTGCACTCACCCTCCGTGCTGATTCCGCC |
| CHP2_SMARCB1_3 | CHP2_SMARCB1_3 | chr22 | 2.4E+07 | 2.4E+07 | + | TCAGCTTTGATGACCATGACCCAGCTGTGATCCATGAGAACGCATCTCAGCCCGAGGTGCTGGTCCCCATCCGGCTGGACATGAGATCGATGGGCAGAAGCTGCGAGACGCCTTCACCTG |
| CHP2_SMARCB1_4 | CHP2_SMARCB1_4 | chr22 | 2.4E+07 | 2.4E+07 | + | CTTGGGAAGGGCAGCGCCCAGGCTGGAGCTGGCCCCGACTCATTGCCCTCCCCACTCCTCTTCCAGGCGGATGAGGCGTCTTGCCAACACGGCCCCGGCCTGGTAACCAGCCCATCAGCACACGGCTCCC |

Location and sequence of hotspot genes used as targets for Thyroid cancer.

***Supplementary Table S4:*** *Somatic alterations and specific changes in tumors samples for all patients*

| Histotype | ID | Sample | Chrom | Start | End | Ref | Alt | Freq Ref | Freq Alt | MAF | Mutation Category | Mutation Region | Gene Symbol | Mutation Type | Aminoacid Change | dbSNP v150 | gnomAD.WXS < 0.01 (1%)? | gnomAD.WGS < 0.01 (1%)? | ExAC < 0.01 (1%)? | COSMIC Coding | COSMIC Non-Coding |
|---|---|---|---|---|---|---|---|---|---|---|---|---|---|---|---|---|---|---|---|---|---|
| FVPTC | 11A | 11A_S22_L001 | 2 | 211713654 | 211713655 | TA | T | 15 | 14 | 48.28 | DEL | intronic | ERBB4 | . | . | rs397987661 | Yes | Yes | Yes | No | No |
| FVPTC | 11A | 11A_S22_L001 | 7 | 140753336 | 140753336 | A | T | 62 | 25 | 28.74 | SNV | exonic | BRAF | nonsynonymous SNV | BRAF:NM_001354609:exon15:c.T1799A:p.V600E,BRAF:NM_004333:exon15:c.T1799A:p.V600E | rs113488022 | Yes | Yes | Yes | Yes | No |
| FVPTC | 12A | 12A_S24_L001 | 4 | 55114072 | 55114072 | C | T | 15 | 16 | 51.61 | SNV | intronic | KDR | . | . | rs7692791 | Yes | Yes | Yes | Yes | No |
| FVPTC | 12A | 12A_S24_L001 | 7 | 140753336 | 140753336 | A | T | 25 | 15 | 37.5 | SNV | exonic | BRAF | nonsynonymous SNV | BRAF:NM_001354609:exon15:c.T1799A:p.V600E,BRAF:NM_004333:exon15:c.T1799A:p.V600E | rs113488022 | Yes | Yes | Yes | Yes | No |
| FVPTC | 13A | 13A_S38_L001 | 13 | 28028155 | 28028155 | T | C | 19 | 26 | 57.78 | SNV | intronic | FLT3 | . | . | rs75580865 | Yes | Yes | Yes | Yes | No |
| FVPTC | 13A | 13A_S38_L001 | 9 | 21971145 | 21971145 | A | C | 6 | 3 | 33.33 | SNV | exonic | CDKN2A | nonsynonymous SNV | CDKN2A:NM_000077:exon2:c.T214G:p.C72G,CDKN2A:NM_001195132:exon2:c.T214G:p.C72G,CDKN2A:NM_001363763:exon2:c.T61G:p.C21G,CDKN2A:NM_058195:exon2:c.T257G:p.L86R | . | Yes | Yes | Yes | Yes | Yes |
| NIFTP | 14A | 14A_S26_L001 | 5 | 171410509 | 171410510 | CT | C | 26 | 11 | 29.73 | DEL | intronic | NPM1 | . | . | rs34323200 | Yes | Yes | Yes | No | No |
| NIFTP | 14A | 14A_S28_L001 | 5 | 171410509 | 171410510 | CT | C | 41 | 16 | 28.07 | DEL | intronic | NPM1 | . | . | rs34323200 | Yes | Yes | Yes | No | No |
| NIFTP | 15A | 15A_S28_L001 | 22 | 23801019 | 23801019 | A | G | 5 | 10 | 66.67 | SNV | exonic | SMARCB1 | synonymous SNV | SMARCB1:NM_001007468:exon4:c.A411G:p.P137P,SMARCB1:NM_003173946:exon4:c.A411G:p.P137P,SMARCB1:NM_001362877:exon4:c.A438G:p.P146P,SMARCB1:NM_003073:exon4:c.A438G:p.P146P | rs35105793 | Yes | Yes | Yes | Yes | Yes |
| NIFTP | 15A | 15A_S28_L001 | 4 | 1806132 | 1806132 | C | T | 9 | 2 | 18.18 | SNV | exonic | FGFR3 | nonsynonymous SNV | FGFR3:NM_022965:exon12:c.C1582T:p.R528W,FGFR3:NM_000142:exon14:c.C1918T:p.R640W,FGFR3:NM_001163213:exon14:c.C1924T:p.R642W,FGFR3:NM_001354809:exon14:c.C1921T:p.R641W,FGFR3:NM_001354810:exon14:c.C1921T:p.R641W | . | Yes | Yes | Yes | Yes | Yes |
| NIFTP | 17A | 17A_S31_L001 | 4 | 55080004 | 55080004 | G | A | 23 | 36 | 61.02 | SNV | exonic | KDR | synonymous SNV | KDR:NM_002253:exon30:c.C4008T:p.T1336T | rs35961234 | Yes | Yes | Yes | Yes | No |
| NIFTP | 17A | 17A_S31_L001 | 5 | 171410509 | 171410510 | CT | C | 27 | 20 | 42.55 | DEL | intronic | NPM1 | . | . | rs34323200 | Yes | Yes | Yes | No | No |
| NIFTP | 18A | 18A_S33_L001 | 11 | 533874 | 533874 | T | C | 2 | 4 | 66.67 | SNV | exonic | HRAS | nonsynonymous SNV | HRAS:NM_001130442:exon3:c.A182G:p.Q61R,HRAS:NM_005343:exon3:c.A182G:p.Q61R,HRAS:NM_176795:exon3:c.A182G:p.Q61R | rs121913233 | Yes | Yes | Yes | Yes | Yes |
| NIFTP | 18A | 18A_S33_L001 | 13 | 28036046 | 28036046 | A | G | 0 | 31 | 100 | SNV | intronic | FLT3 | . | . | rs2491231 | Yes | Yes | Yes | Yes | No |
| NIFTP | 18A | 18A_S33_L001 | 17 | 7676154 | 7676154 | G | C | 6 | 3 | 33.33 | SNV | exonic | TP53 | nonsynonymous SNV | TP53:NM_001126118:exon3:c.C98G:p.P33R,TP53:NM_000546:exon4:c.C215G:p.P72R,TP53:NM_001126112:exon4:c.C215G:p.P72R,TP53:NM_001126113:exon4:c.C215G:p.P72R,TP53:NM_001126114:exon4:c.C215G:p.P72R,TP53:NM_001276695:exon4:c.C98G:p.P33R,TP53:NM_001276696:exon4:c.C98G:p.P33R,TP53:NM_001276760:exon4:c.C98G:p.P33R,TP53:NM_001276761:exon4:c.C98G:p.P33R | rs1042522 | Yes | Yes | Yes | Yes | Yes |
| NIFTP | 18A | 18A_S33_L001 | 19 | 1220322 | 1220322 | T | C | 3 | 5 | 62.5 | SNV | intronic | STK11 | . | . | rs2075606 | Yes | Yes | Yes | Yes | Yes |
| NIFTP | 18A | 18A_S33_L001 | 2 | 211713654 | 211713655 | TA | T | 25 | 7 | 21.88 | DEL | intronic | ERBB4 | . | . | rs397987661 | Yes | Yes | Yes | No | No |
| NIFTP | 18A | 18A_S33_L001 | 3 | 179199217 | 179199217 | A | G | 26 | 16 | 38.1 | SNV | intronic | PIK3CA | . | . | rs3729674 | Yes | Yes | Yes | Yes | Yes |
| NIFTP | 18A | 18A_S33_L001 | 3 | 179209622 | 179209622 | A | G | 26 | 19 | 42.22 | SNV | exonic | PIK3CA | nonsynonymous SNV | PIK3CA:NM_006218:exon7:c.A1173G:p.I391M | rs2230461 | Yes | Yes | Yes | Yes | No |
| NIFTP | 18A | 18A_S33_L001 | 4 | 1806167 | 1806167 | G | A | 0 | 16 | 100 | SNV | exonic | FGFR3 | synonymous SNV | FGFR3:NM_022965:exon12:c.G1617A:p.T539T,FGFR3:NM_000142:exon14:c.G1953A:p.T651T,FGFR3:NM_001163213:exon14:c.G1959A:p.T653T,FGFR3:NM_001354809:exon14:c.G1956A:p.T652T,FGFR3:NM_001354810:exon14:c.G1956A:p.T652T | rs7688609 | Yes | Yes | Yes | Yes | Yes |
| NIFTP | 18A | 18A_S33_L001 | 4 | 54274888 | 54274888 | A | G | 0 | 59 | 100 | SNV | exonic | PDGFRA | synonymous SNV | PDGFRA:NM_001347827:exon12:c.A1701G:p.P567P,PDGFRA:NM_001347829:exon12:c.A1701G:p.P567P,PDGFRA:NM_001347830:exon12:c.A1740G:p.P580P,PDGFRA:NM_006206:exon12:c.A1701G:p.P567P,PDGFRA:NM_001347828:exon13:c.A1776G:p.P592P | rs1873778 | Yes | Yes | Yes | Yes | Yes |
| NIFTP | 18A | 18A_S33_L001 | 5 | 112839920 | 112839920 | T | A | 37 | 35 | 48.61 | SNV | exonic | APC | synonymous SNV | APC:NM_001127511:exon14:c.T4272A:p.P1424P,APC:NM_001354897:exon15:c.T4356A:p.P1452P,APC:NM_001354899:exon15:c.T4242A:p.P1414P,APC:NM_001354901:exon15:c.T4149A:p.P1383P,APC:NM_001354902:exon15:c.T4053A:p.P1351P,APC:NM_001354905:exon15:c.T3846A:p.P1282P,APC:NM_000038:exon16:c.T4326A:p.P1442P,APC:NM_001354895:exon16:c.T4326A:p.P1442P,APC:NM_001354898:exon16:c.T4251A:p.P1417P,APC:NM_001354900:exon16:c.T4203A:p.P1401P,APC:NM_001354903:exon16:c.T4023A:p.P1341P,APC:NM_001354904:exon16:c.T3948A:p.P1316P,APC:NM_001127510:exon17:c.T4326A:p.P1442P,APC:NM_001354896:exon17:c.T4380A:p.P1460P,APC:NM_001354906:exon17:c.T3477A:p.P1159P | rs67622085 | Yes | Yes | Yes | Yes | Yes |
| NIFTP | 18A | 18A_S33_L001 | 5 | 112840073 | 112840073 | G | A | 0 | 68 | 100 | SNV | exonic | APC | synonymous SNV | APC:NM_001127511:exon14:c.G4425A:p.T1475T,APC:NM_001354897:exon15:c.G4509A:p.T1503T,APC:NM_001354899:exon15:c.G4395A:p.T1465T,APC:NM_001354901:exon15:c.G4302A:p.T1434T,APC:NM_001354902:exon15:c.G4206A:p.T1402T,APC:NM_001354905:exon15:c.G3999A:p.T1333T,APC:NM_000038:exon16:c.G4479A:p.T1493T,APC:NM_001354895:exon16:c.G4479A:p.T1493T,APC:NM_001354898:exon16:c.G4404A:p.T1468T,APC:NM_001354900:exon16:c.G4356A:p.T1452T,APC:NM_001354903:exon16:c.G4176A:p.T1392T,APC:NM_001354904:exon16:c.G4101A:p.T1367T,APC:NM_001127510:exon17:c.G4479A:p.T1493T,APC:NM_001354896:exon17:c.G4533A:p.T1511T,APC:NM_001354906:exon17:c.G3630A:p.T1210T | rs41115 | Yes | Yes | Yes | Yes | Yes |
| NIFTP | 18A | 18A_S33_L001 | 5 | 171410509 | 171410510 | CT | C | 13 | 17 | 56.67 | DEL | intronic | NPM1 | . | . | rs34323200 | Yes | Yes | Yes | No | No |
| PTC | 27A | 27A_S34_L001 | 10 | 43118395 | 43118395 | G | T | 0 | 24 | 100 | SNV | exonic | RET | synonymous SNV | RET:NM_001355216:exon10:c.G1545T:p.L515L,RET:NM_020630:exon13:c.G2307T:p.L769L,RET:NM_020975:exon13:c.G2307T:p.L769L | rs1800861 | Yes | Yes | Yes | Yes | Yes |
| PTC | 27A | 27A_S34_L001 | 10 | 43120185 | 43120185 | C | G | 0 | 17 | 100 | SNV | exonic | RET | synonymous SNV | RET:NM_001355216:exon12:c.C1950G:p.S650S,RET:NM_020630:exon15:c.C2712G:p.S904S,RET:NM_020975:exon15:c.C2712G:p.S904S | rs1800863 | Yes | Yes | Yes | Yes | No |
| PTC | 27A | 27A_S34_L001 | 17 | 7676154 | 7676154 | G | C | 0 | 7 | 100 | SNV | exonic | TP53 | nonsynonymous SNV | TP53:NM_001126118:exon3:c.C98G:p.P33R,TP53:NM_000546:exon4:c.C215G:p.P72R,TP53:NM_001126112:exon4:c.C215G:p.P72R,TP53:NM_001126113:exon4:c.C215G:p.P72R,TP53:NM_001126114:exon4:c.C215G:p.P72R,TP53:NM_001276695:exon4:c.C98G:p.P33R,TP53:NM_001276696:exon4:c.C98G:p.P33R,TP53:NM_001276760:exon4:c.C98G:p.P33R,TP53:NM_001276761:exon4:c.C98G:p.P33R | rs1042522 | Yes | Yes | Yes | Yes | Yes |
| PTC | 27A | 27A_S34_L001 | 19 | 1220513 | 1220513 | C | T | 4 | 2 | 33.33 | SNV | intronic | STK11 | . | . | rs565387911 | Yes | Yes | Yes | No | No |
| PTC | 27A | 27A_S34_L001 | 19 | 1220534 | 1220534 | G | A | 4 | 2 | 33.33 | SNV | intronic | STK11 | . | . | . | Yes | Yes | Yes | No | No |
| PTC | 27A | 27A_S34_L001 | 2 | 211713654 | 211713655 | TA | T | 29 | 21 | 42 | DEL | intronic | ERBB4 | . | . | rs397987661 | Yes | Yes | Yes | No | No |
| PTC | 27A | 27A_S34_L001 | 22 | 23834078 | 23834078 | G | A | 2 | 2 | 50 | SNV | ncRNA_intronic | GSTTP2 | . | . | . | Yes | Yes | Yes | No | No |
| PTC | 27A | 27A_S34_L001 | 22 | 23834087 | 23834087 | G | A | 2 | 2 | 50 | SNV | ncRNA_intronic | GSTTP2 | . | . | . | Yes | Yes | Yes | No | No |
| PTC | 27A | 27A_S34_L001 | 3 | 179199217 | 179199217 | A | G | 25 | 20 | 44.44 | SNV | intronic | PIK3CA | . | . | rs3729674 | Yes | Yes | Yes | Yes | Yes |
| PTC | 27A | 27A_S34_L001 | 4 | 1806167 | 1806167 | G | A | 0 | 6 | 100 | SNV | exonic | FGFR3 | synonymous SNV | FGFR3:NM_022965:exon12:c.G1617A:p.T539T,FGFR3:NM_000142:exon14:c.G1953A:p.T651T,FGFR3:NM_001163213:exon14:c.G1959A:p.T653T,FGFR3:NM_001354809:exon14:c.G1956A:p.T652T,FGFR3:NM_001354810:exon14:c.G1956A:p.T652T | rs7688609 | Yes | Yes | Yes | Yes | Yes |
| PTC | 27A | 27A_S34_L001 | 4 | 54274888 | 54274888 | A | G | 0 | 47 | 100 | SNV | exonic | PDGFRA | synonymous SNV | PDGFRA:NM_001347827:exon12:c.A1701G:p.P567P,PDGFRA:NM_001347829:exon12:c.A1701G:p.P567P,PDGFRA:NM_001347830:exon12:c.A1740G:p.P580P,PDGFRA:NM_006206:exon12:c.A1701G:p.P567P,PDGFRA:NM_001347828:exon13:c.A1776G:p.P592P | rs1873778 | Yes | Yes | Yes | Yes | Yes |
| PTC | 27A | 27A_S34_L001 | 4 | 54727298 | 54727298 | A | C | 45 | 39 | 46.43 | SNV | exonic | KIT | nonsynonymous SNV | KIT:NM_000222:exon10:c.A1621C:p.M541L,KIT:NM_001093772:exon10:c.A1609C:p.M537L | rs3822214 | Yes | Yes | Yes | Yes | Yes |
| PTC | 27A | 27A_S34_L001 | 5 | 112840073 | 112840073 | G | A | 28 | 28 | 50 | SNV | exonic | APC | synonymous SNV | APC:NM_001127511:exon14:c.G4425A:p.T1475T,APC:NM_001354897:exon15:c.G4509A:p.T1503T,APC:NM_001354899:exon15:c.G4395A:p.T1465T,APC:NM_001354901:exon15:c.G4302A:p.T1434T,APC:NM_001354902:exon15:c.G4206A:p.T1402T,APC:NM_001354905:exon15:c.G3999A:p.T1333T,APC:NM_000038:exon16:c.G4479A:p.T1493T,APC:NM_001354895:exon16:c.G4479A:p.T1493T,APC:NM_001354898:exon16:c.G4404A:p.T1468T,APC:NM_001354900:exon16:c.G4356A:p.T1452T,APC:NM_001354903:exon16:c.G4176A:p.T1392T,APC:NM_001354904:exon16:c.G4101A:p.T1367T,APC:NM_001127510:exon17:c.G4479A:p.T1493T,APC:NM_001354896:exon17:c.G4533A:p.T1511T,APC:NM_001354906:exon17:c.G3630A:p.T1210T | rs41115 | Yes | Yes | Yes | Yes | Yes |
| PTC | 27A | 27A_S34_L001 | 5 | 171410509 | 171410510 | CT | C | 31 | 10 | 24.39 | DEL | intronic | NPM1 | . | . | rs34323200 | Yes | Yes | Yes | No | No |
| PTC | 28A | 28A_S35_L001 | 4 | 55096378 | 55096378 | T | TG | 4 | 29 | 87.88 | INS | intronic | KDR | . | . | rs3214870 | Yes | Yes | Yes | No | No |
| PTC | 28A | 28A_S35_L001 | 7 | 140753336 | 140753336 | A | T | 32 | 19 | 37.25 | SNV | exonic | BRAF | nonsynonymous SNV | BRAF:NM_001354609:exon15:c.T1799A:p.V600E,BRAF:NM_004333:exon15:c.T1799A:p.V600E | rs113488022 | Yes | Yes | Yes | Yes | No |
| PTC | 29A | 29A_S37_L001 | 10 | 43120185 | 43120185 | C | G | 8 | 13 | 61.9 | SNV | exonic | RET | synonymous SNV | RET:NM_001355216:exon12:c.C1950G:p.S650S,RET:NM_020630:exon15:c.C2712G:p.S904S,RET:NM_020975:exon15:c.C2712G:p.S904S | rs1800863 | Yes | Yes | Yes | Yes | No |
| PTC | 29A | 29A_S37_L001 | 19 | 1220322 | 1220322 | T | C | 5 | 3 | 37.5 | SNV | intronic | STK11 | . | . | rs2075606 | Yes | Yes | Yes | Yes | Yes |
| PTC | 29A | 29A_S37_L001 | 4 | 55106807 | 55106807 | T | A | 20 | 30 | 60 | SNV | exonic | KDR | nonsynonymous SNV | KDR:NM_002253:exon11:c.A1416T:p.Q472H | rs1870377 | Yes | Yes | Yes | Yes | No |
| PTC | 29A | 29A_S37_L001 | 4 | 55114072 | 55114072 | C | T | 21 | 13 | 38.24 | SNV | intronic | KDR | . | . | rs7692791 | Yes | Yes | Yes | Yes | No |
| PTC | 29A | 29A_S37_L001 | 5 | 171410509 | 171410510 | CT | C | 25 | 11 | 30.56 | DEL | intronic | NPM1 | . | . | rs34323200 | Yes | Yes | Yes | No | No |
| PTC | 29A | 29A_S37_L001 | 7 | 140753336 | 140753336 | A | T | 32 | 15 | 31.91 | SNV | exonic | BRAF | nonsynonymous SNV | BRAF:NM_001354609:exon15:c.T1799A:p.V600E,BRAF:NM_004333:exon15:c.T1799A:p.V600E | rs113488022 | Yes | Yes | Yes | Yes | No |
| PTC | 30A | 30A_S39_L001 | 17 | 7676154 | 7676154 | G | C | 3 | 15 | 83.33 | SNV | exonic | TP53 | nonsynonymous SNV | TP53:NM_001126118:exon3:c.C98G:p.P33R,TP53:NM_000546:exon4:c.C215G:p.P72R,TP53:NM_001126112:exon4:c.C215G:p.P72R,TP53:NM_001126113:exon4:c.C215G:p.P72R,TP53:NM_001126114:exon4:c.C215G:p.P72R,TP53:NM_001276695:exon4:c.C98G:p.P33R,TP53:NM_001276696:exon4:c.C98G:p.P33R,TP53:NM_001276760:exon4:c.C98G:p.P33R,TP53:NM_001276761:exon4:c.C98G:p.P33R | rs1042522 | Yes | Yes | Yes | Yes | Yes |
| PTC | 30A | 30A_S39_L001 | 19 | 1220314 | 1220314 | G | A | 1 | 2 | 66.67 | SNV | intronic | STK11 | . | . | . | Yes | Yes | Yes | No | No |
| PTC | 30A | 30A_S39_L001 | 7 | 140753336 | 140753336 | A | T | 43 | 11 | 20.37 | SNV | exonic | BRAF | nonsynonymous SNV | BRAF:NM_001354609:exon15:c.T1799A:p.V600E,BRAF:NM_004333:exon15:c.T1799A:p.V600E | rs113488022 | Yes | Yes | Yes | Yes | No |
| PTC | 20A | 32-1419T_S2_L001 | 19 | 1220322 | 1220322 | T | C | 5 | 4 | 44.44 | SNV | intronic | STK11 | . | . | rs2075606 | Yes | Yes | Yes | Yes | Yes |
| PTC | 20A | 32-1419T_S2_L001 | 4 | 55096379 | 55096379 | G | GA | 47 | 27 | 36.49 | INS | intronic | KDR | . | . | . | Yes | Yes | Yes | No | No |
| PTC | 20A | 32-1419T_S2_L001 | 7 | 140753336 | 140753336 | A | T | 24 | 19 | 44.19 | SNV | exonic | BRAF | nonsynonymous SNV | BRAF:NM_001354609:exon15:c.T1799A:p.V600E,BRAF:NM_004333:exon15:c.T1799A:p.V600E | rs113488022 | Yes | Yes | Yes | Yes | No |
| PTC | 19A | 32-1519T_S4_L001 | 10 | 43118395 | 43118395 | G | T | 0 | 34 | 100 | SNV | exonic | RET | synonymous SNV | RET:NM_001355216:exon10:c.G1545T:p.L515L,RET:NM_020630:exon13:c.G2307T:p.L769L,RET:NM_020975:exon13:c.G2307T:p.L769L | rs1800861 | Yes | Yes | Yes | Yes | Yes |
| PTC | 19A | 32-1519T_S4_L001 | 10 | 43120185 | 43120185 | C | G | 10 | 10 | 50 | SNV | exonic | RET | synonymous SNV | RET:NM_001355216:exon12:c.C1950G:p.S650S,RET:NM_020630:exon15:c.C2712G:p.S904S,RET:NM_020975:exon15:c.C2712G:p.S904S | rs1800863 | Yes | Yes | Yes | Yes | No |
| PTC | 19A | 32-1519T_S4_L001 | 11 | 534242 | 534242 | A | G | 12 | 28 | 70 | SNV | exonic | HRAS | synonymous SNV | HRAS:NM_001130442:exon2:c.T81C:p.H27H,HRAS:NM_005343:exon2:c.T81C:p.H27H,HRAS:NM_176795:exon2:c.T81C:p.H27H | rs12628 | Yes | Yes | Yes | Yes | No |
| PTC | 19A | 32-1519T_S4_L001 | 13 | 28036046 | 28036046 | A | G | 24 | 14 | 36.84 | SNV | intronic | FLT3 | . | . | rs2491231 | Yes | Yes | Yes | Yes | No |
| PTC | 19A | 32-1519T_S4_L001 | 17 | 7676154 | 7676154 | G | C | 13 | 17 | 56.67 | SNV | exonic | TP53 | nonsynonymous SNV | TP53:NM_001126118:exon3:c.C98G:p.P33R,TP53:NM_000546:exon4:c.C215G:p.P72R,TP53:NM_001126112:exon4:c.C215G:p.P72R,TP53:NM_001126113:exon4:c.C215G:p.P72R,TP53:NM_001126114:exon4:c.C215G:p.P72R,TP53:NM_001276695:exon4:c.C98G:p.P33R,TP53:NM_001276696:exon4:c.C98G:p.P33R,TP53:NM_001276760:exon4:c.C98G:p.P33R,TP53:NM_001276761:exon4:c.C98G:p.P33R | rs1042522 | Yes | Yes | Yes | Yes | Yes |
| PTC | 19A | 32-1519T_S4_L001 | 3 | 10142088 | 10142088 | C | T | 22 | 11 | 33.33 | SNV | exonic | VHL | nonsynonymous SNV | VHL:NM_000551:exon1:c.C241T:p.P81S,VHL:NM_001354723:exon1:c.C241T:p.P81S,VHL:NM_198156:exon1:c.C241T:p.P81S | rs104893829 | Yes | Yes | Yes | Yes | Yes |
| PTC | 19A | 32-1519T_S4_L001 | 3 | 179199217 | 179199217 | A | G | 18 | 15 | 45.45 | SNV | intronic | PIK3CA | . | . | rs3729674 | Yes | Yes | Yes | Yes | Yes |
| PTC | 19A | 32-1519T_S4_L001 | 4 | 1806167 | 1806167 | G | A | 0 | 18 | 100 | SNV | exonic | FGFR3 | synonymous SNV | FGFR3:NM_022965:exon12:c.G1617A:p.T539T,FGFR3:NM_000142:exon14:c.G1953A:p.T651T,FGFR3:NM_001163213:exon14:c.G1959A:p.T653T,FGFR3:NM_001354809:exon14:c.G1956A:p.T652T,FGFR3:NM_001354810:exon14:c.G1956A:p.T652T | rs7688609 | Yes | Yes | Yes | Yes | Yes |
| PTC | 19A | 32-1519T_S4_L001 | 4 | 54727298 | 54727298 | A | C | 42 | 39 | 48.15 | SNV | exonic | KIT | nonsynonymous SNV | KIT:NM_000222:exon10:c.A1621C:p.M541L,KIT:NM_001093772:exon10:c.A1609C:p.M537L | rs3822214 | Yes | Yes | Yes | Yes | Yes |
| PTC | 19A | 32-1519T_S4_L001 | 4 | 55114072 | 55114072 | C | T | 12 | 27 | 69.23 | SNV | intronic | KDR | . | . | rs7692791 | Yes | Yes | Yes | Yes | No |
| PTC | 19A | 32-1519T_S4_L001 | 5 | 150054033 | 150054033 | T | G | 0 | 17 | 100 | SNV | exonic | UTR3 | CSF1R | . | rs2066934 | Yes | Yes | Yes | Yes | Yes |
| PTC | 19A | 32-1519T_S4_L001 | 5 | 150054034 | 150054034 | G | A | 0 | 17 | 100 | SNV | exonic | UTR3 | CSF1R | . | rs2066933 | Yes | Yes | Yes | No | No |
| PTC | 19A | 32-1519T_S4_L001 | 5 | 171410509 | 171410510 | CT | C | 19 | 4 | 17.39 | DEL | intronic | NPM1 | . | . | rs34323200 | Yes | Yes | Yes | No | No |
| PTC | 19A | 32-1519T_S4_L001 | 7 | 129206550 | 129206550 | T | T | 36 | 6 | 14.29 | SNV | exonic | SMO | synonymous SNV | SMO:NM_005631:exon6:c.T1227T:p.G409G | . | Yes | Yes | Yes | Yes | No |
| PTC | 19A | 32-1519T_S4_L001 | 7 | 129206552 | 129206552 | T | A | 36 | 6 | 14.29 | SNV | exonic | SMO | nonsynonymous SNV | SMO:NM_005631:exon6:c.T1229A:p.L410Q | . | Yes | Yes | Yes | Yes | No |
| PTC | 19A | 32-1519T_S4_L001 | 7 | 140753336 | 140753336 | A | T | 37 | 26 | 41.27 | SNV | exonic | BRAF | nonsynonymous SNV | BRAF:NM_001354609:exon15:c.T1799A:p.V600E,BRAF:NM_004333:exon15:c.T1799A:p.V600E | rs113488022 | Yes | Yes | Yes | Yes | No |
| NIFTP | 60A | 3322-20-T_S8_L001 | 10 | 43113726 | 43113726 | C | T | 12 | 2 | 14.29 | SNV | intronic | RET | . | . | . | Yes | Yes | Yes | No | No |
| NIFTP | 60A | 3322-20-T_S8_L001 | 10 | 43113727 | 43113727 | T | C | 12 | 2 | 14.29 | SNV | intronic | RET | . | . | . | Yes | Yes | Yes | No | No |
| NIFTP | 60A | 3322-20-T_S8_L001 | 11 | 108365533 | 108365533 | C | A | 34 | 6 | 15 | SNV | exonic | UTR3 | ATM | . | . | Yes | Yes | Yes | No | No |
| NIFTP | 60A | 3322-20-T_S8_L001 | 11 | 108365542 | 108365542 | T | A | 28 | 5 | 15.15 | SNV | exonic | UTR3 | ATM | . | . | Yes | Yes | Yes | No | No |
| NIFTP | 60A | 3322-20-T_S8_L001 | 11 | 534242 | 534242 | A | G | 12 | 18 | 60 | SNV | exonic | HRAS | synonymous SNV | HRAS:NM_001130442:exon2:c.T81C:p.H27H,HRAS:NM_005343:exon2:c.T81C:p.H27H,HRAS:NM_176795:exon2:c.T81C:p.H27H | rs12628 | Yes | Yes | Yes | Yes | No |
| NIFTP | 60A | 3322-20-T_S8_L001 | 13 | 28036046 | 28036046 | A | G | 31 | 14 | 31.11 | SNV | intronic | FLT3 | . | . | rs2491231 | Yes | Yes | Yes | Yes | No |
| NIFTP | 60A | 3322-20-T_S8_L001 | 2 | 211713654 | 211713655 | TA | T | 6 | 13 | 68.42 | DEL | intronic | ERBB4 | . | . | rs397987661 | Yes | Yes | Yes | No | No |
| NIFTP | 60A | 3322-20-T_S8_L001 | 2 | 211947372 | 211947372 | T | C | 16 | 22 | 57.89 | SNV | intronic | ERBB4 | . | . | rs839541 | Yes | Yes | Yes | No | No |
| NIFTP | 60A | 3322-20-T_S8_L001 | 4 | 55106807 | 55106807 | T | A | 15 | 26 | 63.41 | SNV | exonic | KDR | nonsynonymous SNV | KDR:NM_002253:exon11:c.A1416T:p.Q472H | rs1870377 | Yes | Yes | Yes | Yes | No |
| NIFTP | 60A | 3322-20-T_S8_L001 | 4 | 55114072 | 55114072 | C | T | 11 | 11 | 50 | SNV | intronic | KDR | . | . | rs7692791 | Yes | Yes | Yes | Yes | No |
| NIFTP | 60A | 3322-20-T_S8_L001 | 5 | 112840073 | 112840073 | G | A | 25 | 27 | 51.92 | SNV | exonic | APC | synonymous SNV | APC:NM_001127511:exon14:c.G4425A:p.T1475T,APC:NM_001354897:exon15:c.G4509A:p.T1503T,APC:NM_001354899:exon15:c.G4395A:p.T1465T,APC:NM_001354901:exon15:c.G4302A:p.T1434T,APC:NM_001354902:exon15:c.G4206A:p.T1402T,APC:NM_001354905:exon15:c.G3999A:p.T1333T,APC:NM_000038:exon16:c.G4479A:p.T1493T,APC:NM_001354895:exon16:c.G4479A:p.T1493T,APC:NM_001354898:exon16:c.G4404A:p.T1468T,APC:NM_001354900:exon16:c.G4356A:p.T1452T,APC:NM_001354903:exon16:c.G4176A:p.T1392T,APC:NM_001354904:exon16:c.G4101A:p.T1367T,APC:NM_001127510:exon17:c.G4479A:p.T1493T,APC:NM_001354896:exon17:c.G4533A:p.T1511T,APC:NM_001354906:exon17:c.G3630A:p.T1210T | rs41115 | Yes | Yes | Yes | Yes | Yes |
| NIFTP | 60A | 3322-20-T_S8_L001 | 5 | 171410509 | 171410510 | CT | C | 3 | 4 | 57.14 | DEL | intronic | NPM1 | . | . | rs34323200 | Yes | Yes | Yes | No | No |
| NIFTP | 60A | 3322-20-T_S8_L001 | 7 | 55181370 | 55181370 | G | A | 11 | 10 | 47.62 | SNV | exonic | EGFR | synonymous SNV | EGFR:NM_001346941:exon14:c.G1560A:p.Q520Q,EGFR:NM_001346897:exon19:c.G2226A:p.Q742Q,EGFR:NM_001346899:exon19:c.G2226A:p.Q742Q,EGFR:NM_001346898:exon20:c.G2361A:p.Q787Q,EGFR:NM_001346900:exon20:c.G2202A:p.Q734Q,EGFR:NM_005228:exon20:c.G2361A:p.Q787Q | rs1050171 | Yes | Yes | Yes | Yes | No |
| NIFTP | 62A | 3324-20-1_S10_L001 | 4 | 54695526 | 54695526 | T | A | 4 | 2 | 33.33 | SNV | exonic | KIT | nonsynonymous SNV | KIT:NM_000222:exon2:c.T82A:p.S28T,KIT:NM_001093772:exon2:c.T82A:p.S28T | . | Yes | Yes | Yes | No | No |
| NIFTP | 62A | 3324-20-1_S10_L001 | 4 | 54695547 | 54695547 | T | C | 4 | 2 | 33.33 | SNV | exonic | KIT | nonsynonymous SNV | KIT:NM_000222:exon2:c.T103C:p.S35P,KIT:NM_001093772:exon2:c.T103C:p.S35P | . | Yes | Yes | Yes | No | No |
| NIFTP | 62A | 3324-20-1_S10_L001 | 7 | 55181370 | 55181370 | G | A | 0 | 3 | 100 | SNV | exonic | EGFR | synonymous SNV | EGFR:NM_001346941:exon14:c.G1560A:p.Q520Q,EGFR:NM_001346897:exon19:c.G2226A:p.Q742Q,EGFR:NM_001346899:exon19:c.G2226A:p.Q742Q,EGFR:NM_001346898:exon20:c.G2361A:p.Q787Q,EGFR:NM_001346900:exon20:c.G2202A:p.Q734Q,EGFR:NM_005228:exon20:c.G2361A:p.Q787Q | rs1050171 | Yes | Yes | Yes | Yes | No |
| NIFTP | 62A | 3324-20-1_S21_L001 | 4 | 55096378 | 55096378 | T | TG | 77 | 19 | 19.79 | INS | intronic | KDR | . | . | rs3214870 | Yes | Yes | Yes | No | No |
| FVPTC | 67A | 3329-20-T_S12_L001 | 18 | 51076697 | 51076697 | T | A | 0 | 2 | 100 | SNV | exonic | SMAD4 | synonymous SNV | SMAD4:NM_005359:exon11:c.T1368A:p.A456A | . | Yes | Yes | Yes | No | No |
| FVPTC | 67A | 3329-20-T_S23_L001 | 10 | 43118395 | 43118395 | G | T | 0 | 43 | 100 | SNV | exonic | RET | synonymous SNV | RET:NM_001355216:exon10:c.G1545T:p.L515L,RET:NM_020630:exon13:c.G2307T:p.L769L,RET:NM_020975:exon13:c.G2307T:p.L769L | rs1800861 | Yes | Yes | Yes | Yes | Yes |

| | | | | | | | | | | | | | | | | | | | | | | | |
|---|---|---|---|---|---|---|---|---|---|---|---|---|---|---|---|---|---|---|---|---|---|---|---|
| FVPTC | 67A | 3329-20-T_S23_L001 | 11 | 533874 | 533874 | T | C | 13 | 7 | 35 | SNV | exonic | HRAS | nonsynonymous SNV | HRAS:NM_001130442:exon3:c.A182G:p.Q61R,HRAS:NM_005343:exon3:c.A182G:p.Q61R,HRAS:NM_176795:exon3:c.A182G:p.Q61R | rs121913233 | Yes | Yes | Yes | Yes | Yes | Yes | Yes |
| FVPTC | 67A | 3329-20-T_S23_L001 | 11 | 534242 | 534242 | A | G | 27 | 15 | 35.71 | SNV | exonic | HRAS | synonymous SNV | HRAS:NM_001130442:exon2:c.T81C:p.H27H,HRAS:NM_005343:exon2:c.T81C:p.H27H,HRAS:NM_176795:exon2:c.T81C:p.H27H | rs12628 | Yes | Yes | Yes | Yes | Yes | Yes | Yes |
| FVPTC | 67A | 3329-20-T_S23_L001 | 13 | 28036046 | 28036046 | A | G | 0 | 30 | 100 | SNV | intronic | FLT3 | . | . | rs2491231 | Yes | Yes | Yes | Yes | Yes | Yes | No |
| FVPTC | 67A | 3329-20-T_S23_L001 | 2 | 211713654 | 211713656 | TAA | T | 49 | 13 | 20.97 | DEL | intronic | ERBB4 | . | . | rs748883732 | Yes | Yes | Yes | Yes | Yes | No | No |
| FVPTC | 67A | 3329-20-T_S23_L001 | 4 | 1806167 | 1806167 | G | A | 0 | 45 | 100 | SNV | exonic | FGFR3 | synonymous SNV | FGFR3:NM_022965:exon12:c.G1617A:p.T539T,FGFR3:NM_000142:exon14:c.G1953A:p.T651T,FGFR3:NM_001163213:exon14:c.G1959A:p.T653T,FGFR3:NM_001354809:exon14:c.G1956A:p.T652T,FGFR3:NM_001354810:exon14:c.G1956A:p.T652T | rs7688609 | Yes | Yes | Yes | Yes | Yes | Yes | Yes |
| FVPTC | 67A | 3329-20-T_S23_L001 | 4 | 54274888 | 54274888 | A | G | 0 | 56 | 100 | SNV | exonic | PDGFRA | synonymous SNV | PDGFRA:NM_001347827:exon12:c.A1701G:p.P567P,PDGFRA:NM_001347829:exon12:c.A1701G:p.P567P,PDGFRA:NM_001347830:exon12:c.A1740G:p.P580P,PDGFRA:NM_006206:exon12:c.A1701G:p.P567P,PDGFRA:NM_001347828:exon13:c.A1776G:p.P592P | rs1873778 | Yes | Yes | Yes | Yes | Yes | Yes | Yes |
| FVPTC | 67A | 3329-20-T_S23_L001 | 4 | 54285873 | 54285873 | C | T | 22 | 28 | 56 | SNV | exonic | PDGFRA | synonymous SNV | PDGFRA:NM_001347829:exon18:c.C2472T:p.V824V,PDGFRA:NM_001347830:exon18:c.C2511T:p.V837V,PDGFRA:NM_006206:exon18:c.C2472T:p.V824V,PDGFRA:NM_001347828:exon19:c.C2547T:p.V849V | rs2228230 | Yes | Yes | Yes | Yes | Yes | Yes | Yes |
| FVPTC | 67A | 3329-20-T_S23_L001 | 4 | 55096378 | 55096378 | T | TG | 31 | 16 | 34.04 | INS | intronic | KDR | . | . | rs3214870 | Yes | Yes | Yes | Yes | Yes | No | No |
| FVPTC | 67A | 3329-20-T_S23_L001 | 4 | 55114072 | 55114072 | C | T | 34 | 10 | 22.73 | SNV | intronic | KDR | . | . | rs7692791 | Yes | Yes | Yes | Yes | Yes | Yes | No |
| FVPTC | 67A | 3329-20-T_S23_L001 | 5 | 171410509 | 171410510 | CT | C | 27 | 8 | 22.86 | DEL | intronic | NPM1 | . | . | rs34323200 | Yes | Yes | Yes | Yes | Yes | No | No |
| FVPTC | 67A | 3329-20-T_S23_L001 | 7 | 55181370 | 55181370 | G | A | 0 | 21 | 100 | SNV | exonic | EGFR | synonymous SNV | EGFR:NM_001346941:exon14:c.G1560A:p.Q520Q,EGFR:NM_001346897:exon19:c.G2226A:p.Q742Q,EGFR:NM_001346899:exon19:c.G2226A:p.Q742Q,EGFR:NM_001346898:exon20:c.G2361A:p.Q787Q,EGFR:NM_001346900:exon20:c.G2202A:p.Q734Q,EGFR:NM_005228:exon20:c.G2361A:p.Q787Q | rs1050171 | Yes | Yes | Yes | Yes | Yes | Yes | No |
| NIFTP | 68A | 3330-20-T_S22_L001 | 4 | 54274888 | 54274888 | A | G | 0 | 86 | 100 | SNV | exonic | PDGFRA | synonymous SNV | PDGFRA:NM_001347827:exon12:c.A1701G:p.P567P,PDGFRA:NM_001347829:exon12:c.A1701G:p.P567P,PDGFRA:NM_001347830:exon12:c.A1740G:p.P580P,PDGFRA:NM_006206:exon12:c.A1701G:p.P567P,PDGFRA:NM_001347828:exon13:c.A1776G:p.P592P | rs1873778 | Yes | Yes | Yes | Yes | Yes | Yes | Yes |
| NIFTP | 68A | 3330-20-T_S22_L001 | 4 | 55106807 | 55106807 | T | A | 30 | 36 | 54.55 | SNV | exonic | KDR | nonsynonymous SNV | KDR:NM_002253:exon11:c.A1416T:p.Q472H | rs1870377 | Yes | Yes | Yes | Yes | Yes | Yes | No |
| FVPTC | 70A | 3332-20-T_S1_L001 | 10 | 43118395 | 43118395 | G | T | 0 | 39 | 100 | SNV | exonic | RET | synonymous SNV | RET:NM_001355216:exon10:c.G1545T:p.L515L,RET:NM_020630:exon13:c.G2307T:p.L769L,RET:NM_020975:exon13:c.G2307T:p.L769L | rs1800861 | Yes | Yes | Yes | Yes | Yes | Yes | Yes |
| FVPTC | 70A | 3332-20-T_S1_L001 | 11 | 534242 | 534242 | A | G | 39 | 18 | 31.58 | SNV | exonic | HRAS | synonymous SNV | HRAS:NM_001130442:exon2:c.T81C:p.H27H,HRAS:NM_005343:exon2:c.T81C:p.H27H,HRAS:NM_176795:exon2:c.T81C:p.H27H | rs12628 | Yes | Yes | Yes | Yes | Yes | Yes | Yes |
| FVPTC | 70A | 3332-20-T_S1_L001 | 2 | 211713654 | 211713655 | TA | T | 8 | 7 | 46.67 | DEL | intronic | ERBB4 | . | . | rs397987661 | Yes | Yes | Yes | Yes | Yes | No | No |
| FVPTC | 70A | 3332-20-T_S1_L001 | 2 | 29209719 | 29209719 | A | T | 26 | 8 | 23.53 | SNV | intronic | ALK | . | . | . | Yes | Yes | Yes | Yes | Yes | No | No |
| FVPTC | 70A | 3332-20-T_S1_L001 | 3 | 10142169 | 10142169 | C | T | 19 | 4 | 17.39 | SNV | exonic | VHL | nonsynonymous SNV | VHL:NM_000551:exon1:c.C322T:p.R108C,VHL:NM_001354723:exon1:c.C322T:p.R108C,VHL:NM_198156:exon1:c.C322T:p.R108C | . | Yes | Yes | Yes | Yes | Yes | No | No |
| FVPTC | 70A | 3332-20-T_S1_L001 | 3 | 179199217 | 179199217 | A | G | 20 | 18 | 47.37 | SNV | intronic | PIK3CA | . | . | rs3729674 | Yes | Yes | Yes | Yes | Yes | Yes | Yes |
| FVPTC | 70A | 3332-20-T_S1_L001 | 3 | 179209622 | 179209622 | A | G | 8 | 18 | 69.23 | SNV | exonic | PIK3CA | nonsynonymous SNV | PIK3CA:NM_006218:exon7:c.A1173C:p.I391M | rs2230461 | Yes | Yes | Yes | Yes | Yes | Yes | No |
| FVPTC | 70A | 3332-20-T_S1_L001 | 4 | 1806167 | 1806167 | G | A | 0 | 25 | 100 | SNV | exonic | FGFR3 | synonymous SNV | FGFR3:NM_022965:exon12:c.G1617A:p.T539T,FGFR3:NM_000142:exon14:c.G1953A:p.T651T,FGFR3:NM_001163213:exon14:c.G1959A:p.T653T,FGFR3:NM_001354809:exon14:c.G1956A:p.T652T,FGFR3:NM_001354810:exon14:c.G1956A:p.T652T | rs7688609 | Yes | Yes | Yes | Yes | Yes | Yes | Yes |
| FVPTC | 70A | 3332-20-T_S1_L001 | 4 | 1806193 | 1806193 | G | T | 21 | 4 | 16 | SNV | intronic | FGFR3 | . | . | . | Yes | Yes | Yes | Yes | No | No | No |
| FVPTC | 70A | 3332-20-T_S1_L001 | 4 | 1806194 | 1806194 | C | T | 21 | 4 | 16 | SNV | intronic | FGFR3 | . | . | rs7782145772 | Yes | Yes | No | No | No | No | No |
| FVPTC | 70A | 3332-20-T_S1_L001 | 4 | 54274888 | 54274888 | A | G | 27 | 22 | 44.9 | SNV | exonic | PDGFRA | synonymous SNV | PDGFRA:NM_001347827:exon12:c.A1701G:p.P567P,PDGFRA:NM_001347829:exon12:c.A1701G:p.P567P,PDGFRA:NM_001347830:exon12:c.A1740G:p.P580P,PDGFRA:NM_006206:exon12:c.A1701G:p.P567P,PDGFRA:NM_001347828:exon13:c.A1776G:p.P592P | rs1873778 | Yes | Yes | Yes | Yes | Yes | Yes | Yes |
| FVPTC | 70A | 3332-20-T_S1_L001 | 4 | 55114072 | 55114072 | C | T | 0 | 28 | 100 | SNV | intronic | KDR | . | . | rs7692791 | Yes | Yes | Yes | Yes | Yes | Yes | No |
| FVPTC | 70A | 3332-20-T_S1_L001 | 5 | 112840073 | 112840073 | G | A | 26 | 19 | 42.22 | SNV | exonic | APC | synonymous SNV | APC:NM_001127511:exon14:c.G4425A:p.T1475T,APC:NM_001354897:exon15:c.G4509A:p.T1503T,APC:NM_001354899:exon15:c.G4395A:p.T1465T,APC:NM_001354901:exon15:c.G4302A:p.T1434T,APC:NM_001354902:exon15:c.G4206A:p.T1402T,APC:NM_001354905:exon15:c.G3999A:p.T1333T,APC:NM_000038:exon16:c.G4479A:p.T1493T,APC:NM_001354895:exon16:c.G4479A:p.T1493T,APC:NM_001354898:exon16:c.G4404A:p.T1468T,APC:NM_001354898:exon16:c.G4479A:p.T1493T,APC:NM_001354895:exon16:c.G4479A:p.T1493T,APC:NM_001354898:exon16:c.G4404A:p.T1468T,APC:NM_001354900:exon16:c.G4356A:p.T1452T,APC:NM_001354903:exon16:c.G4176A:p.T1392T,APC:NM_001354904:exon16:c.G4101A:p.T1367T,APC:NM_001127510:exon17:c.G4479A:p.T1493T,APC:NM_001354896:exon17:c.G4533A:p.T1511T,APC:NM_001354906:exon17:c.G3630A:p.T1210T | rs41115 | Yes | Yes | Yes | Yes | Yes | Yes | Yes |
| FVPTC | 70A | 3332-20-T_S1_L001 | 5 | 150054033 | 150054033 | T | G | 0 | 16 | 100 | SNV | UTR3 | CSF1R | . | . | rs2066934 | Yes | Yes | Yes | Yes | Yes | Yes | Yes |
| FVPTC | 70A | 3332-20-T_S1_L001 | 5 | 150054034 | 150054034 | G | A | 0 | 16 | 100 | SNV | UTR3 | CSF1R | . | . | rs2066933 | Yes | Yes | Yes | Yes | Yes | No | No |
| FVPTC | 70A | 3332-20-T_S1_L001 | 7 | 129206552 | 129206552 | T | A | 38 | 8 | 17.39 | SNV | exonic | SMO | nonsynonymous SNV | SMO:NM_005631:exon6:c.T1229A:p.L410Q | . | Yes | Yes | Yes | Yes | Yes | Yes | Yes |
| FVPTC | 70A | 3332-20-T_S1_L001 | 7 | 55181370 | 55181370 | G | A | 12 | 10 | 45.45 | SNV | exonic | EGFR | synonymous SNV | EGFR:NM_001346941:exon14:c.G1560A:p.Q520Q,EGFR:NM_001346897:exon19:c.G2226A:p.Q742Q,EGFR:NM_001346899:exon19:c.G2226A:p.Q742Q,EGFR:NM_001346898:exon20:c.G2361A:p.Q787Q,EGFR:NM_001346900:exon20:c.G2202A:p.Q734Q,EGFR:NM_005228:exon20:c.G2361A:p.Q787Q | rs1050171 | Yes | Yes | Yes | Yes | Yes | Yes | No |
| PTC | 38A | 38A_S30_L001 | 10 | 43118395 | 43118395 | G | T | 0 | 32 | 100 | SNV | exonic | RET | synonymous SNV | RET:NM_001355216:exon10:c.G1545T:p.L515L,RET:NM_020630:exon13:c.G2307T:p.L769L,RET:NM_020975:exon13:c.G2307T:p.L769L | rs1800861 | Yes | Yes | Yes | Yes | Yes | Yes | Yes |
| PTC | 38A | 38A_S30_L001 | 13 | 28036046 | 28036046 | A | G | 30 | 17 | 36.17 | SNV | intronic | FLT3 | . | . | rs2491231 | Yes | Yes | Yes | Yes | Yes | Yes | No |
| PTC | 38A | 38A_S30_L001 | 17 | 7676154 | 7676154 | G | C | 0 | 29 | 100 | SNV | exonic | TP53 | nonsynonymous SNV | TP53:NM_001126118:exon3:c.C98G:p.P33R,TP53:NM_000546:exon4:c.C215G:p.P72R,TP53:NM_001126112:exon4:c.C215G:p.P72R,TP53:NM_001126113:exon4:c.C215G:p.P72R,TP53:NM_001276614:exon4:c.C215G:p.P72R,TP53:NM_001276695:exon4:c.C98G:p.P33R,TP53:NM_001276696:exon4:c.C98G:p.P33R,TP53:NM_001276760:exon4:c.C98G:p.P33R,TP53:NM_001276761:exon4:c.C98G:p.P33R | rs1042522 | Yes | Yes | Yes | Yes | Yes | Yes | Yes |
| PTC | 38A | 38A_S30_L001 | 18 | 51059974 | 51059974 | C | T | 67 | 44 | 39.64 | SNV | intronic | SMAD4 | . | . | rs948588 | Yes | Yes | Yes | Yes | Yes | Yes | Yes |
| PTC | 38A | 38A_S30_L001 | 19 | 1220322 | 1220322 | T | C | 4 | 7 | 63.64 | SNV | intronic | STK11 | . | . | rs2075606 | Yes | Yes | Yes | Yes | Yes | Yes | Yes |
| PTC | 38A | 38A_S30_L001 | 2 | 211713654 | 211713655 | TA | T | 54 | 25 | 31.65 | DEL | intronic | ERBB4 | . | . | rs397987661 | Yes | Yes | Yes | Yes | Yes | No | No |
| PTC | 38A | 38A_S30_L001 | 4 | 1806167 | 1806167 | G | A | 0 | 18 | 100 | SNV | exonic | FGFR3 | synonymous SNV | FGFR3:NM_022965:exon12:c.G1617A:p.T539T,FGFR3:NM_000142:exon14:c.G1953A:p.T651T,FGFR3:NM_001163213:exon14:c.G1959A:p.T653T,FGFR3:NM_001354809:exon14:c.G1956A:p.T652T,FGFR3:NM_001354810:exon14:c.G1956A:p.T652T | rs7688609 | Yes | Yes | Yes | Yes | Yes | Yes | Yes |
| PTC | 38A | 38A_S30_L001 | 4 | 1806195 | 1806195 | G | A | 9 | 9 | 50 | SNV | intronic | FGFR3 | . | . | rs3135898 | Yes | Yes | Yes | Yes | Yes | Yes | Yes |
| PTC | 38A | 38A_S30_L001 | 4 | 54274888 | 54274888 | A | G | 0 | 69 | 100 | SNV | exonic | PDGFRA | synonymous SNV | PDGFRA:NM_001347827:exon12:c.A1701G:p.P567P,PDGFRA:NM_001347829:exon12:c.A1701G:p.P567P,PDGFRA:NM_001347830:exon12:c.A1740G:p.P580P,PDGFRA:NM_006206:exon12:c.A1701G:p.P567P,PDGFRA:NM_001347828:exon13:c.A1776G:p.P592P | rs1873778 | Yes | Yes | Yes | Yes | Yes | Yes | Yes |
| PTC | 38A | 38A_S30_L001 | 4 | 55080004 | 55080004 | G | A | 27 | 32 | 54.24 | SNV | exonic | KDR | synonymous SNV | KDR:NM_002253:exon30:c.C4008T:p.T1336T | rs35961234 | Yes | Yes | Yes | Yes | Yes | Yes | No |
| PTC | 38A | 38A_S30_L001 | 4 | 55096378 | 55096378 | T | TG | 54 | 14 | 20.59 | INS | intronic | KDR | . | . | rs3214870 | Yes | Yes | Yes | Yes | Yes | No | No |
| PTC | 38A | 38A_S30_L001 | 4 | 55114072 | 55114072 | C | T | 0 | 33 | 100 | SNV | intronic | KDR | . | . | rs7692791 | Yes | Yes | Yes | Yes | Yes | Yes | No |
| PTC | 38A | 38A_S30_L001 | 5 | 112840073 | 112840073 | G | A | 38 | 41 | 51.9 | SNV | exonic | APC | synonymous SNV | APC:NM_001127511:exon14:c.G4425A:p.T1475T,APC:NM_001354897:exon15:c.G4509A:p.T1503T,APC:NM_001354899:exon15:c.G4395A:p.T1465T,APC:NM_001354901:exon15:c.G4302A:p.T1434T,APC:NM_001354902:exon15:c.G4206A:p.T1402T,APC:NM_001354905:exon15:c.G3999A:p.T1333T,APC:NM_000038:exon16:c.G4479A:p.T1493T,APC:NM_001354895:exon16:c.G4479A:p.T1493T,APC:NM_001354898:exon16:c.G4404A:p.T1468T,APC:NM_001354898:exon16:c.G4479A:p.T1493T,APC:NM_001354895:exon16:c.G4479A:p.T1493T,APC:NM_001354898:exon16:c.G4404A:p.T1468T,APC:NM_001354900:exon16:c.G4356A:p.T1452T,APC:NM_001354903:exon16:c.G4176A:p.T1392T,APC:NM_001354904:exon16:c.G4101A:p.T1367T,APC:NM_001127510:exon17:c.G4479A:p.T1493T,APC:NM_001354896:exon17:c.G4533A:p.T1511T,APC:NM_001354906:exon17:c.G3630A:p.T1210T | rs41115 | Yes | Yes | Yes | Yes | Yes | Yes | Yes |
| PTC | 38A | 38A_S30_L001 | 5 | 171410509 | 171410510 | CT | C | 32 | 11 | 25.58 | DEL | intronic | NPM1 | . | . | rs34323200 | Yes | Yes | Yes | Yes | Yes | No | No |
| PTC | 38A | 38A_S30_L001 | 7 | 116699618 | 116699618 | C | T | 55 | 49 | 47.12 | SNV | exonic | MET | synonymous SNV | MET:NM_000245:exon2:c.C534T:p.S178S,MET:NM_001127500:exon2:c.C534T:p.S178S,MET:NM_001324401:exon2:c.C534T:p.S178S | rs35775721 | Yes | Yes | Yes | Yes | Yes | Yes | Yes |
| PTC | 38A | 38A_S30_L001 | 7 | 116700208 | 116700208 | A | G | 30 | 30 | 50 | SNV | exonic | MET | nonsynonymous SNV | MET:NM_000245:exon2:c.A1124G:p.N375S,MET:NM_001127500:exon2:c.A1124G:p.N375S,MET:NM_001324401:exon2:c.A1124G:p.N375S | rs33917957 | Yes | Yes | Yes | Yes | Yes | No | No |
| PTC | 38A | 38A_S30_L001 | 7 | 55181370 | 55181370 | G | A | 19 | 11 | 36.67 | SNV | exonic | EGFR | synonymous SNV | EGFR:NM_001346941:exon14:c.G1560A:p.Q520Q,EGFR:NM_001346897:exon19:c.G2226A:p.Q742Q,EGFR:NM_001346899:exon19:c.G2226A:p.Q742Q,EGFR:NM_001346898:exon20:c.G2361A:p.Q787Q,EGFR:NM_001346900:exon20:c.G2202A:p.Q734Q,EGFR:NM_005228:exon20:c.G2361A:p.Q787Q | rs1050171 | Yes | Yes | Yes | Yes | Yes | Yes | No |
| PTC | 38A | 38A_S41_L001 | 10 | 43118395 | 43118395 | G | T | 0 | 36 | 100 | SNV | exonic | RET | synonymous SNV | RET:NM_001355216:exon10:c.G1545T:p.L515L,RET:NM_020630:exon13:c.G2307T:p.L769L,RET:NM_020975:exon13:c.G2307T:p.L769L | rs1800861 | Yes | Yes | Yes | Yes | Yes | Yes | Yes |
| PTC | 38A | 38A_S41_L001 | 13 | 28036046 | 28036046 | A | G | 30 | 15 | 33.33 | SNV | intronic | FLT3 | . | . | rs2491231 | Yes | Yes | Yes | Yes | Yes | Yes | No |
| PTC | 38A | 38A_S41_L001 | 17 | 7676154 | 7676154 | G | C | 0 | 21 | 100 | SNV | exonic | TP53 | nonsynonymous SNV | TP53:NM_001126118:exon3:c.C98G:p.P33R,TP53:NM_000546:exon4:c.C215G:p.P72R,TP53:NM_001126112:exon4:c.C215G:p.P72R,TP53:NM_001126113:exon4:c.C215G:p.P72R,TP53:NM_001276614:exon4:c.C215G:p.P72R,TP53:NM_001276695:exon4:c.C98G:p.P33R,TP53:NM_001276696:exon4:c.C98G:p.P33R,TP53:NM_001276760:exon4:c.C98G:p.P33R,TP53:NM_001276761:exon4:c.C98G:p.P33R | rs1042522 | Yes | Yes | Yes | Yes | Yes | Yes | Yes |
| PTC | 38A | 38A_S41_L001 | 18 | 51059974 | 51059974 | C | T | 44 | 51 | 53.68 | SNV | intronic | SMAD4 | . | . | rs948588 | Yes | Yes | Yes | Yes | Yes | Yes | Yes |
| PTC | 38A | 38A_S41_L001 | 19 | 1220322 | 1220322 | T | C | 9 | 3 | 25 | SNV | intronic | STK11 | . | . | rs2075606 | Yes | Yes | Yes | Yes | Yes | Yes | Yes |
| PTC | 38A | 38A_S41_L001 | 2 | 211713654 | 211713655 | TA | T | 48 | 21 | 30.43 | DEL | intronic | ERBB4 | . | . | rs397987661 | Yes | Yes | Yes | Yes | Yes | No | No |
| PTC | 38A | 38A_S41_L001 | 4 | 1806167 | 1806167 | G | A | 0 | 26 | 100 | SNV | exonic | FGFR3 | synonymous SNV | FGFR3:NM_022965:exon12:c.G1617A:p.T539T,FGFR3:NM_000142:exon14:c.G1953A:p.T651T,FGFR3:NM_001163213:exon14:c.G1959A:p.T653T,FGFR3:NM_001354809:exon14:c.G1956A:p.T652T,FGFR3:NM_001354810:exon14:c.G1956A:p.T652T | rs7688609 | Yes | Yes | Yes | Yes | Yes | Yes | Yes |
| PTC | 38A | 38A_S41_L001 | 4 | 1806195 | 1806195 | G | A | 17 | 8 | 32 | SNV | intronic | FGFR3 | . | . | rs3135898 | Yes | Yes | Yes | Yes | Yes | Yes | Yes |
| PTC | 38A | 38A_S41_L001 | 4 | 54274888 | 54274888 | A | G | 2 | 58 | 96.67 | SNV | exonic | PDGFRA | synonymous SNV | PDGFRA:NM_001347827:exon12:c.A1701G:p.P567P,PDGFRA:NM_001347829:exon12:c.A1701G:p.P567P,PDGFRA:NM_001347830:exon12:c.A1740G:p.P580P,PDGFRA:NM_006206:exon12:c.A1701G:p.P567P,PDGFRA:NM_001347828:exon13:c.A1776G:p.P592P | rs1873778 | Yes | Yes | Yes | Yes | Yes | Yes | Yes |
| PTC | 38A | 38A_S41_L001 | 4 | 55080004 | 55080004 | G | A | 32 | 21 | 39.62 | SNV | exonic | KDR | synonymous SNV | KDR:NM_002253:exon30:c.C4008T:p.T1336T | rs35961234 | Yes | Yes | Yes | Yes | Yes | Yes | No |
| PTC | 38A | 38A_S41_L001 | 4 | 55096378 | 55096378 | T | TG | 35 | 20 | 36.36 | INS | intronic | KDR | . | . | rs3214870 | Yes | Yes | Yes | Yes | Yes | No | No |
| PTC | 38A | 38A_S41_L001 | 5 | 112840073 | 112840073 | G | A | 44 | 24 | 35.29 | SNV | exonic | APC | synonymous SNV | APC:NM_001127511:exon14:c.G4425A:p.T1475T,APC:NM_001354897:exon15:c.G4509A:p.T1503T,APC:NM_001354899:exon15:c.G4395A:p.T1465T,APC:NM_001354901:exon15:c.G4302A:p.T1434T,APC:NM_001354902:exon15:c.G4206A:p.T1402T,APC:NM_001354905:exon15:c.G3999A:p.T1333T,APC:NM_000038:exon16:c.G4479A:p.T1493T,APC:NM_001354895:exon16:c.G4479A:p.T1493T,APC:NM_001354898:exon16:c.G4404A:p.T1468T,APC:NM_001354898:exon16:c.G4479A:p.T1493T,APC:NM_001354895:exon16:c.G4479A:p.T1493T,APC:NM_001354898:exon16:c.G4404A:p.T1468T,APC:NM_001354900:exon16:c.G4356A:p.T1452T,APC:NM_001354903:exon16:c.G4176A:p.T1392T,APC:NM_001354904:exon16:c.G4101A:p.T1367T,APC:NM_001127510:exon17:c.G4479A:p.T1493T,APC:NM_001354896:exon17:c.G4533A:p.T1511T,APC:NM_001354906:exon17:c.G3630A:p.T1210T | rs41115 | Yes | Yes | Yes | Yes | Yes | Yes | Yes |
| PTC | 38A | 38A_S41_L001 | 5 | 171410509 | 171410510 | CT | C | 32 | 10 | 23.81 | DEL | intronic | NPM1 | . | . | rs34323200 | Yes | Yes | Yes | Yes | Yes | No | No |
| PTC | 38A | 38A_S41_L001 | 7 | 116699618 | 116699618 | C | T | 60 | 33 | 35.48 | SNV | exonic | MET | synonymous SNV | MET:NM_000245:exon2:c.C534T:p.S178S,MET:NM_001127500:exon2:c.C534T:p.S178S,MET:NM_001324401:exon2:c.C534T:p.S178S | rs35775721 | Yes | Yes | Yes | Yes | Yes | Yes | Yes |
| PTC | 38A | 38A_S41_L001 | 7 | 116700208 | 116700208 | A | G | 37 | 32 | 46.38 | SNV | exonic | MET | nonsynonymous SNV | MET:NM_000245:exon2:c.A1124G:p.N375S,MET:NM_001127500:exon2:c.A1124G:p.N375S,MET:NM_001324401:exon2:c.A1124G:p.N375S | rs33917957 | Yes | Yes | Yes | Yes | Yes | No | No |
| PTC | 38A | 38A_S41_L001 | 7 | 55181370 | 55181370 | G | A | 10 | 15 | 60 | SNV | exonic | EGFR | synonymous SNV | EGFR:NM_001346941:exon14:c.G1560A:p.Q520Q,EGFR:NM_001346897:exon19:c.G2226A:p.Q742Q,EGFR:NM_001346899:exon19:c.G2226A:p.Q742Q,EGFR:NM_001346898:exon20:c.G2361A:p.Q787Q,EGFR:NM_001346900:exon20:c.G2202A:p.Q734Q,EGFR:NM_005228:exon20:c.G2361A:p.Q787Q | rs1050171 | Yes | Yes | Yes | Yes | Yes | Yes | No |
| FVPTC | 39A | 39A_S42_L001 | 4 | 55114072 | 55114072 | C | T | 13 | 6 | 31.58 | SNV | intronic | KDR | . | . | rs7692791 | Yes | Yes | Yes | Yes | Yes | Yes | No |
| FVPTC | 39A | 39A_S42_L001 | 5 | 112839908 | 112839908 | A | G | 24 | 6 | 20 | SNV | exonic | APC | synonymous SNV | APC:NM_001127511:exon14:c.A4260G:p.T1420T,APC:NM_001354897:exon15:c.A4344G:p.T1448T,APC:NM_001354899:exon15:c.A4230G:p.T1410T,APC:NM_001354901:exon15:c.A4137G:p.T1379T,APC:NM_001354902:exon15:c.A4041G:p.T1347T,APC:NM_001354905:exon15:c.A3834G:p.T1278T,APC:NM_000038:exon16:c.A4314G:p.T1438T,APC:NM_001354895:exon16:c.A4314G:p.T1438T,APC:NM_001354898:exon16:c.A4239G:p.T1413T,APC:NM_001354900:exon16:c.A4191G:p.T1397T,APC:NM_001354903:exon16:c.A4011G:p.T1337T,APC:NM_001354904:exon16:c.A3936G:p.T1312T,APC:NM_001127510:exon17:c.A4314G:p.T1438T,APC:NM_001354896:exon17:c.A4368G:p.T1456T,APC:NM_001354906:exon17:c.A3465G:p.T1155T | . | Yes | Yes | Yes | Yes | Yes | Yes | Yes |
| FVPTC | 39A | 39A_S42_L001 | 7 | 140753336 | 140753336 | A | T | 33 | 12 | 26.67 | SNV | exonic | BRAF | nonsynonymous SNV | BRAF:NM_001354609:exon15:c.T1799A:p.V600E,BRAF:NM_004333:exon15:c.T1799A:p.V600E | rs113488022 | Yes | Yes | Yes | Yes | Yes | Yes | No |
| NIFTP | 41A | 41A_S42_L001 | 13 | 28036046 | 28036046 | A | G | 38 | 22 | 36.67 | SNV | intronic | FLT3 | . | . | rs2491231 | Yes | Yes | Yes | Yes | Yes | Yes | No |
| NIFTP | 41A | 41A_S42_L001 | 17 | 7676154 | 7676154 | G | C | 0 | 38 | 100 | SNV | exonic | TP53 | nonsynonymous SNV | TP53:NM_001126118:exon3:c.C98G:p.P33R,TP53:NM_000546:exon4:c.C215G:p.P72R,TP53:NM_001126112:exon4:c.C215G:p.P72R,TP53:NM_001126113:exon4:c.C215G:p.P72R,TP53:NM_001276614:exon4:c.C215G:p.P72R,TP53:NM_001276695:exon4:c.C98G:p.P33R,TP53:NM_001276696:exon4:c.C98G:p.P33R,TP53:NM_001276760:exon4:c.C98G:p.P33R,TP53:NM_001276761:exon4:c.C98G:p.P33R | rs1042522 | Yes | Yes | Yes | Yes | Yes | Yes | Yes |
| PTC | 42A | 42A_S45_L001 | 4 | 54274888 | 54274888 | A | G | 0 | 56 | 100 | SNV | exonic | PDGFRA | synonymous SNV | PDGFRA:NM_001347827:exon12:c.A1701G:p.P567P,PDGFRA:NM_001347829:exon12:c.A1701G:p.P567P,PDGFRA:NM_001347830:exon12:c.A1740G:p.P580P,PDGFRA:NM_006206:exon12:c.A1701G:p.P567P,PDGFRA:NM_001347828:exon13:c.A1776G:p.P592P | rs1873778 | Yes | Yes | Yes | Yes | Yes | Yes | Yes |
| NIFTP | 43A | 43A_S32_L001 | 2 | 211713654 | 211713655 | TA | T | 23 | 33 | 58.93 | DEL | intronic | ERBB4 | . | . | rs397987661 | Yes | Yes | Yes | Yes | Yes | No | No |
| NIFTP | 43A | 43A_S32_L001 | 2 | 211947372 | 211947372 | T | C | 19 | 22 | 53.66 | SNV | intronic | ERBB4 | . | . | rs839541 | Yes | Yes | Yes | Yes | Yes | No | No |
| NIFTP | 43A | 43A_S32_L001 | 4 | 1804404 | 1804404 | T | C | 2 | 4 | 66.67 | SNV | exonic | FGFR3 | nonsynonymous SNV | FGFR3:NM_000142:exon9:c.T1150C:p.F384L,FGFR3:NM_001163213:exon9:c.T1150C:p.F386L,FGFR3:NM_001354809:exon9:c.T1150C:p.F384L,FGFR3:NM_001354810:exon9:c.T1150C:p.F384L | rs77881656 | Yes | Yes | Yes | Yes | Yes | Yes | Yes |
| NIFTP | 43A | 43A_S32_L001 | 4 | 55096378 | 55096378 | T | TG | 0 | 30 | 100 | INS | intronic | KDR | . | . | rs3214870 | Yes | Yes | Yes | Yes | Yes | No | No |
| NIFTP | 43A | 43A_S32_L001 | 4 | 55114072 | 55114072 | C | T | 0 | 38 | 100 | SNV | intronic | KDR | . | . | rs7692791 | Yes | Yes | Yes | Yes | Yes | No | No |
| NIFTP | 43A | 43A_S32_L001 | 5 | 171410509 | 171410510 | CT | C | 35 | 16 | 31.37 | DEL | intronic | NPM1 | . | . | rs34323200 | Yes | Yes | Yes | Yes | Yes | No | No |
| NIFTP | 43A | 43A_S47_L001 | 10 | 43113720 | 43113720 | A | T | 13 | 2 | 13.33 | SNV | intronic | RET | . | . | . | Yes | Yes | Yes | Yes | No | No | No |
| NIFTP | 43A | 43A_S47_L001 | 10 | 43113727 | 43113727 | T | C | 11 | 2 | 15.38 | SNV | intronic | RET | . | . | . | Yes | Yes | Yes | Yes | No | No | No |
| NIFTP | 43A | 43A_S47_L001 | 17 | 7674944 | 7674944 | C | T | 10 | 4 | 28.57 | SNV | exonic | TP53 | nonsynonymous SNV | TP53:NM_001126115:exon2:c.G191A:p.R64Q,TP53:NM_001126116:exon2:c.G191A:p.R64Q,TP53:NM_001126117:exon2:c.G191A:p.R64Q,TP53:NM_001276697:exon2:c.G110A:p.R37Q,TP53:NM_001276698:exon2:c.G110A:p.R37Q,TP53:NM_001276699:exon2:c.G110A:p.R37Q,TP53:NM_001126118:exon5:c.G470A:p.R157Q,TP53:NM_000546:exon6:c.G587A:p.R196Q,TP53:NM_001126112:exon6:c.G587A:p.R196Q,TP53:NM_001126113:exon6:c.G587A:p.R196Q,TP53:NM_001276614:exon6:c.G587A:p.R196Q,TP53:NM_001276695:exon6:c.G470A:p.R157Q,TP53:NM_001276696:exon6:c.G470A:p.R157Q,TP53:NM_001276760:exon6:c.G470A:p.R157Q,TP53:NM_001276761:exon6:c.G470A:p.R157Q | rs483352697 | Yes | Yes | Yes | Yes | Yes | Yes | Yes |

| | | | | | | | | | | | | | | | | | | | | | | |
|---|---|---|---|---|---|---|---|---|---|---|---|---|---|---|---|---|---|---|---|---|---|---|
| NIFTP | 43A | 43A_S47_L001 | 17 | 7676154 | 7676154 | G | C | 0 | 6 | 100 | SNV | exonic | TP53 | nonsynonymous SNV | TP53:NM_001126118:exon3:c.C98C:p.P33R,TP53:NM_000546:exon4:c.C215C:p.P72R,TP53:NM_001126112:exon4:c.C215C:p.P72R,TP53:NM_001126113:exon4:c.C215C:p.P72R,TP53:NM_001126114:exon4:c.C215C:p.P72R,TP53:NM_001276695:exon4:c.C98C:p.P33R,TP53:NM_001276696:exon4:c.C98C:p.P33R,TP53:NM_001276760:exon4:c.C98C:p.P33R,TP53:NM_001276761:exon4:c.C98C:p.P33R | rs1042522 | Yes | Yes | Yes | Yes | Yes |
| NIFTP | 43A | 43A_S47_L001 | 2 | 211713654 | 211713655 | TA | T | 11 | 36 | 76.6 | DEL | intronic | ERBB4 | . | . | rs397987661 | Yes | Yes | Yes | No | No | |
| NIFTP | 43A | 43A_S47_L001 | 2 | 211947372 | 211947372 | T | C | 26 | 16 | 38.1 | SNV | intronic | ERBB4 | . | . | rs839541 | Yes | Yes | Yes | Yes | No | |
| NIFTP | 43A | 43A_S47_L001 | 4 | 1804404 | 1804404 | T | C | 5 | 4 | 44.44 | SNV | exonic | FGFR3 | nonsynonymous SNV | FGFR3:NM_000142:exon9:c.T1150C:p.F384L,FGFR3:NM_001163213:exon9:c.T1156C:p.F386L,FGFR3:NM_001354809:exon9:c.T1150C:p.F384L,FGFR3:NM_001354810:exon9:c.T1150C:p.F384L | rs77881656 | Yes | Yes | Yes | Yes | Yes |
| NIFTP | 43A | 43A_S47_L001 | 4 | 55096379 | 55096379 | G | GA | 30 | 23 | 43.4 | INS | intronic | KDR | . | . | . | Yes | Yes | Yes | No | No | |
| NIFTP | 43A | 43A_S47_L001 | 4 | 55114072 | 55114072 | C | T | 0 | 22 | 100 | SNV | intronic | KDR | . | . | rs7692791 | Yes | Yes | Yes | Yes | No | |
| NIFTP | 43A | 43A_S47_L001 | 5 | 171410509 | 171410510 | CT | C | 33 | 6 | 15.38 | DEL | intronic | NPM1 | . | . | rs34323200 | Yes | Yes | Yes | No | No | |
| NIFTP | 43A | 43A_S47_L001 | 7 | 129205262 | 129205262 | G | A | 16 | 4 | 20 | SNV | exonic | SMO | synonymous SNV | SMO:NM_005631:exon3:c.G597A:p.R199R | . | Yes | Yes | Yes | No | No | |
| PTC | 45A | 45A_S33_L001 | 7 | 140753336 | 140753336 | A | T | 42 | 13 | 23.64 | SNV | exonic | BRAF | nonsynonymous SNV | BRAF:NM_001354609:exon15:c.T1799A:p.V600E,BRAF:NM_004333:exon15:c.T1799A:p.V600E | rs113488022 | No | Yes | Yes | Yes | No | |
| PTC | 45A | 45A_S49_L001 | 7 | 140753336 | 140753336 | A | T | 29 | 15 | 34.09 | SNV | exonic | BRAF | nonsynonymous SNV | BRAF:NM_001354609:exon15:c.T1799A:p.V600E,BRAF:NM_004333:exon15:c.T1799A:p.V600E | rs113488022 | No | Yes | Yes | Yes | No | |
| PTC | 45A | 45A_S49_L001 | 9 | 21971138 | 21971138 | T | G | 12 | 5 | 29.41 | SNV | exonic | CDKN2A | nonsynonymous SNV | CDKN2A:NM_000077:exon2:c.A221C:p.D74A,CDKN2A:NM_001195132:exon2:c.A221C:p.D74A,CDKN2A:NM_001363763:exon2:c.A68C:p.D23A | rs200429615 | Yes | Yes | Yes | Yes | Yes | |
| PTC | 45A | 45A_S49_L001 | 9 | 21971145 | 21971145 | A | C | 12 | 5 | 29.41 | SNV | exonic | CDKN2A | nonsynonymous SNV | CDKN2A:NM_000077:exon2:c.T214G:p.C72G,CDKN2A:NM_001195132:exon2:c.T214G:p.C72G,CDKN2A:NM_001363763:exon2:c.T61G:p.C21G,CDKN2A:NM_058195:exon2:c.T257G:p.L86R | . | Yes | Yes | Yes | Yes | Yes | |
| PTC | 45A | 45A_S49_L001 | 9 | 21971147 | 21971147 | T | G | 12 | 5 | 29.41 | SNV | exonic | CDKN2A | nonsynonymous SNV | CDKN2A:NM_000077:exon2:c.A212C:p.N71T,CDKN2A:NM_001195132:exon2:c.A212C:p.N71T,CDKN2A:NM_001363763:exon2:c.A59C:p.N20T,CDKN2A:NM_058195:exon2:c.A255C:p.Q85H | rs559848002 | Yes | Yes | Yes | No | No | |
| PTC | 47A | 47A_S36_L001 | 13 | 28036046 | 28036046 | A | G | 37 | 18 | 32.73 | SNV | intronic | FLT3 | . | . | rs2491231 | Yes | Yes | Yes | Yes | No | |
| PTC | 47A | 47A_S36_L001 | 17 | 7674892 | 7674892 | T | C | 15 | 9 | 37.5 | SNV | exonic | TP53 | synonymous SNV | TP53:NM_001126115:exon2:c.A243G:p.R81R,TP53:NM_001126116:exon2:c.A243G:p.R81R,TP53:NM_001126117:exon2:c.A243G:p.R81R,TP53:NM_001276697:exon2:c.A162G:p.R54R,TP53:NM_001276698:exon2:c.A162G:p.R54R,TP53:NM_001276699:exon2:c.A162G:p.R54R,TP53:NM_001126118:exon5:c.A522G:p.R174R,TP53:NM_000546:exon6:c.A639G:p.R213R,TP53:NM_001126112:exon6:c.A639G:p.R213R,TP53:NM_001126113:exon6:c.A639G:p.R213R,TP53:NM_001126114:exon6:c.A639G:p.R213R,TP53:NM_001276695:exon6:c.A522G:p.R174R,TP53:NM_001276696:exon6:c.A522G:p.R174R,TP53:NM_001276760:exon6:c.A522G:p.R174R,TP53:NM_001276761:exon6:c.A522G:p.R174R | rs1800372 | Yes | Yes | Yes | Yes | Yes |
| PTC | 47A | 47A_S36_L001 | 17 | 7676154 | 7676154 | G | C | 7 | 4 | 36.36 | SNV | exonic | TP53 | nonsynonymous SNV | TP53:NM_001126118:exon3:c.C98C:p.P33R,TP53:NM_000546:exon4:c.C215C:p.P72R,TP53:NM_001126112:exon4:c.C215C:p.P72R,TP53:NM_001126113:exon4:c.C215C:p.P72R,TP53:NM_001126114:exon4:c.C215C:p.P72R,TP53:NM_001276695:exon4:c.C98C:p.P33R,TP53:NM_001276696:exon4:c.C98C:p.P33R,TP53:NM_001276760:exon4:c.C98C:p.P33R,TP53:NM_001276761:exon4:c.C98C:p.P33R | rs1042522 | Yes | Yes | Yes | Yes | Yes |
| PTC | 47A | 47A_S36_L001 | 2 | 211713654 | 211713655 | TA | T | 40 | 12 | 23.08 | DEL | intronic | ERBB4 | . | . | rs397987661 | Yes | Yes | Yes | No | No | |
| PTC | 47A | 47A_S36_L001 | 2 | 211947372 | 211947372 | T | C | 26 | 20 | 43.48 | SNV | intronic | ERBB4 | . | . | rs839541 | Yes | Yes | Yes | Yes | No | |
| PTC | 47A | 47A_S36_L001 | 4 | 1806167 | 1806167 | G | A | 0 | 19 | 100 | SNV | exonic | FGFR3 | synonymous SNV | FGFR3:NM_022965:exon12:c.G1617A:p.T539T,FGFR3:NM_000142:exon14:c.G1953A:p.T651T,FGFR3:NM_001163213:exon14:c.G1959A:p.T653T,FGFR3:NM_001354809:exon14:c.G1956A:p.T652T,FGFR3:NM_001354810:exon14:c.G1956A:p.T652T | rs7688609 | Yes | Yes | Yes | Yes | Yes |
| PTC | 47A | 47A_S36_L001 | 4 | 1806195 | 1806195 | G | A | 12 | 7 | 36.84 | SNV | intronic | FGFR3 | . | . | rs3135898 | Yes | Yes | Yes | Yes | Yes | |
| PTC | 47A | 47A_S36_L001 | 4 | 54274888 | 54274888 | A | G | 0 | 44 | 100 | SNV | exonic | PDGFRA | synonymous SNV | PDGFRA:NM_001347827:exon12:c.A1701G:p.P567P,PDGFRA:NM_001347829:exon12:c.A1701G:p.P567P,PDGFRA:NM_001347830:exon12:c.A1740G:p.P580P,PDGFRA:NM_006206:exon12:c.A1701G:p.P567P,PDGFRA:NM_001347828:exon13:c.A1776G:p.P592P | rs1873778 | Yes | Yes | Yes | Yes | Yes |
| PTC | 47A | 47A_S36_L001 | 5 | 112840073 | 112840073 | G | A | 0 | 47 | 100 | SNV | exonic | APC | synonymous SNV | APC:NM_001127511:exon14:c.G4425A:p.T1475T,APC:NM_001354897:exon15:c.G4509A:p.T1503T,APC:NM_001354899:exon15:c.G4395A:p.T1465T,APC:NM_001354901:exon15:c.G4302A:p.T1434T,APC:NM_001354902:exon15:c.G4206A:p.T1402T,APC:NM_001354905:exon15:c.G3999A:p.T1333T,APC:NM_000038:exon16:c.G4479A:p.T1493T,APC:NM_001354895:exon16:c.G4479A:p.T1493T,APC:NM_001354898:exon16:c.G4404A:p.T1468T,APC:NM_001354900:exon16:c.G4356A:p.T1452T,APC:NM_001354903:exon16:c.G4176A:p.T1392T,APC:NM_001354904:exon16:c.G4101A:p.T1367T,APC:NM_001127510:exon17:c.G4479A:p.T1493T,APC:NM_001354896:exon17:c.G4533A:p.T1511T,APC:NM_001354906:exon17:c.G3630A:p.T1210T | rs41115 | Yes | Yes | Yes | Yes | Yes |
| PTC | 47A | 47A_S36_L001 | 5 | 171410509 | 171410510 | CT | C | 25 | 8 | 24.24 | DEL | intronic | NPM1 | . | . | rs34323200 | Yes | Yes | Yes | No | No | |
| PTC | 47A | 47A_S36_L001 | 9 | 21971133 | 21971133 | C | T | 12 | 4 | 25 | SNV | exonic | CDKN2A | nonsynonymous SNV | CDKN2A:NM_000077:exon2:c.G226A:p.A76T,CDKN2A:NM_001195132:exon2:c.G226A:p.A76T,CDKN2A:NM_001363763:exon2:c.G73A:p.A25T,CDKN2A:NM_058195:exon2:c.G269A:p.R90H | rs774633329 | Yes | Yes | No | Yes | Yes | |
| PTC | 47A | 47A_S53_L001 | 13 | 28036046 | 28036046 | A | G | 41 | 12 | 22.64 | SNV | intronic | FLT3 | . | . | rs2491231 | Yes | Yes | Yes | Yes | No | |
| PTC | 47A | 47A_S53_L001 | 17 | 7674892 | 7674892 | T | C | 16 | 11 | 40.74 | SNV | exonic | TP53 | synonymous SNV | TP53:NM_001126115:exon2:c.A243G:p.R81R,TP53:NM_001126116:exon2:c.A243G:p.R81R,TP53:NM_001126117:exon2:c.A243G:p.R81R,TP53:NM_001276697:exon2:c.A162G:p.R54R,TP53:NM_001276698:exon2:c.A162G:p.R54R,TP53:NM_001276699:exon2:c.A162G:p.R54R,TP53:NM_001126118:exon5:c.A522G:p.R174R,TP53:NM_000546:exon6:c.A639G:p.R213R,TP53:NM_001126112:exon6:c.A639G:p.R213R,TP53:NM_001126113:exon6:c.A639G:p.R213R,TP53:NM_001126114:exon6:c.A639G:p.R213R,TP53:NM_001276695:exon6:c.A522G:p.R174R,TP53:NM_001276696:exon6:c.A522G:p.R174R,TP53:NM_001276760:exon6:c.A522G:p.R174R,TP53:NM_001276761:exon6:c.A522G:p.R174R | rs1800372 | Yes | Yes | Yes | Yes | Yes |
| PTC | 47A | 47A_S53_L001 | 17 | 7676154 | 7676154 | G | C | 7 | 10 | 58.82 | SNV | exonic | TP53 | nonsynonymous SNV | TP53:NM_001126118:exon3:c.C98C:p.P33R,TP53:NM_000546:exon4:c.C215C:p.P72R,TP53:NM_001126112:exon4:c.C215C:p.P72R,TP53:NM_001126113:exon4:c.C215C:p.P72R,TP53:NM_001126114:exon4:c.C215C:p.P72R,TP53:NM_001276695:exon4:c.C98C:p.P33R,TP53:NM_001276696:exon4:c.C98C:p.P33R,TP53:NM_001276760:exon4:c.C98C:p.P33R,TP53:NM_001276761:exon4:c.C98C:p.P33R | rs1042522 | Yes | Yes | Yes | Yes | Yes |
| PTC | 47A | 47A_S53_L001 | 19 | 1220322 | 1220322 | T | C | 2 | 3 | 60 | SNV | intronic | STK11 | . | . | rs2075606 | Yes | Yes | Yes | Yes | Yes | |
| PTC | 47A | 47A_S53_L001 | 2 | 211713654 | 211713655 | TA | T | 32 | 21 | 39.62 | DEL | intronic | ERBB4 | . | . | rs397987661 | Yes | Yes | Yes | No | No | |
| PTC | 47A | 47A_S53_L001 | 2 | 211947372 | 211947372 | T | C | 25 | 19 | 43.18 | SNV | intronic | ERBB4 | . | . | rs839541 | Yes | Yes | Yes | Yes | No | |
| PTC | 47A | 47A_S53_L001 | 4 | 1806167 | 1806167 | G | A | 0 | 12 | 100 | SNV | exonic | FGFR3 | synonymous SNV | FGFR3:NM_022965:exon12:c.G1617A:p.T539T,FGFR3:NM_000142:exon14:c.G1953A:p.T651T,FGFR3:NM_001163213:exon14:c.G1959A:p.T653T,FGFR3:NM_001354809:exon14:c.G1956A:p.T652T,FGFR3:NM_001354810:exon14:c.G1956A:p.T652T | rs7688609 | Yes | Yes | Yes | Yes | Yes |
| PTC | 47A | 47A_S53_L001 | 4 | 1806195 | 1806195 | G | A | 6 | 7 | 53.85 | SNV | intronic | FGFR3 | . | . | rs3135898 | Yes | Yes | Yes | Yes | Yes | |
| PTC | 47A | 47A_S53_L001 | 4 | 54274888 | 54274888 | A | G | 0 | 42 | 100 | SNV | exonic | PDGFRA | synonymous SNV | PDGFRA:NM_001347827:exon12:c.A1701G:p.P567P,PDGFRA:NM_001347829:exon12:c.A1701G:p.P567P,PDGFRA:NM_001347830:exon12:c.A1740G:p.P580P,PDGFRA:NM_006206:exon12:c.A1701G:p.P567P,PDGFRA:NM_001347828:exon13:c.A1776G:p.P592P | rs1873778 | Yes | Yes | Yes | Yes | Yes |
| PTC | 47A | 47A_S53_L001 | 5 | 112840073 | 112840073 | G | A | 0 | 58 | 100 | SNV | exonic | APC | synonymous SNV | APC:NM_001127511:exon14:c.G4425A:p.T1475T,APC:NM_001354897:exon15:c.G4509A:p.T1503T,APC:NM_001354899:exon15:c.G4395A:p.T1465T,APC:NM_001354901:exon15:c.G4302A:p.T1434T,APC:NM_001354902:exon15:c.G4206A:p.T1402T,APC:NM_001354905:exon15:c.G3999A:p.T1333T,APC:NM_000038:exon16:c.G4479A:p.T1493T,APC:NM_001354895:exon16:c.G4479A:p.T1493T,APC:NM_001354898:exon16:c.G4404A:p.T1468T,APC:NM_001354900:exon16:c.G4356A:p.T1452T,APC:NM_001354903:exon16:c.G4176A:p.T1392T,APC:NM_001354904:exon16:c.G4101A:p.T1367T,APC:NM_001127510:exon17:c.G4479A:p.T1493T,APC:NM_001354896:exon17:c.G4533A:p.T1511T,APC:NM_001354906:exon17:c.G3630A:p.T1210T | rs41115 | Yes | Yes | Yes | Yes | Yes |
| PTC | 47A | 47A_S53_L001 | 4 | 171410509 | 171410510 | CT | C | 20 | 10 | 33.33 | DEL | intronic | NPM1 | . | . | rs34323200 | Yes | Yes | Yes | No | No | |
| FVPTC | 48A | 48A_S43_L001 | 1 | 114713908 | 114713908 | T | C | 48 | 28 | 36.84 | SNV | exonic | NRAS | nonsynonymous SNV | NRAS:NM_002524:exon3:c.A182C:p.Q61R | rs11554290 | Yes | Yes | Yes | Yes | Yes | |
| FVPTC | 48A | 48A_S43_L001 | 10 | 43118395 | 43118395 | G | T | 0 | 34 | 100 | SNV | exonic | RET | synonymous SNV | RET:NM_001355216:exon10:c.G1545T:p.L515L,RET:NM_020630:exon13:c.G2307T:p.L769L,RET:NM_020975:exon13:c.G2307T:p.L769L | rs1800861 | Yes | Yes | Yes | Yes | Yes | |
| FVPTC | 48A | 48A_S43_L001 | 11 | 534242 | 534242 | A | G | 9 | 11 | 55 | SNV | exonic | HRAS | synonymous SNV | HRAS:NM_001130442:exon2:c.T81C:p.H27H,HRAS:NM_005343:exon2:c.T81C:p.H27H,HRAS:NM_176795:exon2:c.T81C:p.H27H | rs12628 | Yes | Yes | Yes | Yes | Yes | |
| FVPTC | 48A | 48A_S43_L001 | 13 | 28036046 | 28036046 | A | G | 0 | 36 | 100 | SNV | intronic | FLT3 | . | . | rs2491231 | Yes | Yes | Yes | Yes | No | |
| FVPTC | 48A | 48A_S43_L001 | 17 | 7676154 | 7676154 | G | C | 9 | 15 | 62.5 | SNV | exonic | TP53 | nonsynonymous SNV | TP53:NM_001126118:exon3:c.C98C:p.P33R,TP53:NM_000546:exon4:c.C215C:p.P72R,TP53:NM_001126112:exon4:c.C215C:p.P72R,TP53:NM_001126113:exon4:c.C215C:p.P72R,TP53:NM_001126114:exon4:c.C215C:p.P72R,TP53:NM_001276695:exon4:c.C98C:p.P33R,TP53:NM_001276696:exon4:c.C98C:p.P33R,TP53:NM_001276760:exon4:c.C98C:p.P33R,TP53:NM_001276761:exon4:c.C98C:p.P33R | rs1042522 | Yes | Yes | Yes | Yes | Yes |
| FVPTC | 48A | 48A_S43_L001 | 2 | 211713654 | 211713655 | TA | T | 8 | 54 | 87.1 | DEL | intronic | ERBB4 | . | . | rs397987661 | Yes | Yes | Yes | No | No | |
| FVPTC | 48A | 48A_S43_L001 | 2 | 211713654 | 211713656 | TAA | T | 8 | 14 | 63.64 | DEL | intronic | ERBB4 | . | . | rs748883732 | Yes | Yes | Yes | No | No | |
| FVPTC | 48A | 48A_S43_L001 | 3 | 179199217 | 179199217 | A | G | 25 | 33 | 56.9 | SNV | intronic | PIK3CA | . | . | rs3729674 | Yes | Yes | Yes | Yes | Yes | |
| FVPTC | 48A | 48A_S43_L001 | 3 | 179209622 | 179209622 | A | G | 37 | 35 | 48.61 | SNV | exonic | PIK3CA | nonsynonymous SNV | PIK3CA:NM_006218:exon7:c.A1173G:p.I391M | rs2230461 | Yes | Yes | Yes | Yes | No | |
| FVPTC | 48A | 48A_S43_L001 | 4 | 1806167 | 1806167 | G | A | 0 | 30 | 100 | SNV | exonic | FGFR3 | synonymous SNV | FGFR3:NM_022965:exon12:c.G1617A:p.T539T,FGFR3:NM_000142:exon14:c.G1953A:p.T651T,FGFR3:NM_001163213:exon14:c.G1959A:p.T653T,FGFR3:NM_001354809:exon14:c.G1956A:p.T652T,FGFR3:NM_001354810:exon14:c.G1956A:p.T652T | rs7688609 | Yes | Yes | Yes | Yes | Yes |
| FVPTC | 48A | 48A_S43_L001 | 4 | 54274888 | 54274888 | A | G | 0 | 69 | 100 | SNV | exonic | PDGFRA | synonymous SNV | PDGFRA:NM_001347827:exon12:c.A1701G:p.P567P,PDGFRA:NM_001347829:exon12:c.A1701G:p.P567P,PDGFRA:NM_001347830:exon12:c.A1740G:p.P580P,PDGFRA:NM_006206:exon12:c.A1701G:p.P567P,PDGFRA:NM_001347828:exon13:c.A1776G:p.P592P | rs1873778 | Yes | Yes | Yes | Yes | Yes |
| FVPTC | 48A | 48A_S43_L001 | 5 | 112840073 | 112840073 | G | A | 35 | 39 | 52.7 | SNV | exonic | APC | synonymous SNV | APC:NM_001127511:exon14:c.G4425A:p.T1475T,APC:NM_001354897:exon15:c.G4509A:p.T1503T,APC:NM_001354899:exon15:c.G4395A:p.T1465T,APC:NM_001354901:exon15:c.G4302A:p.T1434T,APC:NM_001354902:exon15:c.G4206A:p.T1402T,APC:NM_001354905:exon15:c.G3999A:p.T1333T,APC:NM_000038:exon16:c.G4479A:p.T1493T,APC:NM_001354895:exon16:c.G4479A:p.T1493T,APC:NM_001354898:exon16:c.G4404A:p.T1468T,APC:NM_001354900:exon16:c.G4356A:p.T1452T,APC:NM_001354903:exon16:c.G4176A:p.T1392T,APC:NM_001354904:exon16:c.G4101A:p.T1367T,APC:NM_001127510:exon17:c.G4479A:p.T1493T,APC:NM_001354896:exon17:c.G4533A:p.T1511T,APC:NM_001354906:exon17:c.G3630A:p.T1210T | rs41115 | Yes | Yes | Yes | Yes | Yes |
| FVPTC | 48A | 48A_S43_L001 | 5 | 171410509 | 171410510 | CT | C | 22 | 18 | 45 | DEL | intronic | NPM1 | . | . | rs34323200 | Yes | Yes | Yes | No | No | |
| FVPTC | 48A | 48A_S43_L001 | 7 | 55181370 | 55181370 | G | A | 0 | 28 | 100 | SNV | exonic | EGFR | synonymous SNV | EGFR:NM_001346941:exon14:c.G1560A:p.Q520Q,EGFR:NM_001346897:exon19:c.G2226A:p.Q742Q,EGFR:NM_001346899:exon19:c.G2226A:p.Q742Q,EGFR:NM_001346898:exon20:c.G2361A:p.Q787Q,EGFR:NM_001346900:exon20:c.G2202A:p.Q734Q,EGFR:NM_005228:exon20:c.G2361A:p.Q787Q | rs1050171 | Yes | Yes | Yes | Yes | No |
| NIFTP | 49A | 49A_S37_L001 | 5 | 171410509 | 171410510 | CT | C | 22 | 16 | 42.11 | DEL | intronic | NPM1 | . | . | rs34323200 | Yes | Yes | Yes | No | No | |
| NIFTP | 49A | 49A_S54_L001 | 5 | 171410509 | 171410510 | CT | C | 35 | 9 | 20.45 | DEL | intronic | NPM1 | . | . | rs34323200 | Yes | Yes | Yes | No | No | |
| PTC | 50A | 50A_S56_L001 | 10 | 43118395 | 43118395 | G | T | 12 | 18 | 60 | SNV | exonic | RET | synonymous SNV | RET:NM_001355216:exon10:c.G1545T:p.L515L,RET:NM_020630:exon13:c.G2307T:p.L769L,RET:NM_020975:exon13:c.G2307T:p.L769L | rs1800861 | Yes | Yes | Yes | Yes | Yes | |
| PTC | 50A | 50A_S56_L001 | 13 | 28036046 | 28036046 | A | G | 0 | 42 | 100 | SNV | intronic | FLT3 | . | . | rs2491231 | Yes | Yes | Yes | Yes | No | |
| PTC | 50A | 50A_S56_L001 | 17 | 7676154 | 7676154 | G | C | 0 | 14 | 100 | SNV | exonic | TP53 | synonymous SNV | TP53:NM_001126118:exon3:c.C98C:p.P33R,TP53:NM_000546:exon4:c.C215C:p.P72R,TP53:NM_001126112:exon4:c.C215C:p.P72R,TP53:NM_001126113:exon4:c.C215C:p.P72R,TP53:NM_001126114:exon4:c.C215C:p.P72R,TP53:NM_001276695:exon4:c.C98C:p.P33R,TP53:NM_001276696:exon4:c.C98C:p.P33R,TP53:NM_001276760:exon4:c.C98C:p.P33R,TP53:NM_001276761:exon4:c.C98C:p.P33R | rs1042522 | Yes | Yes | Yes | Yes | Yes |
| PTC | 50A | 50A_S56_L001 | 19 | 1220322 | 1220322 | T | C | 0 | 2 | 100 | SNV | intronic | STK11 | . | . | rs2075606 | Yes | Yes | Yes | Yes | Yes | |
| PTC | 50A | 50A_S56_L001 | 19 | 1220420 | 1220420 | G | A | 0 | 2 | 100 | SNV | exonic | STK11 | nonsynonymous SNV | STK11:NM_000455:exon4:c.G512A:p.G171D | . | No | Yes | Yes | No | No | |
| PTC | 50A | 50A_S56_L001 | 2 | 29209719 | 29209719 | A | T | 14 | 4 | 22.22 | SNV | intronic | ALK | . | . | . | Yes | Yes | Yes | No | No | |
| PTC | 50A | 50A_S56_L001 | 4 | 1806167 | 1806167 | G | A | 0 | 20 | 100 | SNV | exonic | FGFR3 | synonymous SNV | FGFR3:NM_022965:exon12:c.G1617A:p.T539T,FGFR3:NM_000142:exon14:c.G1953A:p.T651T,FGFR3:NM_001163213:exon14:c.G1959A:p.T653T,FGFR3:NM_001354809:exon14:c.G1956A:p.T652T,FGFR3:NM_001354810:exon14:c.G1956A:p.T652T | rs7688609 | Yes | Yes | Yes | Yes | Yes |
| PTC | 50A | 50A_S56_L001 | 4 | 54274888 | 54274888 | A | G | 0 | 32 | 100 | SNV | exonic | PDGFRA | synonymous SNV | PDGFRA:NM_001347827:exon12:c.A1701G:p.P567P,PDGFRA:NM_001347829:exon12:c.A1701G:p.P567P,PDGFRA:NM_001347830:exon12:c.A1740G:p.P580P,PDGFRA:NM_006206:exon12:c.A1701G:p.P567P,PDGFRA:NM_001347828:exon13:c.A1776G:p.P592P | rs1873778 | Yes | Yes | Yes | Yes | Yes |
| PTC | 50A | 50A_S56_L001 | 4 | 54285873 | 54285873 | C | T | 15 | 10 | 40 | SNV | exonic | PDGFRA | synonymous SNV | PDGFRA:NM_001347829:exon18:c.C2472T:p.V824V,PDGFRA:NM_001347830:exon18:c.C2511T:p.V837V,PDGFRA:NM_006206:exon18:c.C2472T:p.V824V,PDGFRA:NM_001347828:exon19:c.C2547T:p.V849V | rs2228230 | Yes | Yes | Yes | Yes | Yes |
| PTC | 50A | 50A_S56_L001 | 5 | 112840073 | 112840073 | G | A | 0 | 40 | 100 | SNV | exonic | APC | synonymous SNV | APC:NM_001127511:exon14:c.G4425A:p.T1475T,APC:NM_001354897:exon15:c.G4509A:p.T1503T,APC:NM_001354899:exon15:c.G4395A:p.T1465T,APC:NM_001354901:exon15:c.G4302A:p.T1434T,APC:NM_001354902:exon15:c.G4206A:p.T1402T,APC:NM_001354905:exon15:c.G3999A:p.T1333T,APC:NM_000038:exon16:c.G4479A:p.T1493T,APC:NM_001354895:exon16:c.G4479A:p.T1493T,APC:NM_001354898:exon16:c.G4404A:p.T1468T,APC:NM_001354900:exon16:c.G4356A:p.T1452T,APC:NM_001354903:exon16:c.G4176A:p.T1392T,APC:NM_001354904:exon16:c.G4101A:p.T1367T,APC:NM_001127510:exon17:c.G4479A:p.T1493T,APC:NM_001354896:exon17:c.G4533A:p.T1511T,APC:NM_001354906:exon17:c.G3630A:p.T1210T | rs41115 | Yes | Yes | Yes | Yes | Yes |
| PTC | 50A | 50A_S56_L001 | 5 | 171410509 | 171410510 | CT | C | 12 | 4 | 25 | DEL | intronic | NPM1 | . | . | rs34323200 | Yes | Yes | Yes | No | No | |
| PTC | 50A | 50A_S56_L001 | 7 | 55181369 | 55181369 | A | T | 14 | 4 | 22.22 | SNV | exonic | EGFR | nonsynonymous SNV | EGFR:NM_001346941:exon14:c.A1559T:p.Q520L,EGFR:NM_001346897:exon19:c.A2225T:p.Q742L,EGFR:NM_001346899:exon19:c.A2225T:p.Q742L,EGFR:NM_001346898:exon20:c.A2360T:p.Q787L,EGFR:NM_001346900:exon20:c.A2201T:p.Q734L,EGFR:NM_005228:exon20:c.A2360T:p.Q787L | . | Yes | Yes | Yes | Yes | No |
| PTC | 50A | 50A_S56_L001 | 9 | 21971115 | 21971115 | C | T | 10 | 2 | 16.67 | SNV | exonic | CDKN2A | nonsynonymous SNV | CDKN2A:NM_000077:exon2:c.G244A:p.V82M,CDKN2A:NM_001195132:exon2:c.G244A:p.V82M,CDKN2A:NM_001363763:exon2:c.G91A:p.V31M,CDKN2A:NM_058195:exon2:c.G287A:p.R96H | . | Yes | Yes | Yes | Yes | Yes |
| PTC | 50A | 50A_S56_L001 | 9 | 21971124 | 21971124 | T | G | 10 | 2 | 16.67 | SNV | exonic | CDKN2A | nonsynonymous SNV | CDKN2A:NM_000077:exon2:c.A235C:p.T79P,CDKN2A:NM_001195132:exon2:c.A235C:p.T79P,CDKN2A:NM_001363763:exon2:c.A82C:p.T28P,CDKN2A:NM_058195:exon2:c.A278C:p.H93P | . | Yes | Yes | Yes | Yes | Yes |
| PTC | 50A | 50A_S56_L001 | 9 | 21971127 | 21971127 | G | A | 8 | 2 | 20 | SNV | exonic | CDKN2A | nonsynonymous SNV | CDKN2A:NM_000077:exon2:c.C232T:p.L78F,CDKN2A:NM_001195132:exon2:c.C232T:p.L78F,CDKN2A:NM_001363763:exon2:c.C79T:p.L27F,CDKN2A:NM_058195:exon2:c.C275T:p.S92F | . | Yes | Yes | Yes | No | No |
| FVPTC | 54A | 54A_Undetermined_S0_L001 | 10 | 43118395 | 43118395 | G | T | 2 | 17 | 89.47 | SNV | exonic | RET | synonymous SNV | RET:NM_001355216:exon10:c.G1545T:p.L515L,RET:NM_020630:exon13:c.G2307T:p.L769L,RET:NM_020975:exon13:c.G2307T:p.L769L | rs1800861 | Yes | Yes | Yes | Yes | Yes | |
| FVPTC | 54A | 54A_Undetermined_S0_L001 | 11 | 534242 | 534242 | A | G | 7 | 6 | 46.15 | SNV | exonic | HRAS | synonymous SNV | HRAS:NM_001130442:exon2:c.T81C:p.H27H,HRAS:NM_005343:exon2:c.T81C:p.H27H,HRAS:NM_176795:exon2:c.T81C:p.H27H | rs12628 | Yes | Yes | Yes | Yes | Yes | |

| | | | | | | | | | | | | | | | | | | | | | |
|---|---|---|---|---|---|---|---|---|---|---|---|---|---|---|---|---|---|---|---|---|---|
| FVPTC | 54A | 54A_Undetermined_S0_L001 | 17 | 7673789 | 7673789 | A | G | 5 | 2 | 28.57 | SNV | exonic | TP53 | synonymous SNV | TP53:NM_001126115:exon4:c.T435C:p.C145C,TP53:NM_001126116:exon4:c.T435C:p.C145C,TP53:NM_001126117:exon4:c.T435C:p.C145C,TP53:NM_001276697:exon4:c.T354C:p.C118C,TP53:NM_001276698:exon4:c.T354C:p.C118C,TP53:NM_001276699:exon4:c.T354C:p.C118C,TP53:NM_001126118:exon7:c.T714C:p.C238C,TP53:NM_000546:exon8:c.T831C:p.C277C,TP53:NM_001126112:exon8:c.T831C:p.C277C,TP53:NM_001126113:exon8:c.T831C:p.C277C,TP53:NM_001126114:exon8:c.T831C:p.C277C,TP53:NM_001276695:exon8:c.T714C:p.C238C,TP53:NM_001276696:exon8:c.T714C:p.C238C,TP53:NM_001276760:exon8:c.T714C:p.C238C,TP53:NM_001276761:exon8:c.T714C:p.C238C | rs1057523347 | Yes | Yes | Yes | Yes | Yes |
| FVPTC | 54A | 54A_Undetermined_S0_L001 | 17 | 7676154 | 7676154 | G | C | 1 | 3 | 75 | SNV | exonic | TP53 | nonsynonymous SNV | TP53:NM_001126118:exon3:c.C98G:p.P33R,TP53:NM_000546:exon4:c.C215G:p.P72R,TP53:NM_001126112:exon4:c.C215G:p.P72R,TP53:NM_001126113:exon4:c.C215G:p.P72R,TP53:NM_001126114:exon4:c.C215G:p.P72R,TP53:NM_001276695:exon4:c.C98G:p.P33R,TP53:NM_001276696:exon4:c.C98G:p.P33R,TP53:NM_001276760:exon4:c.C98G:p.P33R,TP53:NM_001276761:exon4:c.C98G:p.P33R | rs1042522 | Yes | Yes | Yes | Yes | Yes |
| FVPTC | 54A | 54A_Undetermined_S0_L001 | 2 | 211713654 | 211713655 | TA | T | 27 | 19 | 41.3 | DEL | intronic | ERBB4 | . | . | rs397987661 | Yes | Yes | Yes | No | No |
| FVPTC | 54A | 54A_Undetermined_S0_L001 | 2 | 211947372 | 211947372 | T | C | 12 | 7 | 36.84 | SNV | intronic | ERBB4 | . | . | rs839541 | Yes | Yes | Yes | Yes | No |
| FVPTC | 54A | 54A_Undetermined_S0_L001 | 3 | 179199217 | 179199217 | A | G | 22 | 5 | 18.52 | SNV | intronic | PIK3CA | . | . | rs3729674 | Yes | Yes | Yes | Yes | Yes |
| FVPTC | 54A | 54A_Undetermined_S0_L001 | 4 | 1806167 | 1806167 | G | A | 0 | 8 | 100 | SNV | exonic | FGFR3 | synonymous SNV | FGFR3:NM_022965:exon12:c.G1617A:p.T539T,FGFR3:NM_000142:exon14:c.G1953A:p.T651T,FGFR3:NM_001163213:exon14:c.G1959A:p.T653T,FGFR3:NM_001354809:exon14:c.G1956A:p.T652T,FGFR3:NM_001354810:exon14:c.G1956A:p.T652T | rs7688609 | Yes | Yes | Yes | Yes | Yes |
| FVPTC | 54A | 54A_Undetermined_S0_L001 | 4 | 54274888 | 54274888 | A | G | 0 | 24 | 100 | SNV | exonic | PDGFRA | synonymous SNV | PDGFRA:NM_001347827:exon12:c.A1701G:p.P567P,PDGFRA:NM_001347829:exon12:c.A1701G:p.P567P,PDGFRA:NM_001347830:exon12:c.A1740G:p.P580P,PDGFRA:NM_006206:exon12:c.A1701G:p.P567P,PDGFRA:NM_001347828:exon13:c.A1776G:p.P592P | rs1873778 | Yes | Yes | Yes | Yes | Yes |
| FVPTC | 54A | 54A_Undetermined_S0_L001 | 4 | 55096378 | 55096378 | T | TG | 15 | 14 | 48.28 | INS | intronic | KDR | . | . | rs3214870 | Yes | Yes | Yes | No | No |
| FVPTC | 54A | 54A_Undetermined_S0_L001 | 4 | 55106807 | 55106807 | T | A | 8 | 11 | 57.89 | SNV | exonic | KDR | nonsynonymous SNV | KDR:NM_002253:exon11:c.A1416T:p.Q472H | rs1870377 | Yes | Yes | Yes | Yes | No |
| FVPTC | 54A | 54A_Undetermined_S0_L001 | 5 | 112840073 | 112840073 | G | A | 12 | 17 | 58.62 | SNV | exonic | APC | synonymous SNV | APC:NM_001127511:exon14:c.G4425A:p.T1475T,APC:NM_001354897:exon15:c.G4509A:p.T1503T,APC:NM_001354899:exon15:c.G4395A:p.T1465T,APC:NM_001354901:exon15:c.G4302A:p.T1434T,APC:NM_001354902:exon15:c.G4206A:p.T1402T,APC:NM_001354905:exon15:c.G3999A:p.T1333T,APC:NM_000038:exon16:c.G4479A:p.T1493T,APC:NM_001354895:exon16:c.G4479A:p.T1493T,APC:NM_001354898:exon16:c.G4404A:p.T1468T,APC:NM_001354900:exon16:c.G4356A:p.T1452T,APC:NM_001354903:exon16:c.G4176A:p.T1392T,APC:NM_001354904:exon16:c.G4101A:p.T1367T,APC:NM_001127510:exon17:c.G4479A:p.T1493T,APC:NM_001354896:exon17:c.G4533A:p.T1511T,APC:NM_001354906:exon17:c.G3630A:p.T1210T | rs41115 | Yes | Yes | Yes | Yes | Yes |
| FVPTC | 54A | 54A_Undetermined_S0_L001 | 7 | 55181370 | 55181370 | G | A | 3 | 5 | 62.5 | SNV | exonic | EGFR | synonymous SNV | EGFR:NM_001346941:exon14:c.G1560A:p.Q520Q,EGFR:NM_001346897:exon19:c.G2226A:p.Q742Q,EGFR:NM_001346899:exon19:c.G2226A:p.Q742Q,EGFR:NM_001346898:exon20:c.G2361A:p.Q787Q,EGFR:NM_001346900:exon20:c.G2202A:p.Q734Q,EGFR:NM_005228:exon20:c.G2361A:p.Q787Q | rs1050171 | Yes | Yes | Yes | Yes | No |
| FVPTC | 55A | 55A_Undetermined_S0_L001 | 10 | 43118395 | 43118395 | G | T | 3 | 15 | 83.33 | SNV | exonic | RET | synonymous SNV | RET:NM_001355216:exon10:c.G1545T:p.L515L,RET:NM_020630:exon13:c.G2307T:p.L769L,RET:NM_020975:exon13:c.G2307T:p.L769L | rs1800861 | Yes | Yes | Yes | Yes | Yes |
| FVPTC | 55A | 55A_Undetermined_S0_L001 | 13 | 28036046 | 28036046 | A | G | 14 | 15 | 51.72 | SNV | intronic | FLT3 | . | . | rs2491231 | Yes | Yes | Yes | Yes | No |
| FVPTC | 55A | 55A_Undetermined_S0_L001 | 17 | 7676154 | 7676154 | G | C | 3 | 14 | 82.35 | SNV | exonic | TP53 | nonsynonymous SNV | TP53:NM_001126118:exon3:c.C98G:p.P33R,TP53:NM_000546:exon4:c.C215G:p.P72R,TP53:NM_001126112:exon4:c.C215G:p.P72R,TP53:NM_001126113:exon4:c.C215G:p.P72R,TP53:NM_001126114:exon4:c.C215G:p.P72R,TP53:NM_001276695:exon4:c.C98G:p.P33R,TP53:NM_001276696:exon4:c.C98G:p.P33R,TP53:NM_001276760:exon4:c.C98G:p.P33R,TP53:NM_001276761:exon4:c.C98G:p.P33R | rs1042522 | Yes | Yes | Yes | Yes | Yes |
| FVPTC | 55A | 55A_Undetermined_S0_L001 | 2 | 211947372 | 211947372 | T | C | 22 | 7 | 24.14 | SNV | intronic | ERBB4 | . | . | rs839541 | Yes | Yes | Yes | Yes | No |
| FVPTC | 55A | 55A_Undetermined_S0_L001 | 4 | 1806167 | 1806167 | G | A | 0 | 16 | 100 | SNV | exonic | FGFR3 | synonymous SNV | FGFR3:NM_022965:exon12:c.G1617A:p.T539T,FGFR3:NM_000142:exon14:c.G1953A:p.T651T,FGFR3:NM_001163213:exon14:c.G1959A:p.T653T,FGFR3:NM_001354809:exon14:c.G1956A:p.T652T,FGFR3:NM_001354810:exon14:c.G1956A:p.T652T | rs7688609 | Yes | Yes | Yes | Yes | Yes |
| FVPTC | 55A | 55A_Undetermined_S0_L001 | 4 | 54274888 | 54274888 | A | G | 2 | 34 | 94.44 | SNV | exonic | PDGFRA | synonymous SNV | PDGFRA:NM_001347827:exon12:c.A1701G:p.P567P,PDGFRA:NM_001347829:exon12:c.A1701G:p.P567P,PDGFRA:NM_001347830:exon12:c.A1740G:p.P580P,PDGFRA:NM_006206:exon12:c.A1701G:p.P567P,PDGFRA:NM_001347828:exon13:c.A1776G:p.P592P | rs1873778 | Yes | Yes | Yes | Yes | Yes |
| FVPTC | 55A | 55A_Undetermined_S0_L001 | 4 | 55106807 | 55106807 | T | A | 34 | 12 | 26.09 | SNV | exonic | KDR | nonsynonymous SNV | KDR:NM_002253:exon11:c.A1416T:p.Q472H | rs1870377 | Yes | Yes | Yes | Yes | No |
| FVPTC | 55A | 55A_Undetermined_S0_L001 | 5 | 112840073 | 112840073 | G | A | 17 | 19 | 52.78 | SNV | exonic | APC | synonymous SNV | APC:NM_001127511:exon14:c.G4425A:p.T1475T,APC:NM_001354897:exon15:c.G4509A:p.T1503T,APC:NM_001354899:exon15:c.G4395A:p.T1465T,APC:NM_001354901:exon15:c.G4302A:p.T1434T,APC:NM_001354902:exon15:c.G4206A:p.T1402T,APC:NM_001354905:exon15:c.G3999A:p.T1333T,APC:NM_000038:exon16:c.G4479A:p.T1493T,APC:NM_001354895:exon16:c.G4479A:p.T1493T,APC:NM_001354898:exon16:c.G4404A:p.T1468T,APC:NM_001354900:exon16:c.G4356A:p.T1452T,APC:NM_001354903:exon16:c.G4176A:p.T1392T,APC:NM_001354904:exon16:c.G4101A:p.T1367T,APC:NM_001127510:exon17:c.G4479A:p.T1493T,APC:NM_001354896:exon17:c.G4533A:p.T1511T,APC:NM_001354906:exon17:c.G3630A:p.T1210T | rs41115 | Yes | Yes | Yes | Yes | Yes |
| FVPTC | 55A | 55A_Undetermined_S0_L001 | 5 | 171410509 | 171410510 | CT | C | 26 | 14 | 35 | DEL | intronic | NPM1 | . | . | rs34323200 | Yes | Yes | Yes | No | No |
| FVPTC | 55A | 55A_Undetermined_S0_L001 | 7 | 55181370 | 55181370 | G | A | 7 | 10 | 58.82 | SNV | exonic | EGFR | synonymous SNV | EGFR:NM_001346941:exon14:c.G1560A:p.Q520Q,EGFR:NM_001346897:exon19:c.G2226A:p.Q742Q,EGFR:NM_001346899:exon19:c.G2226A:p.Q742Q,EGFR:NM_001346898:exon20:c.G2361A:p.Q787Q,EGFR:NM_001346900:exon20:c.G2202A:p.Q734Q,EGFR:NM_005228:exon20:c.G2361A:p.Q787Q | rs1050171 | Yes | Yes | Yes | Yes | No |
| FVPTC | 57A | 57A_S63_L001 | 10 | 43120185 | 43120185 | C | G | 9 | 13 | 59.09 | SNV | exonic | RET | synonymous SNV | RET:NM_001355216:exon12:c.C1950G:p.S650S,RET:NM_020630:exon15:c.C2712G:p.S904S,RET:NM_020975:exon15:c.C2712G:p.S904S | rs1800863 | Yes | Yes | Yes | Yes | No |
| FVPTC | 57A | 57A_S63_L001 | 11 | 533874 | 533874 | T | C | 9 | 9 | 50 | SNV | exonic | HRAS | nonsynonymous SNV | HRAS:NM_001130442:exon3:c.A182G:p.Q61R,HRAS:NM_005343:exon3:c.A182G:p.Q61R,HRAS:NM_176795:exon3:c.A182G:p.Q61R | rs121913233 | Yes | Yes | Yes | Yes | Yes |
| FVPTC | 57A | 57A_S63_L001 | 2 | 211713654 | 211713655 | TA | T | 13 | 32 | 71.11 | DEL | intronic | ERBB4 | . | . | rs397987661 | Yes | Yes | Yes | No | No |
| FVPTC | 57A | 57A_S63_L001 | 2 | 211713654 | 211713656 | TAA | T | 13 | 14 | 51.85 | DEL | intronic | ERBB4 | . | . | rs748883732 | Yes | Yes | Yes | No | No |
| FVPTC | 57A | 57A_S63_L001 | 2 | 211947372 | 211947372 | T | C | 21 | 19 | 47.5 | SNV | intronic | ERBB4 | . | . | rs839541 | Yes | Yes | Yes | Yes | No |
| FVPTC | 57A | 57A_S63_L001 | 3 | 179209622 | 179209622 | A | G | 17 | 34 | 66.67 | SNV | exonic | PIK3CA | nonsynonymous SNV | PIK3CA:NM_006218:exon7:c.A1173G:p.I391M | rs2230461 | Yes | Yes | Yes | Yes | No |
| FVPTC | 57A | 57A_S63_L001 | 4 | 1806167 | 1806167 | G | A | 0 | 16 | 100 | SNV | exonic | FGFR3 | synonymous SNV | FGFR3:NM_022965:exon12:c.G1617A:p.T539T,FGFR3:NM_000142:exon14:c.G1953A:p.T651T,FGFR3:NM_001163213:exon14:c.G1959A:p.T653T,FGFR3:NM_001354809:exon14:c.G1956A:p.T652T,FGFR3:NM_001354810:exon14:c.G1956A:p.T652T | rs7688609 | Yes | Yes | Yes | Yes | Yes |
| FVPTC | 57A | 57A_S63_L001 | 4 | 55114072 | 55114072 | C | T | 23 | 15 | 39.47 | SNV | intronic | KDR | . | . | rs7692791 | Yes | Yes | Yes | Yes | No |
| FVPTC | 57A | 57A_S63_L001 | 5 | 112840073 | 112840073 | G | A | 19 | 29 | 60.42 | SNV | exonic | APC | synonymous SNV | APC:NM_001127511:exon14:c.G4425A:p.T1475T,APC:NM_001354897:exon15:c.G4509A:p.T1503T,APC:NM_001354899:exon15:c.G4395A:p.T1465T,APC:NM_001354901:exon15:c.G4302A:p.T1434T,APC:NM_001354902:exon15:c.G4206A:p.T1402T,APC:NM_001354905:exon15:c.G3999A:p.T1333T,APC:NM_000038:exon16:c.G4479A:p.T1493T,APC:NM_001354895:exon16:c.G4479A:p.T1493T,APC:NM_001354898:exon16:c.G4404A:p.T1468T,APC:NM_001354900:exon16:c.G4356A:p.T1452T,APC:NM_001354903:exon16:c.G4176A:p.T1392T,APC:NM_001354904:exon16:c.G4101A:p.T1367T,APC:NM_001127510:exon17:c.G4479A:p.T1493T,APC:NM_001354896:exon17:c.G4533A:p.T1511T,APC:NM_001354906:exon17:c.G3630A:p.T1210T | rs41115 | Yes | Yes | Yes | Yes | Yes |
| FVPTC | 57A | 57A_S63_L001 | 5 | 171410509 | 171410510 | CT | C | 10 | 28 | 73.68 | DEL | intronic | NPM1 | . | . | rs34323200 | Yes | Yes | Yes | No | No |
| FVPTC | 57A | 57A_S63_L001 | 7 | 55181370 | 55181370 | G | A | 0 | 36 | 100 | SNV | exonic | EGFR | synonymous SNV | EGFR:NM_001346941:exon14:c.G1560A:p.Q520Q,EGFR:NM_001346897:exon19:c.G2226A:p.Q742Q,EGFR:NM_001346899:exon19:c.G2226A:p.Q742Q,EGFR:NM_001346898:exon20:c.G2361A:p.Q787Q,EGFR:NM_001346900:exon20:c.G2202A:p.Q734Q,EGFR:NM_005228:exon20:c.G2361A:p.Q787Q | rs1050171 | Yes | Yes | Yes | Yes | No |
| PTC | 7A | 7A_S17_L001 | 2 | 211713654 | 211713655 | TA | T | 27 | 29 | 51.79 | DEL | intronic | ERBB4 | . | . | rs397987661 | Yes | Yes | Yes | No | No |
| PTC | 7A | 7A_S17_L001 | 2 | 211947372 | 211947372 | T | C | 26 | 18 | 40.91 | SNV | intronic | ERBB4 | . | . | rs839541 | Yes | Yes | Yes | No | No |
| PTC | 7A | 7A_S17_L001 | 7 | 140753336 | 140753336 | A | T | 50 | 15 | 23.08 | SNV | exonic | BRAF | nonsynonymous SNV | BRAF:NM_001354609:exon15:c.T1799A:p.V600E,BRAF:NM_004333:exon15:c.T1799A:p.V600E | rs113488022 | Yes | Yes | Yes | Yes | No |
| PTC | 7A | 7A_S17_L001 | 9 | 21971128 | 21971128 | A | G | 13 | 5 | 27.78 | SNV | exonic | CDKN2A | nonsynonymous SNV | CDKN2A:NM_058195:exon2:c.T274C:p.S92P | rs1064793313 | Yes | Yes | Yes | No | No |
| FVPTC | 8A | 8A_S19_L001 | 1 | 114713908 | 114713908 | T | C | 46 | 21 | 31.34 | SNV | exonic | NRAS | nonsynonymous SNV | NRAS:NM_002524:exon3:c.A182C:p.Q61R | rs11554290 | Yes | Yes | Yes | Yes | No |
| FVPTC | 8A | 8A_S19_L001 | 10 | 43118395 | 43118395 | G | T | 0 | 14 | 100 | SNV | exonic | RET | synonymous SNV | RET:NM_001355216:exon10:c.G1545T:p.L515L,RET:NM_020630:exon13:c.G2307T:p.L769L,RET:NM_020975:exon13:c.G2307T:p.L769L | rs1800861 | Yes | Yes | Yes | Yes | Yes |
| FVPTC | 8A | 8A_S19_L001 | 13 | 28028155 | 28028155 | T | C | 25 | 29 | 53.7 | SNV | intronic | FLT3 | . | . | rs75580865 | Yes | Yes | Yes | Yes | No |
| FVPTC | 8A | 8A_S19_L001 | 13 | 28036046 | 28036046 | A | G | 0 | 30 | 100 | SNV | intronic | FLT3 | . | . | rs2491231 | Yes | Yes | Yes | Yes | No |
| FVPTC | 8A | 8A_S19_L001 | 17 | 7676154 | 7676154 | G | C | 0 | 12 | 100 | SNV | exonic | TP53 | nonsynonymous SNV | TP53:NM_001126118:exon3:c.C98G:p.P33R,TP53:NM_000546:exon4:c.C215G:p.P72R,TP53:NM_001126112:exon4:c.C215G:p.P72R,TP53:NM_001126113:exon4:c.C215G:p.P72R,TP53:NM_001126114:exon4:c.C215G:p.P72R,TP53:NM_001276695:exon4:c.C98G:p.P33R,TP53:NM_001276696:exon4:c.C98G:p.P33R,TP53:NM_001276760:exon4:c.C98G:p.P33R,TP53:NM_001276761:exon4:c.C98G:p.P33R | rs1042522 | Yes | Yes | Yes | Yes | Yes |
| FVPTC | 8A | 8A_S19_L001 | 2 | 211713654 | 211713655 | TA | T | 9 | 13 | 59.09 | DEL | intronic | ERBB4 | . | . | rs397987661 | Yes | Yes | Yes | No | No |
| FVPTC | 8A | 8A_S19_L001 | 4 | 1806167 | 1806167 | G | A | 0 | 12 | 100 | SNV | exonic | FGFR3 | synonymous SNV | FGFR3:NM_022965:exon12:c.G1617A:p.T539T,FGFR3:NM_000142:exon14:c.G1953A:p.T651T,FGFR3:NM_001163213:exon14:c.G1959A:p.T653T,FGFR3:NM_001354809:exon14:c.G1956A:p.T652T,FGFR3:NM_001354810:exon14:c.G1956A:p.T652T | rs7688609 | Yes | Yes | Yes | Yes | No |
| FVPTC | 8A | 8A_S19_L001 | 4 | 54274888 | 54274888 | A | G | 0 | 46 | 100 | SNV | exonic | PDGFRA | synonymous SNV | PDGFRA:NM_001347827:exon12:c.A1701G:p.P567P,PDGFRA:NM_001347829:exon12:c.A1701G:p.P567P,PDGFRA:NM_001347830:exon12:c.A1740G:p.P580P,PDGFRA:NM_006206:exon12:c.A1701G:p.P567P,PDGFRA:NM_001347828:exon13:c.A1776G:p.P592P | rs1873778 | Yes | Yes | Yes | Yes | Yes |
| FVPTC | 8A | 8A_S19_L001 | 4 | 55096378 | 55096378 | T | TG | 17 | 19 | 52.78 | INS | intronic | KDR | . | . | rs3214870 | Yes | Yes | Yes | No | No |
| FVPTC | 8A | 8A_S19_L001 | 4 | 55114072 | 55114072 | C | T | 0 | 20 | 100 | SNV | intronic | KDR | . | . | rs7692791 | Yes | Yes | Yes | Yes | No |
| FVPTC | 8A | 8A_S19_L001 | 5 | 112840073 | 112840073 | G | A | 0 | 62 | 100 | SNV | exonic | APC | synonymous SNV | APC:NM_001127511:exon14:c.G4425A:p.T1475T,APC:NM_001354897:exon15:c.G4509A:p.T1503T,APC:NM_001354899:exon15:c.G4395A:p.T1465T,APC:NM_001354901:exon15:c.G4302A:p.T1434T,APC:NM_001354902:exon15:c.G4206A:p.T1402T,APC:NM_001354905:exon15:c.G3999A:p.T1333T,APC:NM_000038:exon16:c.G4479A:p.T1493T,APC:NM_001354895:exon16:c.G4479A:p.T1493T,APC:NM_001354898:exon16:c.G4404A:p.T1468T,APC:NM_001354900:exon16:c.G4356A:p.T1452T,APC:NM_001354903:exon16:c.G4176A:p.T1392T,APC:NM_001354904:exon16:c.G4101A:p.T1367T,APC:NM_001127510:exon17:c.G4479A:p.T1493T,APC:NM_001354896:exon17:c.G4533A:p.T1511T,APC:NM_001354906:exon17:c.G3630A:p.T1210T | rs41115 | Yes | Yes | Yes | Yes | Yes |
| FVPTC | 8A | 8A_S19_L001 | 5 | 150054034 | 150054034 | G | A | 2 | 4 | 66.67 | SNV | UTR3 | CSF1R | . | . | rs2066933 | Yes | Yes | Yes | No | No |
| FVPTC | 8A | 8A_S19_L001 | 5 | 171410509 | 171410510 | CT | C | 31 | 15 | 32.61 | DEL | intronic | NPM1 | . | . | rs34323200 | Yes | Yes | Yes | No | No |
| FVPTC | 8A | 8A_S19_L001 | 7 | 116699618 | 116699618 | C | T | 33 | 42 | 56 | SNV | exonic | MET | synonymous SNV | MET:NM_000245:exon2:c.C534T:p.S178S,MET:NM_001127500:exon2:c.C534T:p.S178S,MET:NM_001324401:exon2:c.C534T:p.S178S | rs35775721 | Yes | Yes | Yes | Yes | Yes |
| FVPTC | 8A | 8A_S19_L001 | 7 | 116700208 | 116700208 | A | G | 17 | 24 | 58.54 | SNV | exonic | MET | nonsynonymous SNV | MET:NM_000245:exon2:c.A1124G:p.N375S,MET:NM_001127500:exon2:c.A1124G:p.N375S,MET:NM_001324401:exon2:c.A1124G:p.N375S | rs33917957 | Yes | Yes | Yes | Yes | Yes |
| FVPTC | 8A | 8A_S19_L001 | 7 | 55181370 | 55181370 | G | A | 0 | 15 | 100 | SNV | exonic | EGFR | synonymous SNV | EGFR:NM_001346941:exon14:c.G1560A:p.Q520Q,EGFR:NM_001346897:exon19:c.G2226A:p.Q742Q,EGFR:NM_001346899:exon19:c.G2226A:p.Q742Q,EGFR:NM_001346898:exon20:c.G2361A:p.Q787Q,EGFR:NM_001346900:exon20:c.G2202A:p.Q734Q,EGFR:NM_005228:exon20:c.G2361A:p.Q787Q | rs1050171 | Yes | Yes | Yes | Yes | No |
| NIFTP | 9A | 9A_S20_L001 | 5 | 150054033 | 150054033 | T | G | 0 | 12 | 100 | SNV | UTR3 | CSF1R | . | . | rs2066934 | Yes | Yes | Yes | Yes | Yes |
| NIFTP | 9A | 9A_S20_L001 | 5 | 150054034 | 150054034 | G | A | 0 | 12 | 100 | SNV | UTR3 | CSF1R | . | . | rs2066933 | Yes | Yes | Yes | No | No |
| NIFTP | 1A | T1A_S5_L001 | 17 | 7676154 | 7676154 | G | C | 0 | 14 | 100 | SNV | exonic | TP53 | nonsynonymous SNV | TP53:NM_001126118:exon3:c.C98G:p.P33R,TP53:NM_000546:exon4:c.C215G:p.P72R,TP53:NM_001126112:exon4:c.C215G:p.P72R,TP53:NM_001126113:exon4:c.C215G:p.P72R,TP53:NM_001126114:exon4:c.C215G:p.P72R,TP53:NM_001276695:exon4:c.C98G:p.P33R,TP53:NM_001276696:exon4:c.C98G:p.P33R,TP53:NM_001276760:exon4:c.C98G:p.P33R,TP53:NM_001276761:exon4:c.C98G:p.P33R | rs1042522 | Yes | Yes | Yes | Yes | Yes |
| NIFTP | 2A | T2A_S7_L001 | 1 | 114713908 | 114713908 | T | C | 51 | 14 | 21.54 | SNV | exonic | NRAS | nonsynonymous SNV | NRAS:NM_002524:exon3:c.A182C:p.Q61R | rs11554290 | Yes | Yes | Yes | Yes | Yes |
| NIFTP | 2A | T2A_S7_L001 | 9 | 21971138 | 21971138 | T | G | 8 | 3 | 27.27 | SNV | exonic | CDKN2A | nonsynonymous SNV | CDKN2A:NM_000077:exon2:c.A221C:p.D74A,CDKN2A:NM_001195132:exon2:c.A221C:p.D74A,CDKN2A:NM_001363763:exon2:c.A68C:p.D23A | rs200429615 | Yes | Yes | Yes | Yes | Yes |
| NIFTP | 3A | T3A_S9_L001 | 13 | 28036046 | 28036046 | A | G | 22 | 14 | 38.89 | SNV | intronic | FLT3 | . | . | rs2491231 | Yes | Yes | Yes | Yes | No |
| NIFTP | 3A | T3A_S9_L001 | 9 | 21971134 | 21971134 | G | A | 14 | 4 | 22.22 | SNV | exonic | CDKN2A | nonsynonymous SNV | CDKN2A:NM_058195:exon2:c.C268T:p.R90C | . | No | Yes | Yes | Yes | Yes |
| PTC | 4A | T4A_S11_L001 | 7 | 140753336 | 140753336 | A | T | 54 | 26 | 32.5 | SNV | exonic | BRAF | nonsynonymous SNV | BRAF:NM_001354609:exon15:c.T1799A:p.V600E,BRAF:NM_004333:exon15:c.T1799A:p.V600E | rs113488022 | Yes | Yes | Yes | Yes | No |
| NIFTP | 5A | T5A_S13_L001 | 15 | 90088685 | 90088686 | TC | T | 10 | 4 | 28.57 | DEL | exonic | IDH2 | frameshift substitution | IDH2:NM_001290114:exon2:c.45_46delinsA:p.T16Lfs*15,IDH2:NM_001289910:exon4:c.279_280delinsA:p.T94Lfs*15,IDH2:NM_002168:exon4:c.435_436delinsA:p.T146Lfs*15 | rs747216375 | No | Yes | No | No | No |
| NIFTP | 5A | T5A_S13_L001 | 19 | 1223066 | 1223066 | C | T | 10 | 4 | 28.57 | SNV | exonic | STK11 | synonymous SNV | STK11:NM_000455:exon8:c.C1002T:p.S334S | rs1057521267 | Yes | Yes | Yes | No | No |
| NIFTP | 5A | T5A_S13_L001 | 5 | 171410509 | 171410511 | CTT | C | 37 | 8 | 17.78 | DEL | intronic | NPM1 | . | . | rs766749752 | Yes | Yes | Yes | No | No |
| PTC | 6A | T6A_S15_L001 | 5 | 150054033 | 150054033 | T | G | 0 | 14 | 100 | SNV | UTR3 | CSF1R | . | . | rs2066934 | Yes | Yes | Yes | Yes | Yes |
| PTC | 6A | T6A_S15_L001 | 5 | 150054034 | 150054034 | G | A | 0 | 14 | 100 | SNV | UTR3 | CSF1R | . | . | rs2066933 | Yes | Yes | Yes | No | No |
| PTC | 6A | T6A_S15_L001 | 5 | 171410509 | 171410510 | CT | C | 30 | 12 | 28.57 | DEL | intronic | NPM1 | . | . | rs34323200 | Yes | Yes | Yes | No | No |
| PTC | 6A | T6A_S15_L001 | 7 | 140753336 | 140753336 | A | T | 35 | 22 | 38.6 | SNV | exonic | BRAF | nonsynonymous SNV | BRAF:NM_001354609:exon15:c.T1799A:p.V600E,BRAF:NM_004333:exon15:c.T1799A:p.V600E | rs113488022 | Yes | Yes | Yes | Yes | No |
| PTC | 6A | T6A_S15_L001 | 9 | 130874931 | 130874931 | C | T | 18 | 6 | 25 | SNV | exonic | ABL1 | synonymous SNV | ABL1:NM_005157:exon7:c.C1149T:p.G383G,ABL1:NM_007313:exon7:c.C1206T:p.G402G | . | Yes | Yes | Yes | No | No |

Detailed information regarding all somatic mutations evaluated in this study for tumor samples of the patients.
FVPTC: follicular variant of papillary thyroid carcinoma; PTC: papillary thyroid carcinoma; NIFTP: Non-Invasive Follicular Thyroid neoplasm with Papillary-like nuclear features.
SNV: Single Nucleotide Variant; INS: Insertion; DEL: Deletion. ncRNA: non-coding RNA; UTR: Untranslated Region.